CHALMERS
UNIVERSITY OF TECHNOLOGY

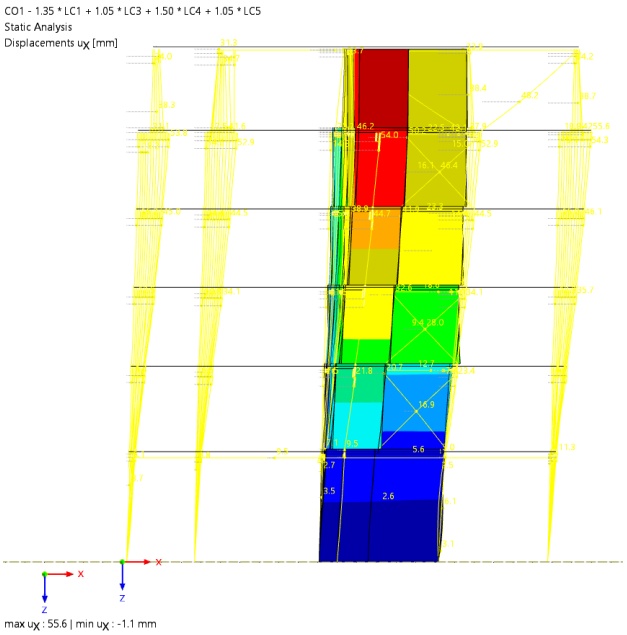

Stiffness of dowel-type timber connections and its influence on structures

Finite element analysis of high performance timber connections and their impact in a case study

Master's thesis in Master Program Structural engineering and building technology

DINA ABDALLAH
ANTON DIMMING

Department of Architecture and Civil Engineering
CHALMERS UNIVERSITY OF TECHNOLOGY
Gothenburg, Sweden 2023

Master's thesis ACEX30

Stiffness of dowel-type timber connections and its influence on structures

Finite element analysis of high performance timber connections and their impact in a case study

DINA ABDALLAH
ANTON DIMMING

CHALMERS
UNIVERSITY OF TECHNOLOGY

Department of Architecture and Civil Engineering
Division of Structural Engineering
Lightweight Structures Group
Chalmers University of Technology
Gothenburg, Sweden 2023

Stiffness of dowel-type timber connections and its influence on structures
Finite element analysis of high performance timber connections and their impact in a case study

DINA ABDALLAH
ANTON DIMMING

Supervisor: Dr. Elzbieta Lukaszewska, AFRY
Examiner: Assist. Professor Robert Jockwer, Department of Architecture and Civil Engineering.

Department of Architecture and Civil Engineering
Division of Structural engineering
Lightweight Structures Group
Chalmers University of Technology
SE-412 96 Gothenburg
Telephone +46 31 772 1000

Cover: An finite element analysis of the building of the study case in RFEM software. The resulted deformation scaled up and caused by mainly wind load acting on the x-direction.

Department of Architecture and Civil Engineering
Gothenburg, Sweden 2023

Stiffness of dowel-type timber connections and its influence on structures
Finite element analysis of high performance timber connections and their impact in a case study
DINA ABDALLAH, ANTON DIMMING
Department of Architecture and Civil Engineering
Chalmers University of Technology

Abstract

Timber is one of the oldest construction materials and are used for many purposes in the field. Although, timber has not been prioritized as a structural material for multi-storey buildings, today's new technologies which generate engineering wood products, allow to build in larger scale than ever before. Connections between timber members in structural systems are critical details, but detailed design standards and guidelines for large-scale timber connections are still lacking.

The stiffness and ductility of timber connections are important parameters for the response of a structural system. However the methods for evaluating stiffness in standards such as Eurocode 5 are limited. For this reason, detailed information on stiffness and ductility of connections might be neglected in design process. This might results in inefficient material utilisation and unknown effects. Therefor, the aim of this thesis is to analyze the stiffness of timber connections, and the impact the stiffness can have on a structural system.

The research is accomplished by identifying and using appropriate modeling methods for dowel-type timber connections, and then investigating the design of a 5-storey building with timber beam-column structural system. Firstly, the rotational stiffness of the most used connection in the case study was calculated by finite element analysis in Abaqus. Then, modified variations of the chosen connection were analysed to study the influence of different design choices on the rotational stiffness. Lastly, the calculated stiffness is inserted to the joints of the model of the reference building in RFEM software to study the contribution of connection's stiffness to internal forces and global deformations.

The findings of this thesis can be summed up to that other than those provided by the standards, there are applicable methods that provide more sophisticated load-deformation relations and estimate stiffness for dowel-type timber connections. For the studied case, the stiffness of the beam-to-column connections had limited impact on the global deformations and some impact on internal forces in the structural system. In addition, accounting for stiffness in the joints of a timber beam reduces the span moment and might allow for reduced design cross-sectional area. However, some more aspects and parameters than the treated ones in this thesis should be taken into account when rising the stiffness and ductility of a connection.

Keywords: Rotational stiffness, ductility, glulam, dowel-type connection, structural system, shear plane, FEM, Eurocode.

Acknowledgements

This master thesis was written from an initiative of our supervisor Dr. Elzbieta Lukaszewska. We would like to thank Dr. Elzbieta Lukaszewska for all her support and ideas, and for providing us good conditions to carry out this thesis. We also thank our examiner, Assistant Professor Robert Jockwer for all the guidance and feedback, and for exchanging his knowledge and expertise with us throughout the whole project. The writing was carried out at the Afry office in Gothenburg and we appreciate the great hospitality that we had there during the spring semester. Finally, we thank our opponents Amilia Engdahl and Noora Khoulani for their valuable feedback and constructive criticism.

Dina Abdallah, Anton Dimming, Gothenburg, july 2023

Contents

List of Figures

List of Tables

1
Introduction

1.1 Background

Timber was one of the earliest construction materials to be used by human beings in the history. Timber has shown durability of a lifetime beyond 100 years and less environmental impacts compared with other construction materials, which is very relevant in a time when sustainability is becoming essential. Although timber has been very popular for one-storey houses, it was replaced with concrete or steel to build taller buildings and bridges.

The interest in timber in Europe has been increasing in recent years to build higher and in longer spans. The development of timber technologies (i.e. glulam, CLT and LVL) has allowed longer spans with minimized cross-section areas. As interest of building larger structures with timber is increasing, still among clients and in the construction industry there are commonly expectations considering the costs, that modern large timber structures are a more expensive alternative than its counterparts. Proofing that selecting timber is an economic alternative is important, and developing techniques and methods that reduces the design and construction costs could make timber structures an even more attractive alternative. [Ottenhaus et al., 2021] states that connections are among the most expensive parts in timber structures, and at the same time the most complex. Connections require time consuming design process and the production of them could be demanding. Figure 1.1 shows a schematic overview of how the design procedure of connections in structures could look like.

According to [Ottenhaus et al., 2021] Stiffness and ductility of connections in large timber structures are one of the most critical aspects in the design. Connections are often the weaker link in the structure and the design of them will have influence in how the structure performs. Both in terms of preventing brittle and devastating collapse, but also providing structural properties that will affect the response of the total structure.

Since the connections are the sensitive parts of a structure, it is still common in the design procedure to sustain a more secure assumption and design the connections between elements in the structure as pinned, when modelling the structures

to obtain design loads on both connections and other load carrying elements. As the stiffness and ductility might affect load paths and load redistribution in a structure, assuming no stiffness in connections will result in different stress distribution compared to reality, and by that redesigning of the structural components might be necessary.

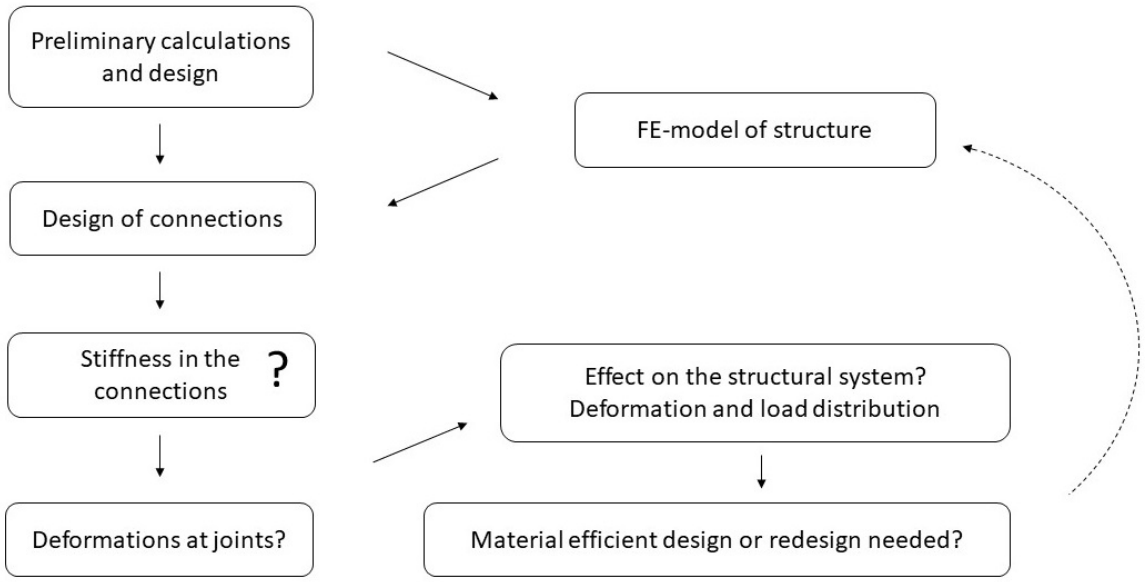

Figure 1.1: *Overview of possible design procedure for connections in structure*

1.2 Aim

The aim of the project is to analyze the stiffness and ductility of timber connections, and the impact the stiffness can have on a structural system.

By gathering information about stiffness properties for a set of timber connections, and by generating models and investigating the influence of some design choices on the connection's stiffness, the calculated stiffness values are used to determine if there is a necessity of considering the stiffness when designing timber structural systems.

1.3 Objectives

The objectives that are addressed to achieve the aim of this project are:

- To study the theory needed for analysing stiffness and ductility of timber connections.

- To study the basic concepts about some structural systems of timber and use a reference building as a case study.

- To select a set of connection alternatives that would fulfil the structural demands for the reference building and would be applicable regarding geometries and architectural contexts.

- To study and evaluate the performance of connections with regard to requirements that exist in large timber structures.

- To simulate the stiffness with the planar load-deformation relation of the selected connections.

- To verify the results of the simulations with simplified hand calculations.

- To apply the results and stiffness data of the connections into a finite element model of the structural system of the reference building and study the effect of the stiffness on system level.

1.4 Limitations

Some limitations are preliminary determined to make the scope of the project reasonable with regards to the time frame. The project will focus on connections in a multi-story beam-column system building, composed mainly with glulam elements. The evaluation of connections will mainly include structural aspects e.g. capacity, stiffness and deflections. The connections that will be studied are connecting beams and columns and structural analysis will mostly consider the planar behavior of the connections. The stiffness of connections will be analysed but the calculations and simulations will not consider long term effects and the material models don't include damage of the materials other than plasticity. The effect that moisture might have on timber and possibly also the results will not be studied either. The case study that is implemented to analyse global behaviour of a building and its structural system is modeled with given dimensions of the structural elements. The purpose with the analysis is to study stiffness of connections on a system level and only a few load cases will be considered.

1.5 Method

Seeking to achieve the aim and objectives for the project, the work is split into phases.

- The first phase includes preparation with a literature study and a case study to become more familiar with the subject and problem.

- The second phase is about delimiting and focusing the work. To narrow in and identify relevant solution for connections within the context. A suitable method for modelling the strength and load-deformation behaviour of the connections will be adopted.

- In the third phase connections will be analysed and modelled, then the modelling and result will be verified. A parametric study adapted for variations of the studied connections will also be made, in order identify important design aspects and improve the connections. Also to perform a sensitivity study.

- In the fourth phase the structural system of the reference building will be modeled in finite element software RFEM by Dlubal. Stiffness parameters that have been generated for connections will be implemented as spring constants and the effect of this will be studied.

The literature study contains four main parts. The first part presents material properties of wood and timber as a building material. After the first part some aspects about structural systems will be reviewed and some basics of structural systems of timber will be treated in order to describe contexts for timber connections. Then, relevant theory, standards, guidelines and previous knowledge on the design and structural behavior of timber connection are studied. Thereafter, the reader is presented to some aspects about finite element modelling of timber structures and timber connections. The theory that are the basis for the method and analysis will be presented.

An existing glulam beam-column structural system is investigated to help determine which connections the project will treat and further analyse. The purpose is also to investigate how the mechanical behaviour of the studied connections influence the structural system at a global level.

After selecting the connections to be studied, the connections are modelled in Abaqus CAE to be analysed. The planar load deformation relation and failure modes of the connections will be simulated. The analyses are adapted to calculate rotational stiffness and vertical stiffness. The implemented analyses are thereafter verified with analytical calculations to check the accuracy of the models.

At last, the global analysis of the structural system is performed in RFEM and the knowledge about stiffness of connections present in the building will be implemented in the model. The FE-model will be loaded with different relevant loads and results with and without stiffness assignments at joints will be compared.

2

Theory

2.1 Wood and timber

Wood is a growing material, which highly influences its material properties. It consists of fibres that are made up of wood cell walls which are arranged in the longitudinal direction of the tree trunk. [Soutsos and Domone, 2010] describe that the main functions which the material structure of wood provides for trees are to transport nutrients and water, carry the weight of the tree trunk and crown, and to store the essential fluids with nutrients that trees need. There are two main types of wood, hardwood and softwood which have some differences in the cell structure, the wood cell's functions, how they grow which shows different material properties compared to one another.

[Göts et al., 1989] explains that the structure of wood cells are similar like thin hollow straws and consist mostly of cellulose. In trees these cell wall structures are more or less densely arranged together like in bundles. The wood cells are generated and grow in an outer zone of the trunk called cambium and [Soutsos and Domone, 2010] detail how the material structure are contained or cemented together in a matrix of lignin and hemicellulose . These are some of the basic characteristics which why wood is an orthotropic material with different mechanical properties in different directions.

Wood as a construction material has high strength and stiffness compared to its weight. According to [Soutsos and Domone, 2010] The wood's properties vary depending several factors, for instance on environmental conditions during the growth and varying characteristics for different species. However, stiffness and strength also differ at the same tree trunk due to anisotropy of the material structure, variations of density of wood cells within the trunk, rate of growth and imperfections like knots. Tested wood specimens show high sensitivity to the direction of loading where a significant difference in capacity can be observed between loading parallel or perpendicular to grain. These directions relative to the trunk are explained in figure 2.1

In the fibre or grain direction wood is very strong in compression and rather stronger in tension. The perpendicular-to-grain compression strength is several times weaker than strength in the parallel direction. Wood has its lowest strength for tension loading in the direction perpendicular to the grain.

Wood in structural members are referred to as timber. Due to the variations of properties influencing the homogeneity and quality of wood, structural timber also shows a lot of variations in material properties that are independent of the grain direction. Therefor timber are graded and sorted in different standardized strength classes.

2.1.1 Matateriał orientation

Wood can be defined as an orthotropic material with 3 orthogonal planes of symmetry, longitudinal, radial and tangential. Not only the load-carrying capacity and stiffness is influenced by these directions, [Burström, 2001] highlights that also the loss of moisture and therefore the rate of shrinkage and swelling are affected by the orthotropic structure of wood. A common way to define the different directions with coresponding stress components are visualized in figure 2.1

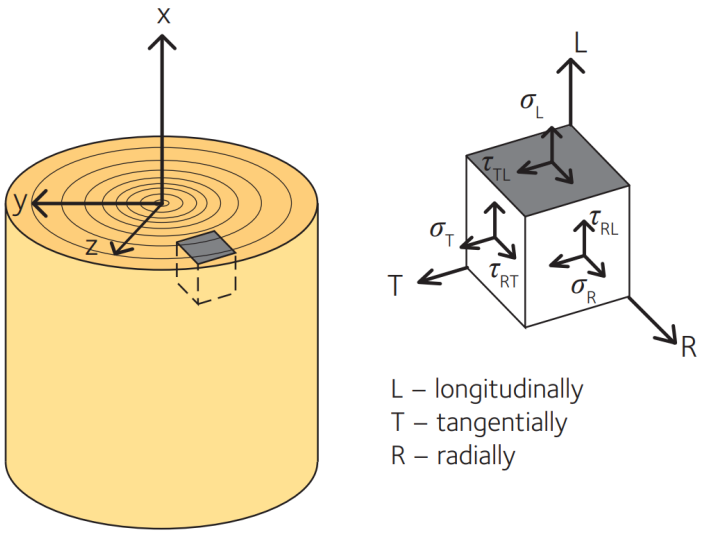

Figure 2.1: *Definition of stress components and their orientation in wood. Shear stress as τ and normal stress as σ [Swedish Wood, 2022a]*

In timber design codes and contexts, the longitudinal direction in figure 2.1 are also referred to as the *parallel to grain direction*, while the tangential and radial are equivalent with the *perpendicular to grain direction*.

2.1.2 Material properties variations

As wood and timber has variations in its material properties that are of interest in design of timber structures, different distribution functions based on real material test data are used for standardising values.

The distribution functions are implemented to deal with the uncertainty and typically material properties such as characteristic values and mean values are defined

and applied for design practices. The characteristic value of a material properties are some of the basic concepts for structural design according to *Eurocode 1* [CEN, 2002] , usually as the lower 5% percentile of the normal distribution. Figure 2.2 shows an example of material properties distributions, the modulus of elasticity parallel to the grain for glulam material class GL30c.

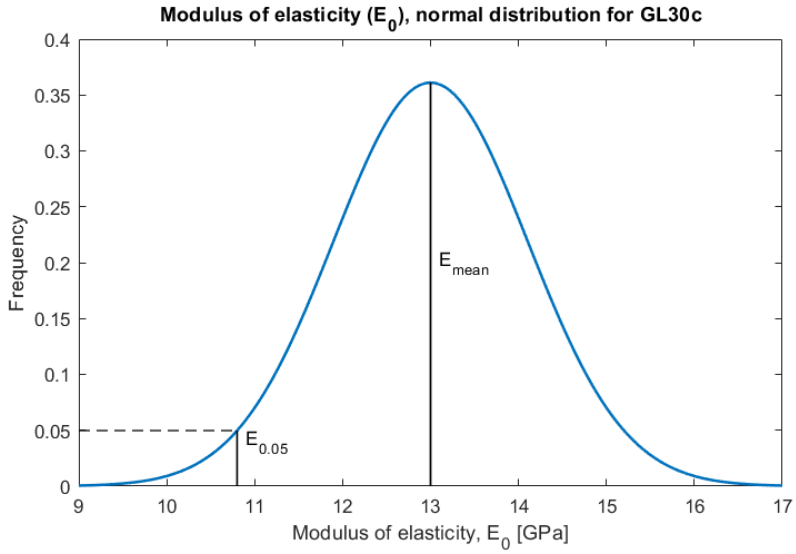

Figure 2.2: *Normal distribution for modulus of elasticity parallel to the grain for GL30c*

The variation of material properties of timber follows different distributions for other different parameters like density, strength in different directions as well as the stiffness. As the characteristic strengths are used in design of timber structures, there can be 5 % probability that the actual strength of a member is lower than assumed. However this risk is further minimized by using safety factors for the strength as well as design load combination factors that add margin to the expected loads that act on the structure. For design situations when the stiffness are evaluated, as in [Swedish Wood, 2022b] the average values are typically applied for analysing deflections.

2.1.3 Glulam

Glued-laminated timber or Glulam is one of so-called engineered wood products. As presented by [Swedish Wood, 2022a] glulam consists of planed laminates of structural timber glued together. the number and size of laminates can vary according to the desired cross-section dimensions in structural timber. However, all the lumbers are sawed and glued at the same fibre direction, parallel with the length of the member.

The capacity of a glulam structure is determined by the mechanical properties of the included lumbers. The Glulam produced in Sweden can be assorted by the class code GLXXYs. Further explained by [Swedish Wood, 2022a] XX stands for the bending

capacity and can be between 22 or 32. Y stands for homogeneous (h) or combined (c) where combined refers to a cross-section with higher capacity laminates at the top and bottom (where the maximum tensile and compressive stresses take place). s, if inserted, indicates to that the structure is split and has lower strength than the ordinary.

The glulam strength class is not only determined by the wood's properties, but also by the defects in the wood. [Harte, 2001] among others identify the most crucial wood defect as knots, where the area and location of knots in a member has an important role in its strength reduction. [Swedish Wood, 2022a] visualizes and explains that when comparing two members with same dimension with origin from the same wood, one is entirely sawed as one member and the other is of glued laminates, the latter displays higher mean strength and less variations of the material properties. This relies on that occurance of knots in glulam are more distributed along and across the timber member, which minimizes the probability of one big knot existing in a critical location and this utilizes the material more effectively. Figure 2.3 visualizes the frequency and difference of distribution of strength of glulam and sawn timber for different specimens.

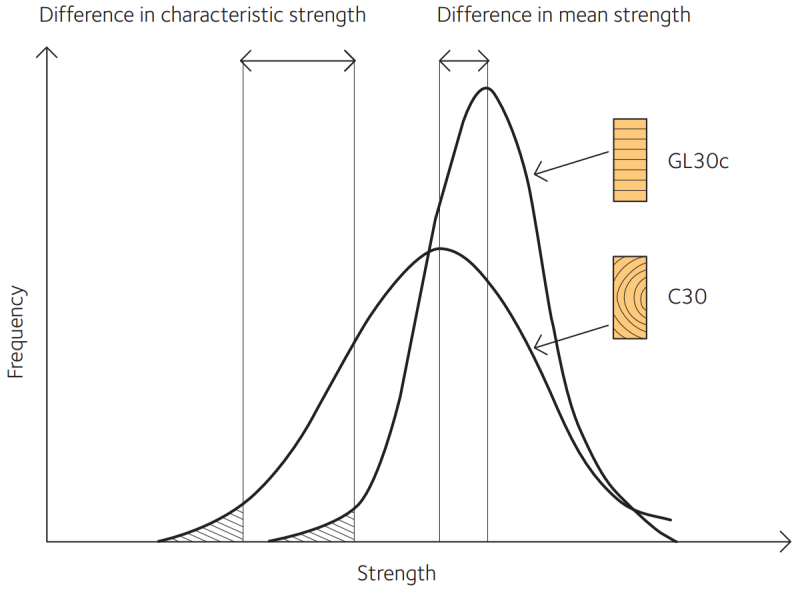

Figure 2.3: *Curves based on functions for strength distribution, glulam GL30c and timber C30 [Swedish Wood, 2022a]*

Beside a high strength-to-weight ratio, glulam has several more advantages. The feature of finger joints enable producing large-scale structures with long spans. Glulam also allows for large variability of different shapes for structural members that can be used in construction. The glulam members could be aesthetically appealing in structures and are often apparent in a buildings.

2.2 Timber structural systems

In this section, some structural systems of timber that are suitable for larger buildings will be reviewed. According to [Göts et al., 1989] one can fundamentally categorize structural systems made of timber for buildings into open structures and closed structures. Open structures, often carried out as different types of frame structures, separates the load carrying function and stabilising function from other functions such as the weather protection, thermal protection and finishes. In closed structures the walls contributing to these other functions can also be the main load carrying elements. Examples of closed structures are buildings made with massive cross laminated timber walls, log houses or different type of wall structures composed with wood based panels.

[Kaufmann et al., 2018] states that timber construction has made a leap thanks to several new technical developments since the shift to the 21st century. This combined with the potential for wood as a renewable and sustainable building material has accelerated the focus and aim at building an increasing share of the taller multi-story buildings with timber.

2.2.1 Timber frames

Timber frames as structural systems for buildings have been used for centuries and the building techniques used today are the result of many years of development. [Göts et al., 1989] presents different ways of arranging the load bearing elements in frames and the hierarchy of which order beams and columns support one another. The type and amount of connections that are needed to stabilise and hold the structure together would differ for different types of frame systems.

Some benefits with frame systems are their flexibility for different designs and purposes, large open floor areas can be achieved within buildings, the possibility for prefabrication with quick construction process, and the possibility for future adaptation and repurposing for the buildings. [Swedish Wood, 2022b] highlights another aspect, that is the propagation of sound between floors and walls through flank transmission which occurs in a greater extent if walls are solid and load carrying.

The most material and cost efficient way of organising a multi story frame structure is to align the vertical load carrying elements. In this way vertical loads can take a straight path to the ground without inducing bending or shear in horizontal beams or slabs.

2.2.1.1 Distribution of moments in beams

The load distribution in frame structures is depending on the stiffness in its members and joints between members. These characteristic influence if the structures are more or less statically indeterminate or statically determined. For beams present in a frame structure [Caprio et al., 2022] presented a way to evaluate and graphically visualise the moment distribution in the mid span and end of a beam depending on the stiffness in its end supports. A stiffness ratio k_b can be defined according to equation 2.1.

$$k_b = \frac{K_{el} \cdot L}{E \cdot I} \tag{2.1}$$

- Where K_{el} is the stiffness at the supports in [Nm/rad]
- L is the beam length
- E is Young's modulus of the cross-section
- I is the area momentof inertia of the cross-section

For a timber beam, the ductility and stiffness of its connections might determine the moment redistribution between the support joints and the beam span. For simply supported beams, i.e. no stiff joints are interacting, the maximum moment is fully taken by the beam span $M_s = M_{max}$. For rigid joints, the support moment will be twice as big as the span moment, see figure 2.4. Between these two extreme cases, the moments distribute with relation to the stiffness ratio between mid span and end support according to equation 2.2 and 2.3 respectively.

$$M_f = \frac{1}{8} - \frac{K_{el} \cdot L}{24 \cdot EI + 12 \cdot K_{el} \cdot L} \cdot qL^2 \tag{2.2}$$

$$M_s = \frac{K_{el} \cdot L}{24 \cdot EI + 12 \cdot K_{el} \cdot L} \cdot qL^2 \tag{2.3}$$

In figure 2.4 the equations 2.2 and 2.3 for M_f and M_s are modified and plotted with the variation of k_b and in relation to M_{max}. Where M_{max} are calculated as:

$$M_{max} = \frac{q \cdot L^2}{8} \tag{2.4}$$

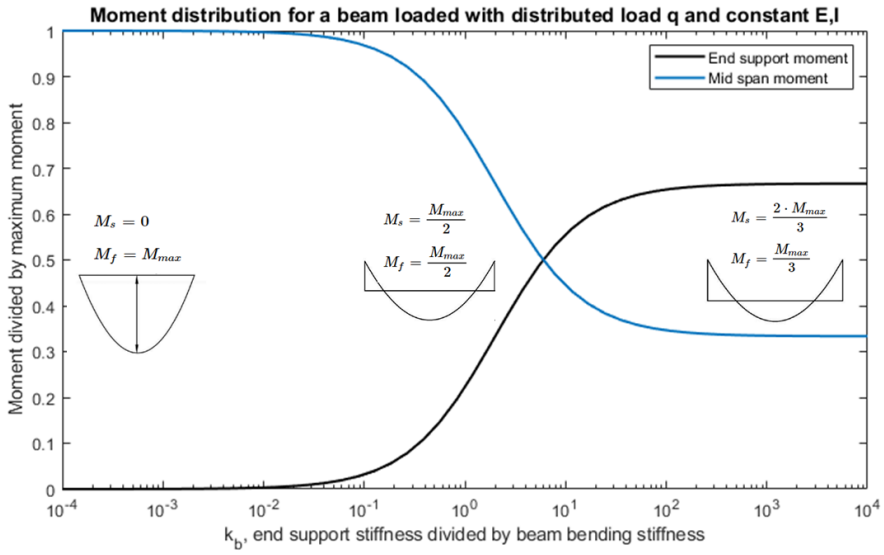

Figure 2.4: *Moment distribution between end support moment and mid span moment in a beam, where furthest to the left is the case of simply supported and furthest to the right the beam is fully fixed*

The most optimal beam joint could be the one that minimizes the demand of high moment capacity either in end support or mid span. This is the case where a perfect interplay between joints and beam occurs and the moments are distributed equally.

In figure 2.5 an example of the effect of stiffness in timber frame connections are presented. The results from analysis of static model of three identical timber frames in RFEM Dlubal are visualized. The frames have different rotational stiffness in connections between beams and columns. One case with pinned, one case with fully rigid, one case with semi-rigid of 15 MNm/rad and the magnitude of the bending moment on each case are plotted.

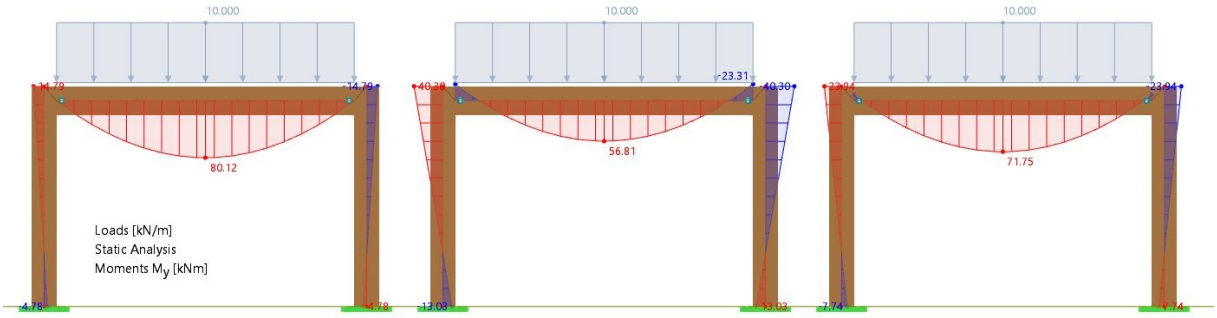

Figure 2.5: *Three identical frames of GL30c with cross section 430x630mm for columns and 430x720mm for beams modeled in RFEM Dlubal, showing moment distribution. First frame from left have pinned connections, second frame have moment rigid connections and the third frame have semi rigid-moment connection of 15 MNm/rad*

2.2.1.2 Girder on column system

With this concept for a strucutral system, columns are not continuous, but are instead one story high and longitudinal continuous girders rest at the top of the columns. For every next story new columns are placed on top of the girders and the pattern continues in this manner. Floor structures like slabs or joists are carried between, supported with connections, or on top of the continuous girders. [Göts et al., 1989] and [Swedish Wood, 2016] gives examples for these supporting connections and they can typically be joist hangers, beam hangers with hinge, slotted in T-steel plates with screws or dowels, pairs of inclined screws penetrating both the main beams and the secondary beams in the end grain, and also ridge attachments when joist rest on top of the primary girders. Some of these type of connections are presented in figure 2.10

Since the continuous girders strength in compression perpendicular to the grain would not be enough to support the load from the stories above transferred through the columns, [Göts et al., 1989] writes that timber or metal connections like gussets or penetrating reinforcement in the girders are needed for transferring loads to the column below without overloading the girders in compression.

Benefits with this type of structure is that the continuous girders supporting floor structures allows higher material utilization since bending moment is not concentrated at the spans as for simply supported beams. Because of this stresses and deflections are reduced and the spans between columns can be made longer with the same beam cross-section. The dynamic vibration response of the floors will also be improved with this layout. Another advantage is that cantilever easily can continue to support balconies or other structures without using additional connections. figure 2.6 shows the concept for this structural system.

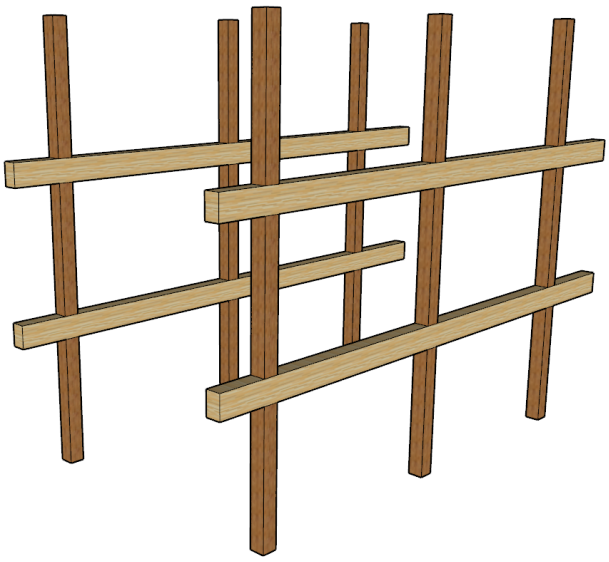

Figure 2.6: *Conceptual sketch of continuous girder frame system*

2.2.1.3 Tie beam system

For this system columns are continuous and the beams supporting floors are fitted in between columns and connected to them. [Swedish Wood, 2016] suggests that the columns could be prefabricated as continuous elements to reach the full height of the building. Advantages with continuous columns for multi story buildings is the horizontal stiffness and redundancy since there are fewer joints interrupting the stiffness and load paths that transfer shear and bending between stories. However, [Göts et al., 1989] writes that this type of system requires a lot of high performance connections for every joint between beams and columns. Building cantilevers that extends from columns is also not as convenient as for the continuous girder system.

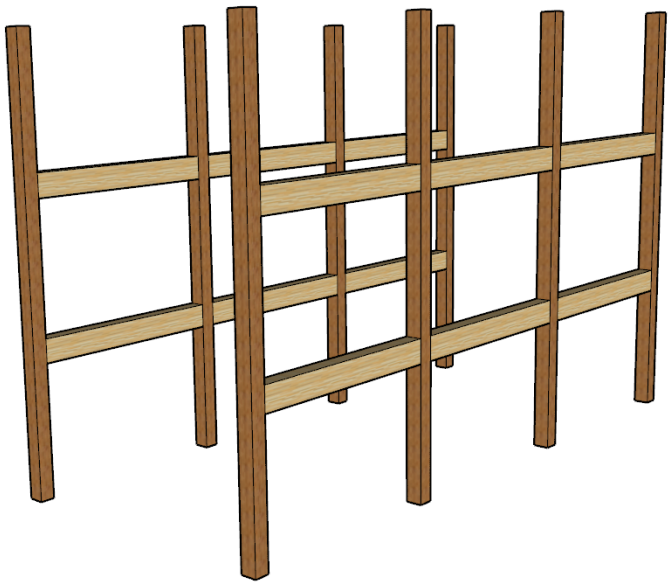

Figure 2.7: *Conceptual sketch of tie beam system*

The connections that support beams at each storey could be designed more or less moment rigid. More moment rigid connections would not only transfer vertical loads from the storeys but also transfer moments from the beam spans to the columns. At the same time, moment rigid frames in the building would also convert horizontal loads on the building to moments in the frame structures, possibly relieve the load level taken by bracing systems. As stiffness attracts loads in structures, in such a case, there will be interaction between forces in bracing components and connections depending on their different stiffness. Figure 2.8 illustrates a principal planar behaviour of two systems, one with pinned connections and the other one with moment rigid connections. It can be seen how the structure with moment rigid connection acts as a whole system avoiding extreme local deformations, unlike the structure with pinned connections.

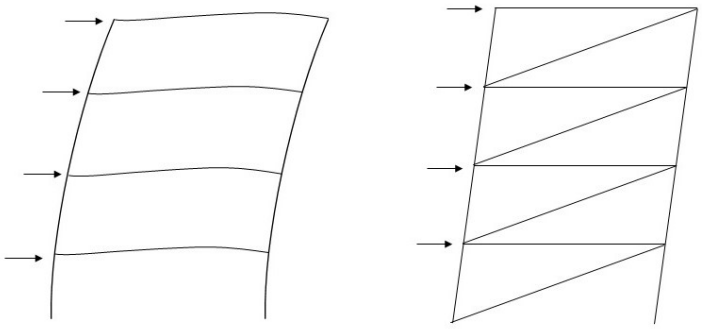

Figure 2.8: *Principal sketch of frame action under horizontal loads with moment rigid connections at beams and columns (right), and a braced frame with pinned connections (left)*

2.2.1.4 Twin girder system

In a twin girder system the horizontal beams are split and mounted on each side of the columns so that both columns and beams are continuous. In this manner a stiff and efficient frame system can be created. [Göts et al., 1989] enlightens that since the girders are connected on the sides of the columns laterally loaded connection can be designed quite easily, mainly to carry shear forces. The floor structure rest on top of the girders. It could be necessary with extension of the ends of the girders at the outer columns in order to allow for sufficient spacing between the and grain and connection.

2.2.1.5 Split column system

The split columns means that twin pair of columns are used on each side on a continuous girder. This system also allows for using both continuous beams and columns like the twin girder system design and laterally loaded connections between columns and beams can quite easily be carried out. However [Göts et al., 1989] writes that one drawback with this layout is that the columns are weaker and more prone to buckling since their cross section is reduced.

2.2.1.6 Bracing

[Swedish Wood, 2022a] present important aspects about horizontally stability of structures. To ensure horizontal stability of frame structures where the frame is not moment rigid enough for horizontal loads, some kind of bracing elements are needed for transferring horizontal forces to the ground. Other important functions that bracing systems should ensure are to limit horizontal deformation and to increase load carrying capacity by preventing instability like buckling and tilting.

The bracing structure could be diagonal truss element that act in tension, compression or both, that are installed in the frames. These could for instance be solid timber trusses or slender steel bars that only act in tension. Other ways of stabilizing structures for vertical planes could be with shear walls such as panel walls or

massive cross laminated timber walls.

Bracing also has to act in horizontal planes of the structures, in floors and roofs. For these actions trusses and stays can act within the floor and roof structure. If floors are made of slabs these forces could be carried as shear in the plane of the slabs.

2.3 Connections

Described by [Dorn and Bader, 2016], timber connection is the concept that implies how one or more timber elements are assembled to transfer forces between the respective structural parts. The complexity varies for different connections, one connection can for instance be very simple and only include two timber members, like in figure 2.9 where two timber beams are connected to only act in compression.

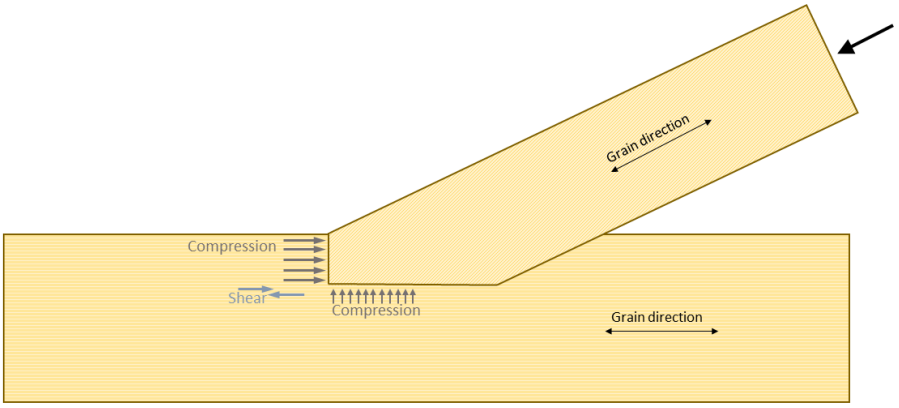

Figure 2.9: *Conceptual figure of a timber connection with induced forces when loaded in compression, without any connector or fastener*

A connection could also be created by a composition of attached connectors and fasteners that transfer forces between, into or from timber elements. A timber connector could be seen as a structural element that transfer forces between timber elements, and fasteners are used for transferring forces between timber and connectors or directly to another timber member.

Connectors and fasteners should be able to transfer all the forces that the connected members are designed to withstand. Fasteners can be laterally or axially loaded, withstanding shear, bending and withdrawal forces. According to [Porteous and Kermani, 2013] nails are one of the most common type of fastener in timber construction, and are usually more suitable for structures with lighter loads. When the withdrawal capacity is of higher importance and higher strength are required [Porteous and Kermani, 2013] writes that screws would be the more appropriate option. Dowels and bolts are suitable for higher loads when neither screws or nails provide sufficient capacity. [Porteous and Kermani, 2013] also explains that bolts could act both in axial loading and lateral loading while dowels which have a smooth cylindrical shape only provide strength for lateral loads.

Nowadays, the market of timber connectors is enriched with plenty of modern products and solutions for a lot of different joints. In figure 2.10, examples of common connectors and some situations for their field of use are displayed. The table includes conceptual steel-to-timber type of joints, The forces they are designed to transfer and their application field.

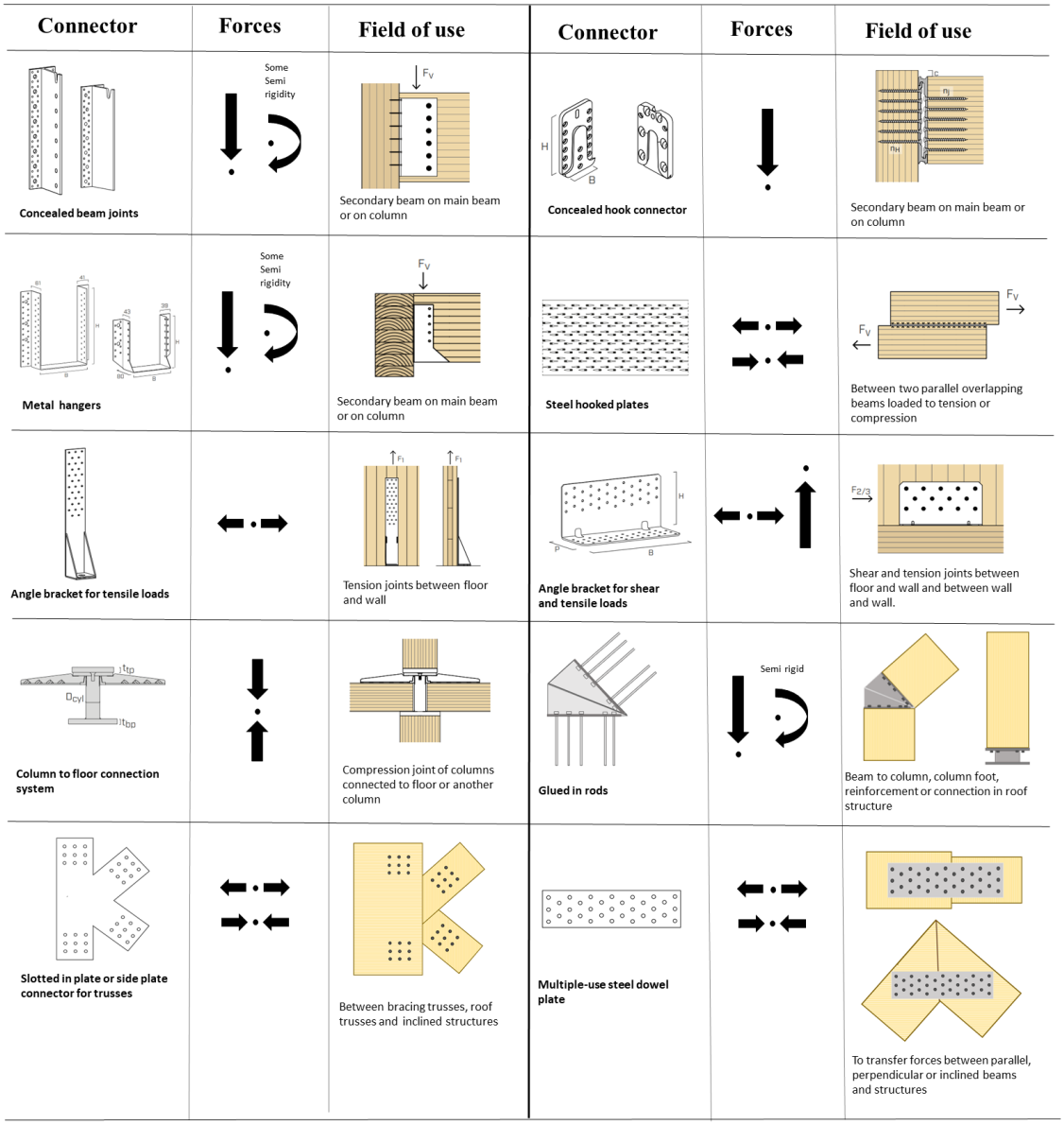

Figure 2.10: *Examples of different types of connectors with the forces they transfer and their field of use. The arrows pointing towards each other is a symbol for compression. The arrows pointing away from each other is a symbol for tension. The rotated and vertical arrows is a symbol for moment and shear force respectively. Some images are from [Rothoblaas, 2019]*

The suitability of different types of connections is influenced by the the angle between the members to be connected, the actions and forces to be transferred, as well as the orientation of the fiber direction of the members relative to one another. For parallel members as in figure 2.11, the connection transfer the applied forces between the members by the overlapping shear plane. The members in figure 2.11 could also transfer some moment, and with increasing load unless brittle failure the connections would eventually act like a plastic hinge.

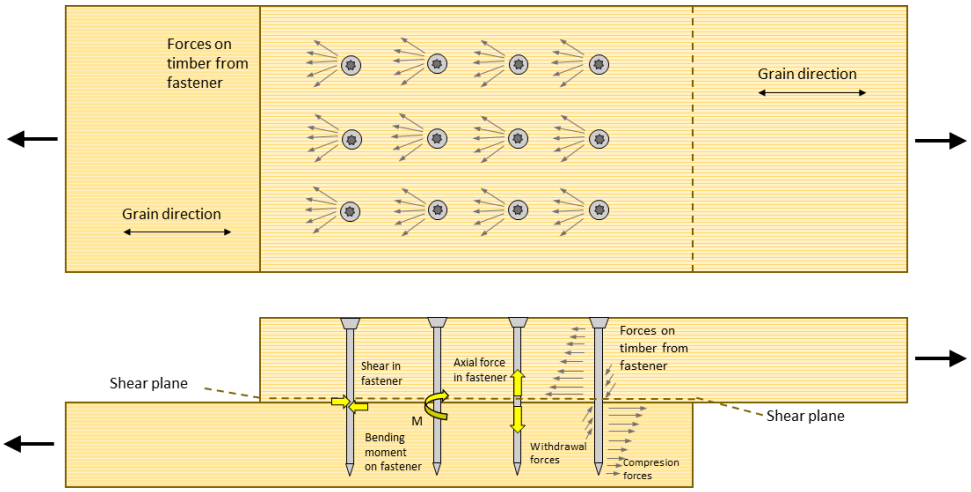

Figure 2.11: *Conceptual figure of a timber to timber connection loaded in tension parallel to the grain and what forces that then can be induced in the embedding timber and in the fasteners*

[Gečys and Daniūnas, 2017] claims that most timber connections could be considered more or less semi-rigid and the design choices of the connection will highly influence this semi rigidity and the relation between the moment that the connection resist with some rotation in the joint. Figure 2.12 shows a conceptual way of connecting two perpendicular components, in this case a beam to column, and what reaction forces that can be induced in the embedding timber near the fasteners. The beam is loaded with shear forces and bending moment and the forces are transferred to the column through the connector and fasteners as displayed in the figure.

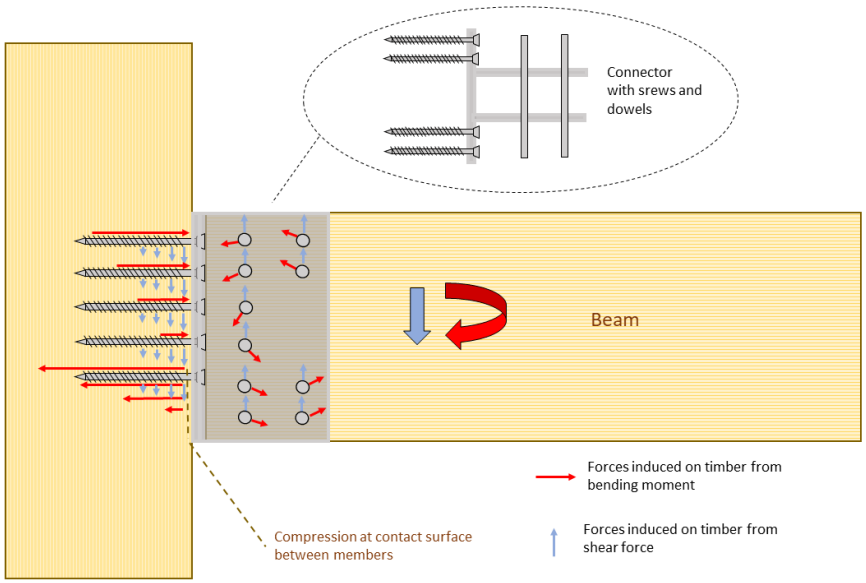

Figure 2.12: *Conceptual figure of a semi rigid beam to column connection loaded with shear and moment and what forces that then can be induced in the embedding timber and in the fasteners*

Connectors like cover plates, as the one illustrated in figure 2.12, or slotted in plates are subjected to a lot of different forces and complicated stress patterns which would vary depending on the type of forces it transfers. The metal of connectors should be ductile and these could typically be manufactured in steel of different grades or aluminium alloys.

Explained by [Geiser et al., 2022], the design of connector plates thickness and material properties are important for avoiding "the notch effect" which might damage fasteners and in worst case cause cut of. Therefore it's recommended that the strength of connector plates are lower than the fasteners with a specified margin. [Geiser et al., 2022] writes that besides providing strength, the fasteners play the most important role for providing ductility to connections in terms of developing plastic hinges. The thickness of fasteners as well as the mechanical properties of the material of fasteners are two decisive aspects for appropriate design.

2.4 Guidelines and standards for design of timber connections

In this chapter contents from different standards, guidelines and studies regarding structural aspects about timber connections are reviewed. Some aspects treated in the European standard; Eurocode 5 and the Swiss standard SIA265 are mainly refereed to and compared. A state of the art report for design of timber connections by the *European Cooperation In Science And Technology* are also referred to as [Sandhaas et al., 2018].

2.4.1 Eurocode

Eurocode 1 (EN 1990) prescribes the *Basis of structural design*, which contains guidelines of safety, serviceability and durability of structures. one of the basic requirements in Eurocode is:
(2.1 (2)) "A structure shall be designed to have adequate:
- structural resistance,
- serviceability, and
- durability."
And it continues with the rule:
(2.1 (6)) "The basic requirements should be met (inter alia) by appropriate design and detailing".
Therefore, in order to fulfill the design principles of the timber structures, detailing (connections) needs to be properly designed.

In Eurocode 5 (EN 1995-1-1) for *Design of timber structures*, It is prescribed how to design several types of timber joints. This standard includes guidelines for calculating capacities of different types of fasteners loaded in different directions with respect to grain directions, what diameters and spacing of fasteners should be selected and how material properties of wood are considered. Several types of failure modes of laterally loaded fasteners are covered by the standard and some consideration for multiple fastener joints are presented. For analysing stiffness in the serviceability limit state and ultimate limit state of connections the codes are limited. The main feature that are provided for this purpose is the slip modulus for planar shear action on fastener to timber at connections.

2.4.2 Swiss Standard

The Swiss standard in its edition SIA 265:2003 [Schweizer Norm, 2003] for *Timber structures* provides design codes that in general are similar to the Eurocode 5 but in some cases could become subject for comparison or complement. The requirements in SIA 265 as Eurocode 5, also guide the design of timber connection in term of timber thickness, fastener diameters and distances between fasteners in different load-to-grain directions.

Bellow are some important aspects regarding timber connection design stated in SIA 265:

- The total structural capacity of connections usually deviates and is smaller than the sum of the capacity of each fastener in a connection.

- When verifying capacity of a connection the general stresses in the surrounding timber regions should be checked against failure in the timber. Reduction of the timber cross-section may be considered and and SIA 265 specifies that tension perpendicular to the fiber direction that can be induced in different situations should be noticed.

- Eccentricities that induce additional loads within the connection should be identified and dealt with.

- The load distribution and magnitude of load acting at different fasteners in connections are proportional to the stiffness of each fastener.

As Eurocde 5, SIA 265 emphasizes the influence of the number of fasteners on the connection capacity. The design resistance values should be calculated considering groups of fasteners or fasteners in a row in case of laterally or axially loading which can reduce the strength of connections. SIA 265 defines a simplified calculation for ductility factor of a connection and generally prescribes the type of connection to be associated to different ductility classes.

2.4.3 Failure modes

2.4.3.1 Laterally loaded steel-to-timber connections

In in Eurocode 5, some of the failure modes of laterally loaded connections are defined. The decisive failure of a connections depends on the thickness of the metallic plate, the thickness of the timber member, the diameter of the fastener and the number of shear planes. Furthermore, the capacity of the connection is determined by the the embedment strength of the timber member, the yield and the withdrawal strength of the fastener. However, the definitions in Eurocode 5 assume that the metallic plate is designed to be stiff enough to withstand any failure, see figure 2.13.

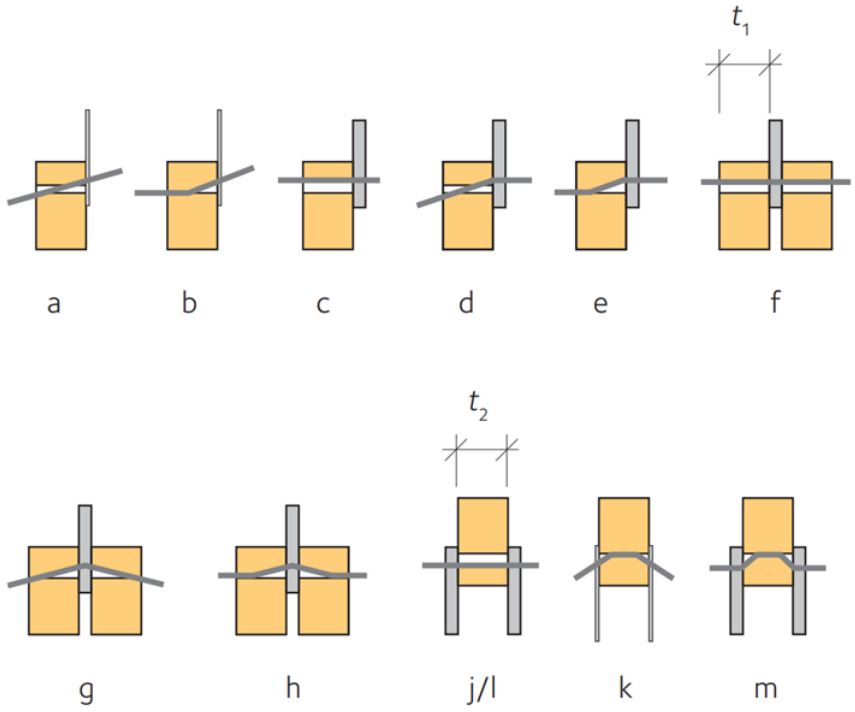

Figure 2.13: *European yield model failure modes for steel-to-timber doweled connections [Swedish Wood, 2022b]*

Eurocode 5 presents equations to calculate the capacity of one fastener in a connection as shown in Appendix A.5. The failure mode among the modes presented in EC5 that shows the smallest fastener load-carrying capacity is the decisive one. However, there are no equations proposed in order to calculate the total capacity of a multiple fastener connection other than using reduction factors for groups of fasteners.

2.4.3.2 Brittle failure

[Porteous and Kermani, 2013] states that equations for calculating capacities for the failure modes in 2.13 are valid if brittle failure can be excluded. When loading a timber connection timber can develop brittle failures before reaching the yield capacity of the connection, for instance, splitting, row shear, block shear and net tension failure as shown in figure 2.14. Eurocode 5 provides requirements as for instances fastener spacing and distances to edges for fasteners that are recommended for avoiding brittle failure at the connection. [Geiser et al., 2022] refers to an aspect that are one basis for recommendations in Eurocode 5 for avoiding splitting. This is how to organise groups of fasteners to avoid restraint forces from shrinking that can cause splitting. For this it is recommended that fasteners are placed not to far from one another as well as using few fasteners or allowing the wood to move. However according to [Sandhaas et al., 2018] Eurocode 5 lack equations for calculating loads that generate capacities for brittle failure modes and only methods for the ductile

capacity behaviour of timber connections are presented.

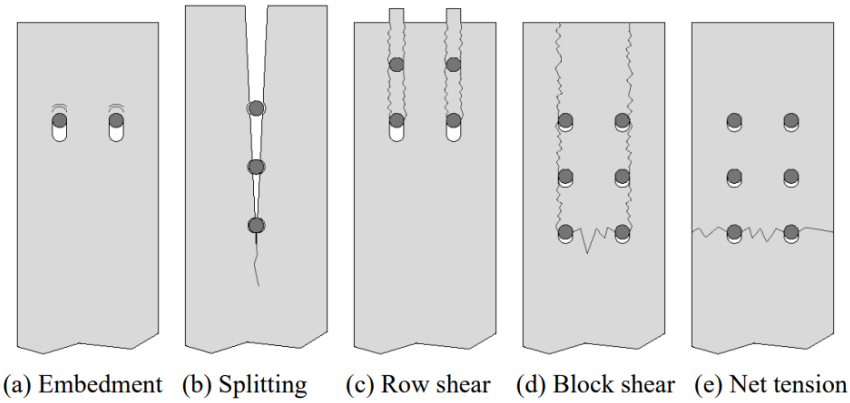

Figure 2.14: *Brittle failure modes in a dowel-type timber connection, image from [Sandhaas et al., 2018]*

[Sandhaas et al., 2018] presents some guidelines to calculate the timber strength against brittle failures in connections, inter alia, *the New Zealand draft.* Figure 2.15 shows an illustration of steel-to-timber connection with denotation of the geometrical parameters that are used in the proposed expressions by [Sandhaas et al., 2018]

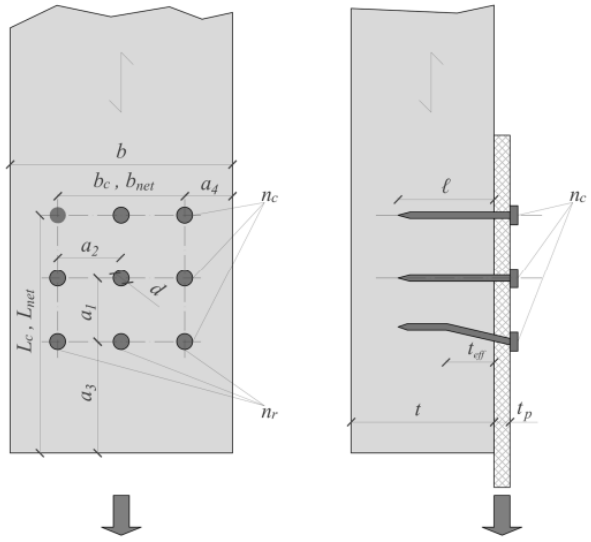

Figure 2.15: *Denotation of geometrical parameters used in this chapter, image from [Sandhaas et al., 2018]*

The row-shear capacity according to the New Zealand standard draft is given by equation 2.5.

$$F_{row,Rd} = \phi_w \cdot RS_i \cdot n_r \cdot k_1 \cdot k_{12} \tag{2.5}$$

Where RS_i is the characteristic row shear strength and is given by:
$RS_i = 0.75 \cdot f_{v,k} \cdot K_{LS} \cdot n_c \cdot 2 \cdot a_{cri} \cdot h$

- ϕ and k - are code calibration parameters
- a_{cri} - the smallest of a1 and a3
- $f_{v,k}$ - the characteristic shear strength of a row
- K_{LS} - the loading surface factor, equals 1.00 for inner members, and 0.65 for outer members

The block-shear capacity according to the New Zealand standard draft is given by equation 2.6.

$$F_{block,Rd} = \phi_w \cdot (RS_i + 1.25 \cdot f_{t,0,k} \cdot A_{GT-net}) \cdot k_1 \cdot k_{12} \tag{2.6}$$

- RS_i - the characteristic row shear strength along two shear planes of the outer row of the connection
- A_{GT-net} - net tension area between the two outer rows

The net tensile capacity according to the New Zealand standard draft is given by equation 2.7.

$$F_{net,Rd} = \phi_w \cdot R_t \cdot k_1 \cdot k_{12} = \phi_w \cdot f_{t,0,k} \cdot A_n \cdot k_1 \cdot k_{12} \tag{2.7}$$

- R_t - the head tensile plane
- A_n - the net cross-sectional area

2.4.3.3 Splitting

Splitting failure in parallel-to-grain direction is not included neither in EC5 nor New Zealand draft. [Hanhijärvi and Kevarinmäki, 2008] propose experimental-based expressions to calculate splitting of double and mulit-shear plane timber connections. The splitting may occur only in the outer part of the member, it might generate at the end of the timber or in the hole closest to the end of the timber. The calculating model posited by [Hanhijärvi and Kevarinmäki, 2008] considers the possible combination of the different failure modes at different parts, where the determinant capacity is the smallest one.

Splitting capacity of a connection can be calculated in the hole and at the end of the member according to equation 2.8 and 2.9 respectively.

$$F_{spl,hole,Rd} = \frac{k_{90,cnctr} \cdot n_{ef} \cdot 10 \cdot f_{t,90,k} \cdot t_{ef} \cdot a_3}{s_{t90,hole}} \tag{2.8}$$

$$F_{spl,end,Rd} = \frac{k_{90,cnctr} \cdot n_{ef} \cdot 10 \cdot f_{t,90,k} \cdot t_{ef} \cdot a_3}{s_{t90,end}} \tag{2.9}$$

- $k_{90,cnctr}$ - a stress concentration factor equal to 0.7

- n_{ef} - the effective number of fasteners equal to $n^{0.9}$
- $f_{t,90,k}$ - the perpendicular-to-grain tensile strength
- t - the thickness of the specimen

$s_{t90,hole}$ and $s_{t90,end}$ is the ratio between the maximum and average perpendicular-to-grain stress and is calculated by equation 2.10 and 2.11 for the hole and end stress respectively.

$$s_{t90,hole} = max(1, 0.65 \cdot \frac{a_3}{a_4}) \tag{2.10}$$

$$s_{t90,end} = \frac{2.7}{cosh(\frac{a_3}{a_4} - 1.4)} \tag{2.11}$$

Furthermore, in order to obtain more accurate calculations, it was noticed from the experiments that the elastic bending of the dowel has an impact on the connection capacity. Therefore, the dowel deformation is taken into account by reducing the timber member thickness according to equation 2.12.

$$t_{ef} = t \cdot min(1, \frac{d}{0.6 \cdot d_{gr}}) \tag{2.12}$$

where $d_{gr,1} = 2.45 \cdot \sqrt{\frac{f_{h,m}}{f_{y,m}}} \cdot t$

- d_{gr} - factor of a dowel rigidity
- $f_{h,m}$ - the mean embedment strength equal to $1.5 f_{h,0,k}$
- $f_{y,m}$ - the mean yield strength of the dowel

2.4.4 Deformations and Non-linear behaviour of timber connections

It is by [Sandhaas et al., 2018] explained that deformations of a connection between timber members results from the combination of non elastic and elastic deformations in the timber and steel. Connections with higher ductility rather then brittle behaviour are prone to develop more non-linear like deformations. The intermediate part of the load deformation relation curves of connections could be expected to approximately show linear relation, while at low loads, there could be an initial slip at the connections. For high loads relative to the strength of the connection, plasticity develops unless brittle failure. The stiffness of the connection in serviceability state is usually linked to, or mentioned as the linear elastic range of the deformation. Figure 2.16 shows the concepts of plastic deformation of laterally loaded fastener joints.

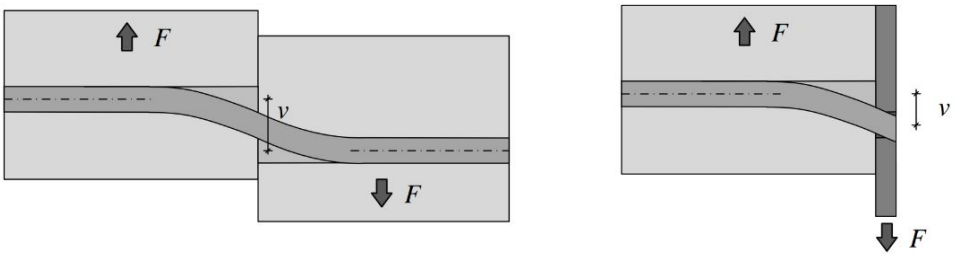

Figure 2.16: *Plastic deformations in a timber to timber joint and in a timber to steel joint by [Sandhaas et al., 2018]*

The non-linearity in timber connection is explained by [Dorn and Bader, 2016] to be embodied in three stages of plastic deformation before failure is obtained; embedment of timber, yielding of a single fastener and yielding of the whole connection. The embedment strength of timber depends on the wood properties at the surrounding surface to the fastener. Then, the load-carrying capacity of a single fastener relies on the material properties and slenderness of the fastener. The response of a multi-fastener connector is majorly affected by the load combination at the connection. Nevertheless, the load-to-grain direction has a significant impact which increases with larger stresses.

In general SIA265 states that nonlinear material relationships can be assumed for structural timber members that could react with plastic strains, but since timber has brittle failure in tension, non linear material behaviour should only be utilized in zones exposed to compression.

2.4.5 Ductility

Ductility has several different definitions in structural engineering, but it is generally defined as the opposite of brittleness. A material is ductile means that it develops relatively large deformations when loading and before reaching its load-capacity limit. Ductility can be utilized as an alert to potential failure and therefore it's an important aspect to design for in structural components.

In timber structures, the joints play a critical role in the structure's stiffness, load-carrying capacity and ductility which is explained by [Ottenhaus et al., 2021]. Due to the timber's linear and brittle behaviour, the metallic connections are the only residual ductile elements of the structure to act as plastic hinges in case of overloading, which are usually called as "potential" ductile elements (PDE).

Under the loading of a timber connection, timber and steel behave differently. In order to obtain ductility, the fasteners should be modelled with a lower capacity than the timber member. This allows the metallic fasteners to progressively start yielding before timber reaching its capacity and compose brittle damages. Since plasticity develops progressively in a connection, the yielding point will be approximately derived. [Ottenhaus et al., 2021] discuss some methods to calculate ductility in connections. Although, the authors emphasize that the analyses are still distinctive for

each case and too complicated to simplify into general designing standardization.

However, the Swiss structural code, SIA 265 (2003) recommends to calculate the ductility factor D_s of a connection according to the relative, deformation-based definitions:

$$D_s = \frac{w_u}{w_y} \tag{2.13}$$

Where it defines: *(6.1.2.2) The required ductility factor of the connection is a function of the desired structural behaviour and exploitation of plastic force redistributions in the system.*

w_u and w_y are defined in the connection load deformation curve in figure 2.17 where also K_{ser} of the connection would become:

$$K_{ser} = \frac{F_y}{w_y} \tag{2.14}$$

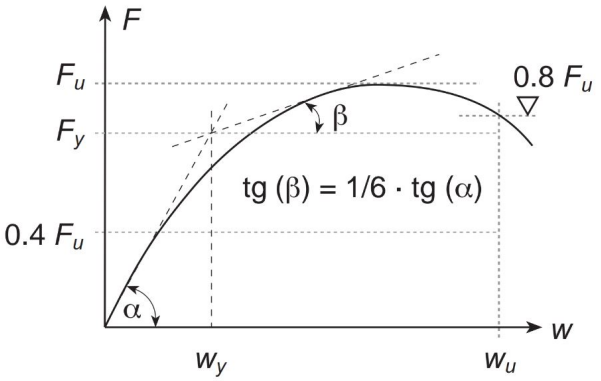

Figure 2.17: *Definition of connection ductility and stiffness by SIA265 (2003)*

SIA 265 (2003) classifies the structures depending on its ductile behaviour from A (negligible) to D (high ductility). In addition, some requirements for dowel-type fasteners to be design in class B, C or D are prescribed.

Eurocode 8 (EN 1998-1) is generated for *Design of structures for earthquake resistance*. Eurocode 8 assorts timber structures in low, medium and high ductility classes. This classes represents the structure's energy dissipation capacity under seismic actions depending on its type of connection. It provides detailing rules and upper limit factors for designing timber connections with ductile behaviour. However, in Sweden, no seismic loads are considered in the structural design. Although ductility is needed for further types of loading along the structure's service life, Eurocode is still lacking rules or recommendations considering these loads.

2.4.6 Stiffness of fasteners in timber

2.4.6.1 Stiffness of laterally loaded connections based on Eurocode 5

[Porteous and Kermani, 2013] explains that most timber connections shows semi rigid rotational behavior, which is in the range between $k = 0$ to $k = \infty$ where infinite stiffness means fully rigidity. The bending moment in a timber connection can be expressed as:

$$M = k\upsilon_r \tag{2.15}$$

- where υ_r is the rotation at the connector induced by its connected structural members.

For connections that can exhibit a proper ductile behaviour, [Porteous and Kermani, 2013] describes that Eurocode 5 permits that the effect of the stiffness in a connection can be utilized in structural analyses. When analysing the behaviour of connections in a structure different values for k should be considered based on the purpose with the analysis. In service state analysis k_{ser} can be used and in the ultimate limit state a reduced value k_u is adapted.

To calculate the rotational stiffness parameter $k_{ser}[Nm/rad]$ per shear plane for a connection, Eurocode 5 suggests a method where the stiffness of every individual connector contributes to the total stiffness.

$$k_{ser} = (\frac{K_{ser}}{(1 + k_{def})}) \cdot \sum_{i=1}^{n}(x_i^2 + y_i^2) \tag{2.16}$$

- K_{ser} is the slip modulus for an individual fastener per shear plane.
- k_{def} factor for deformation depending on material and moisture
- n is the total number of fasteners in the corresponding shear plane in the connection
- x_i and y_i coordinates for fastener i with respect to the shear center in the studied connection

In a similar manner the total stiffens in the vertical and horizontal stiffness for a connection, $K_{V,u}$ and $K_{H,u}$ can be calculated by knowing all individual fasteners slip modulus per shear plane and the number of fasteners. For a fastener connecting timber to timber the slip modulus K_{ser} given in $[N/mm]$ per shear plane can be calculated with the following expressions:

For screws, dowels and, bolts without or with clearance, and nails with pre-drilling:

$$\rho_m^{1.5} \cdot d \div 23 \tag{2.17}$$

For nails without predrilling K_{ser} becomes:

$$\rho_m^{1.5} \cdot d^{0.8} \div 30 \tag{2.18}$$

- ρ_m is the mean density of the timber or engineered wood product, embedding the fastener.

- d is the diameter of the fastener in $[mm]$.

Based on k_{ser} the following simplified approach is adopted to account for stiffness in the Ultimate limit state:

$$K_u = \frac{2}{3} \cdot K_{ser} \tag{2.19}$$

The stiffness modulus K_{ser} can according to Eurocode 5 be assumed and analysed for loading with a load level up to 40% of the maximum load which the individual fastener can resist. [Porteous and Kermani, 2013] also write that the slip modulus can be assumed to behave linear elastically in this range up to 40% of the ultimate load.

The initial slip u_{inst} is the slip immediately induced by a load for the linear relationship K_{ser} can for an individual fastener be calculated accordingly:

$$u_{inst} = \frac{F}{K_{ser}} + c \tag{2.20}$$

- F is the load in $[N]$ acting on the fastener

- c is added if there are spacing around fasteners, typically 1 mm

The definition of K_{ser} and K_u based on load deformation curves are presented in figure 2.18

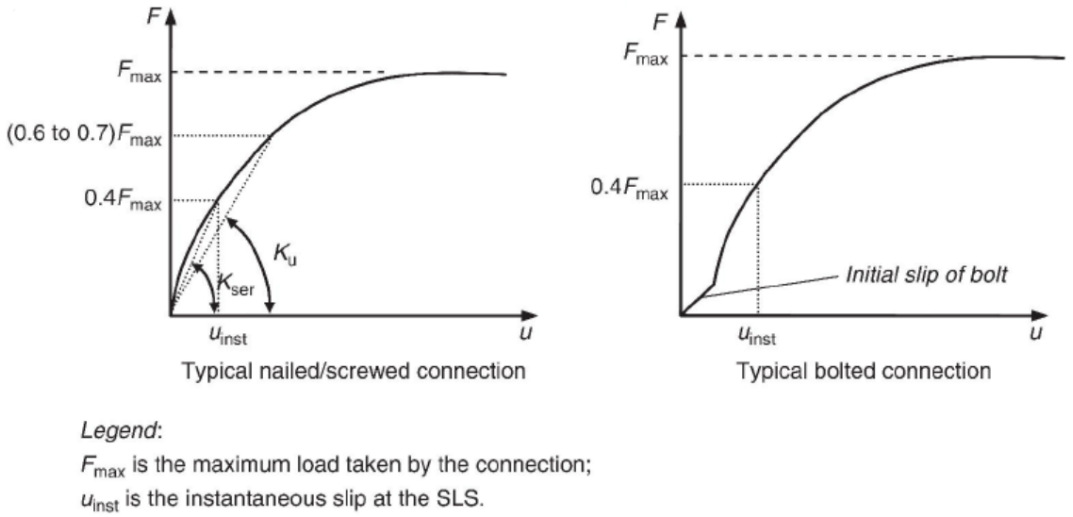

Figure 2.18: *Definition of K_{ser} and K_u according to Eurocode 5 in relation to the maximum load F_{max} [Porteous and Kermani, 2013]*

When one of the timber members in at the shear plane of the connection is replaced with a metal connector, theoretically half of the contribution to the slip of the fastener in the shear plane is eliminated. Hence K_{ser} would in such a case be multiplied with a factor 2. In metal to timber connection, there could however be gaps between fasteners and the metal plate, some part could yield and there might occur some rotation of the fastener. Because of this the slip modulus should be treated with caution when analysing sensitive structures and Eurocode 5 suggest some unspecified reduction instead of just using $2 \cdot K_{ser}$.

One way of utilizing known stiffness properties of connections in computer analysis of structural systems like frames is to model the connections between elements as elastic springs. The stiffness modulus could then be represented as linear elastic spring elements, representing stiffness in different degrees of freedom. According to [Porteous and Kermani, 2013] this is an applicable method to simulate semi-rigid connections with its expected rotation - moment relation. With the same principle one can also consider the stiffness in the axial and vertical directions at the joint.

2.4.6.2 Supplements to Eurocode 5 approaches

There is a consensus among researchers that methods to determine stiffness of timber connections in Eurocode 5 are to simplified. Calculations might sometimes not be as accurate and reliable. [Sandhaas et al., 2018] states that the Eurocode 5 model for analyticaly calculating stiffness of fasteners does not account for thickness of the timber and failure mode of fastener. There are other significant factors that in some cases effect the slip modulus for laterally loaded fasteners and some of these are reviewed here.

[Kuhlmann and Gauß, 2019] observed deviations between measured stiffness values for individual dowels and bolts and predicted values accordingly with Eurocode 5 and there are several suggested reasons for this. The initial stiffness from the tests at approximately 10% of the maximum load showed values of 1/3 of the stiffness that develops at reloading in the range between 10-40% of the maximum load. [Kuhlmann and Gauß, 2019] explains that at initial loading levels there are plastic deformations at the surfaces embedding the fasteners. This initial plasticity might contribute to cause the lower stiffness.

Reinforcement in connections and the direction of the load acting on fasteners also shows effect on the stiffness that develop. Tests of loading fasteners with tension perpendicular to the grain in the study by [Kuhlmann and Gauß, 2019] were performed with threaded screws as reinforcement, centred in the specimen and perpendicular to the fastener. This type of reinforcement at sensitive connections was recommended as an conclusion by the paper. For the action parallel to the grain tests were performed with and without reinforcement and the measured stiffness then showed 20% increase with the reinforcement. A comparison between the stiffness of the same type of fasteners for different orientation of the loading of the fastener with respect to the grain direction showed an impact for dowels but not so much for bolts.

In addition to the type of fastener [Kuhlmann and Gauß, 2019] furthermore states that the slenderness or stiffness of the fastener itself will impact the slip modulus of the fastener in the connection and might cause different results than the simplified approach in Eurocode 5. For joints that show sensitivity to the stiffness, they recommended that analytical calculations for determining k_{ser} in Eurocode 5 should be avoided when analysing internal forces at the connections.

[Jockwer et al., 2022] reviewed parameters that affect the stiffness and ductility of dowel type connections. Based on tests with fastener groups laterally loaded in tension, fastener diameter and several fasteners in a row was identified as the most influencing parameters for the slip modulus at a connection in serviceability limit state. One conclusion was that the the relationship between the fastener diameter and slip modulus may not be linear as suggested from the Eurocode 5 method. When elastic and plastic deformation occurs in and around fasteners the load- deformation behaviour deviates from a linear dependency of fastener diameter. However the stiffness could be expected to follow a linear relation with fastener diameter provided that the fastener are fully embedded in the timber.

[Dorn and Bader, 2016] also claim that the design guidelines for stiffness of fasteners supplied in Eurocode 5 are overly simplified and not sufficient. They specify that no stiffness values suitable that are for describing the deformations of fasteners at limit loads are provided.

2.4.6.3 Stiffness in laterally loaded connections according to the swiss standard SIA265

The swiss standard SIA265 [Schweizer Norm, 2003] provides a similar approach for considering stiffness in laterally loaded timber connections as Eurocode 5. The stiffness for connections and fasteners are also referred to as K_{ser} and K_u in the swiss standard. It is stated that the provided values for K_{ser} and K_u only should be assumed for strcuters in service class 1 and for short term loading.

For dowels, screws, bolts and nails with predrilled holes, in timber to timber connections, K_{ser} could be calculated with the following expressions:

for parallel actions, load to grain angle = 0°:

$$K_{ser} = 3 \cdot \rho_k^{0.5} \cdot d^{1.7} \tag{2.21}$$

for perpendicular actions, load to grain angle = 90°:

$$K_{ser} = 1.5 \cdot \rho_k^{0.5} \cdot d^{1.7} \tag{2.22}$$

As in Eurocode 5, K_{ser} of fasteners in metal to timber connections could be doubled from the timber to timber value. In SIA265 K_u is also calculated in an equal way as in Eurocode 5, see equation 2.19. It is in the standard suggest that the K_{ser} values for actions on fasteners in between parallel and perpendicular angels to the grain can be obtained by linear interpolation. Figure 2.19 presents a comparison of K_{ser}

from the Swiss standard and Eurocode 5, based on the same material but varying fastener diameters.

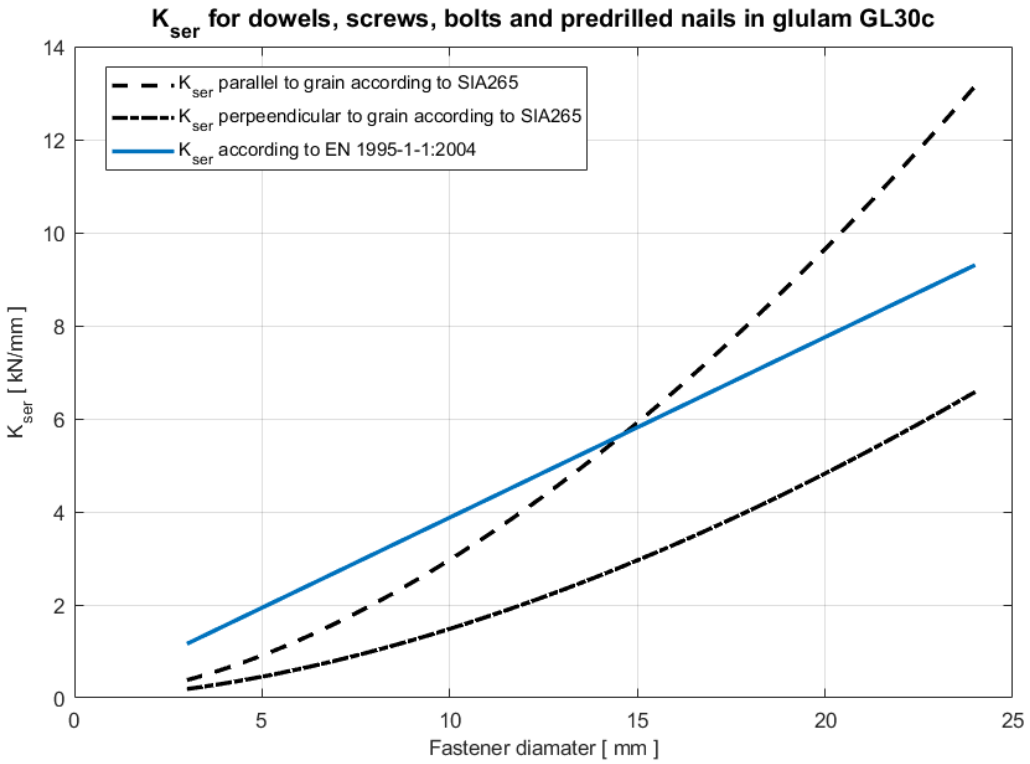

Figure 2.19: *Graphical comparison of K_{ser} from SIA265 and EN 1995-1-1:2004 in material GL30c, $\rho_k = 390kg/m^3$ and $\rho_{mean} = 430kg/m^3$. One shear plane with timber to timber connection*

In figure 2.19 it can be observed that Eurocode 5 might overestimate stiffness for fasteners smaller than 14 mm diameter, and might underestimate stiffness for larger fastener in some cases. Assuming that the stiffness is equal regardless load to grain angle might also give larger errors for fasteners with larger diameter.

2.4.6.4 Stiffness in laterally loaded connections according to the former german standard DIN 1052:2008

Presented by [Sandhaas et al., 2018], the former german standard DIN 1052:2008 defines the connection stiffness in the serviceability limit state very similar to Eurocode 5. For nails without predrilling equation 2.23.

$$K_{ser} = \rho_k^{1.5} \cdot d^{0.8} \div 25 \tag{2.23}$$

For connections with other types of fasteners such as bolts, dowels and nails with predrilling the stiffness is calculated as equation 2.24.

$$K_{ser} = \rho_k^{1.5} \cdot d \div 20 \tag{2.24}$$

- d is screw diameter
- ρ_k is the characteristic density of the timber or engineered wood product, embedding the fastener.

2.4.6.5 Withdrawal stiffness of screws

Eurocode 5 [Eurocode 5, 2004] provides equations for calculating withdrawal capacities for fasteners like nails and screws but are lacking equations for analytically determine withdrawal stiffness of fasteners. There are different research where some suggestions for calaculating whithdrawal stiffens for screws are provided. However equations presented below from literature show a rather wide spread of the calculated stiffness which is difficult to interpret. These analytical equations for calculating axial stiffness of screws are here noted as (I), (II), (III), (IV). It is noted by Eurocode 5 that the failuare modes of axially loaded screws occur for small deformations.

The axial withdrawal stiffness of screws was in a study by [Johanides et al., 2021] analytically calculated according to equation 2.25.

$$(I)K_{ser,ax} = 780 \cdot d^{0.2} \cdot l_{ef}^{0.7} \tag{2.25}$$

- d is nominal screw diameter [mm]
- l_{ef} is the length of the screw where threads are embedded in timber [mm]

[Tomasi et al., 2010] refers to an equation 2.26 provided by the German Institute of Building Technology for calculating withdrawal and penetration stiffness of axially loaded screws [N/mm]:

$$(II)K_{ser,ax} = 30 \cdot l_{ef} \cdot d \tag{2.26}$$

[Mirdad et al., 2022] studied stiffness and withdrawal behaviour of self tapping screws with different inclination in relation the the grain of the timber, and refereed to previous studies where the following equation (III) was adapted for axial load deformation of screws in laminated timber products. It is valid for screws with insertion angle perpendicular to the grain and give $K_{ser,ax}$ in [N/mm]. This equation also considers the density ρ of the timber product.

$$(III)K_{ser,ax} = 77.6 \cdot \rho^{0.75} \cdot d^{-0.7} \cdot l_{ef}^{0.4} \tag{2.27}$$

The study by [Mirdad et al., 2022] resulted in an purposed equation for calculating the stiffness per unit are in $[N/mm^3]$ for screws with arbitrary insertion angle α with respect to the parallel grain direction. The following equation based on test results with coefficients obtained with regression analysis is presented.

$$(IV)K_{ser,ax} = \frac{0.173 \cdot l_{ef}^{0.414} \cdot \rho^{0.715} \cdot d^{-0.512}}{5.092 \cdot cos^2\alpha + 6.351 \cdot sin^2\alpha} \tag{2.28}$$

The stiffness in [N/mm] to $[N/mm^3]$ was by [Mirdad et al., 2022] converted by dividing with:

$$\pi \cdot d \cdot l_{ef} \tag{2.29}$$

Figure 2.20 compares these four equations for screws with 7 mm nominal diameter and with varying penetrating length of threads

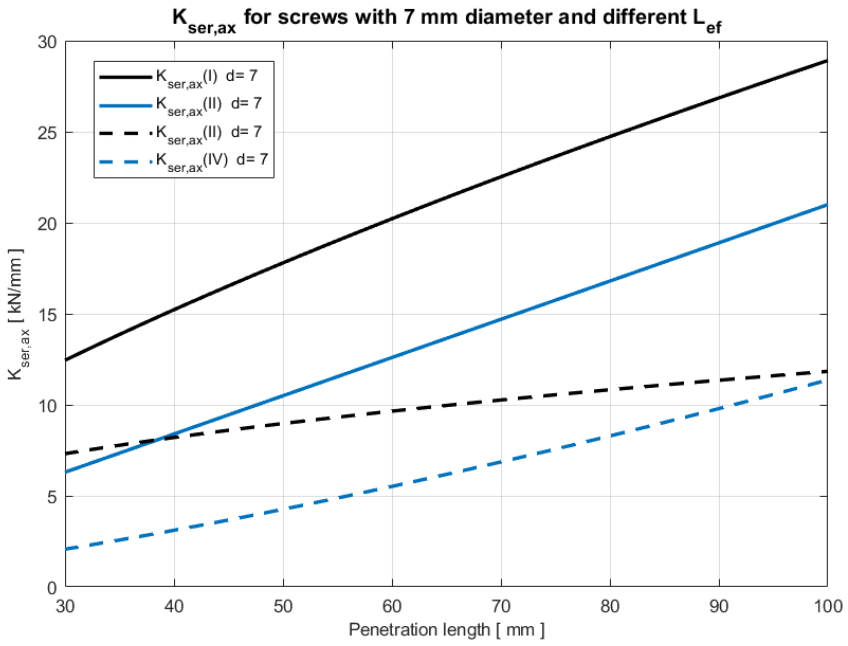

Figure 2.20: *Graphical comparison of $K_{ser,ax}$ from equation (I), (II), (II), (IV) with varying screw diameter and effective penetration length*

2.5 Finite element modelling of structural timber and connections

2.5.1 Examples of methods for modelling stiffness in timber connections

2.5.1.1 The component method

The component method explained by [Kuhlmann and Gauß, 2019], is a method for modelling stiffness and strength in connections and has been used in several studies to show realistic results compared to physical deformation tests on timber connections.

With this method, geometries, components, or parts of the connections are represented as spring elements and these spring elements are organized in suitable manner to simulate how the real connection would deform under decided loading. One component could for instance be an individual fasteners or the total stiffness for a group of fasteners in a specific direction, or the rotational stiffness of the group based on the polar moment of inertia of the fasteners. The results from the spring system can

be complied to one equivalent stiffness parameter that can be used for modelling the connection in a structural systems

To model a realistic behaviour it is important that the stiffness of each component is generated or calculated correctly. The stiffness values could also be based on real tests if possible. This information are the critical input data for successful modelling. [Kuhlmann and Gauß, 2019] proposes that a catalogue with different components and methods to determine their stiffness and capacity could be a possible solution for increasing the practical use of the component method. Such a catalogue would simplify the use of the component method for evaluation and design of connections and structures.

It is possible to simulate non linear behaviour of the timber connection. The stiffness in the components could be updated for different levels of loading, based on deformation conditions, how fasteners would behave like linear elasticity and plasticity. The load displacement curves for individual fasteners should preferably be defined as accurately as possible when implementing the stiffness into a component model. However a simplified but still useful approach is to divide the non linear deformation curve into three linear ranges to represent the initial elastic deformation, plasticity and failure of connections with sufficient accuracy. A full non linear connection model requires much detailed information and time to develop.

One challenge with component modelling is to include realistic modelling of effects that might occur for higher loads if splitting in the joint occurs as well as interactions between the components. Stiffness in different parts of connections might affect each other in unforeseen ways when interacting under loading. [Kuhlmann and Gauß, 2019] concludes that the splitting of timber would have an impact to the stiffens of a joint at high loads.

2.5.1.2 Solid Finite element modelling in 3 dimensions

Detailed modelling of connections with solid 3D elements is a complex method but can with suitable material models and interaction with criterion for contact between surfaces give detailed results and realistic mechanical behaviour with stress and deformations. [Sandhaas et al., 2018] explains that the main drawback is the time consuming work that is required both for developing a reliable model and also the large computing effort that is required by the software. In order to capture the real material mechanics and interaction with steel and timber, linear and plastic material properties has to be assigned with yielding and failure criteria. [Kuhlmann and Gauß, 2019] also claims that for regular basis design procedures full 3D FE-modelling of timber connections might be to advanced.

However the plasticity and brittle failure of timber can be expressed in FE-modeling with the Hill criterion and Hoffman criterion. These criterion shows the principles of how FE-softwares could include non linear material behaviour of a plastic orthotropic material model. [Xu et al., 2012] explains that the Hill Criterion could state a stress combination in 3 dimensions that would be the condition for the yield strength, and

hence tells the FE-model when the material is yielding. [Xu et al., 2012] continues and explains that since the Hill criterion can not describe the difference in strength between compression and tension and also not brittle material failure, the Hoffman criterion can be used as a modification of the Hill criterion for allowing a realistic material failure model that consideres damage of the material.

Hill criterion in three dimensions can be expressed as a modification of the Von Mises yield criterion accordingly:

$$\begin{aligned}[a_1(\sigma_y - \sigma_z)^2 + a_2(\sigma_z - \sigma_x)^2 + a_3(\sigma_x - \sigma_y)^2 + \\ 3a_4\tau_{xz}^2 + 3a_5\tau_{yz}^2 + 3a_6\tau_{xy}^2]/\sqrt{2} = 1\end{aligned} \tag{2.30}$$

With constants a_1 to a_6 becoming:

$$a_1 = a_2 = \frac{1}{f_{c,0}^2}, a_3 = \frac{2}{f_{c,90}^2} - \frac{1}{f_{c,0}^2}, a_4 = a_5 = a_6 = \frac{2}{3f_v^2} \tag{2.31}$$

In the study by [Xu et al., 2012] where a bending stiffness test of a connection was compared with two simulated models, one with the Hill yield criterion and one with the Hoffman damage criterion, it was observed that the model that included the Hoffman damage criterion showed more accurate results.

2.5.1.3 Modelling of dowel type connections - beam on elastic foundation

[Kuhlmann, 2022] writes that dowel type fasteners loaded laterally can be modeled within the embedding timber as beam elements on elastic foundations. These types of FE-models could be created in 2 dimensions, as beams supported on linear or non linear elastic springs that simulates the deformation in the fastener and the timber. These types FE-models are then accounting for both displacement in the fastener and embedding wood. The models can simulate the mechanical behaviour of the connections for loading in two dimension, and captures the interaction of the different stiffness between the metal fastener and the wood. [Sandhaas et al., 2018] explains how the stiffness of the springs that represent the embedment of the fastener in the timber can be assigned, and this are refered to in section 2.5.2.4.

2.5.1.4 Connection zone in global FE modelling of structural systems

For modeling global behaviour of strucutral systems, there are in some finite element software possible to assign stiffness at supports and connections as spring constants. This is the case for RFEM by Dlubal, but there are also other approaches for implementing the stiffness of connections in FE-models.

In a dynamic evaluation of the serviceability behaviour of a 14 story glulam truss - frame building in Norway, a parametric approach was conducted by [Malo et al., 2016] to account for stiffness at some connections. Axial stiffness of connections were introduced by modifying the cross sectional area of elements within a connection zone

at the ends of every bracing truss.

In this building the influence on global deflections by semi rigid rotational stiffness in connections was first evaluated by comparing two extreme cases. One where the rotational stiffness in every node were simply hinged, and one with fully rotational rigidity. It was concluded that difference between the cases were insignificant for the result on horizontal deflections of the building and its natural frequencies. Instead the axial stiffness for the connections between the bracing trusses were of higher interest.

In the structural analysis only one type of connection were implemented in the modelling. [Malo et al., 2016] writes that physical tests on this connection resulted in that the initial axial stiffness K_{sec} up to 50% of the maximum load was 260 kN/mm. The stiffness for cyclic loading and unloading K_{cyc} was 780 kN/mm. The calculated K_{ser} from Eurocode 5 was by comparison 447 kN/mm. These tested stiffness values was corresponding to a fraction of 0.35 and 1 of the axial stiffness $E \cdot A$ in the truss members.

To account for the stiffness in the modelling, the length of the connection zone at trusses were set to the sectional height of the truss member. Then the cross-sectional area at these zones were modified down to 10-40% of the real truss member area.

2.5.2 Theory for the implementation of FEM modelling

The finite element modelling implementations are mainly based on a draft; *Guidelines for a Finite Element Based Design of Timber Structures* by [Kuhlmann, 2022], as well as the report by [Sandhaas et al., 2018]. Some additional theory are also gathered from other literature.

2.5.2.1 Non linear modelling of timber

According to [Kuhlmann, 2022] different non linear material behaviour is suitable for modelling the plastic behaviour for situations with loading in compression perpendicular and parallel to the grain of timber.

In compression perpendicular and parallel to the grain the plasticity behaviour can be modeled with a tri-linear or bi-linear stiffness approach. [Kuhlmann, 2022] also mentions that stress-strain curves with "*multilinear or curved without/with softening*" and experimentally determined curves could be a possible option as well.

There are different types of nonlinear analyses. The proper type for implementation is case specific and is influenced by what kind of problem is to be studied and what type of non-linearity is relevant. Some different levels of modeling for timber structure analysis are presented by [Kuhlmann, 2022] in figure 2.21

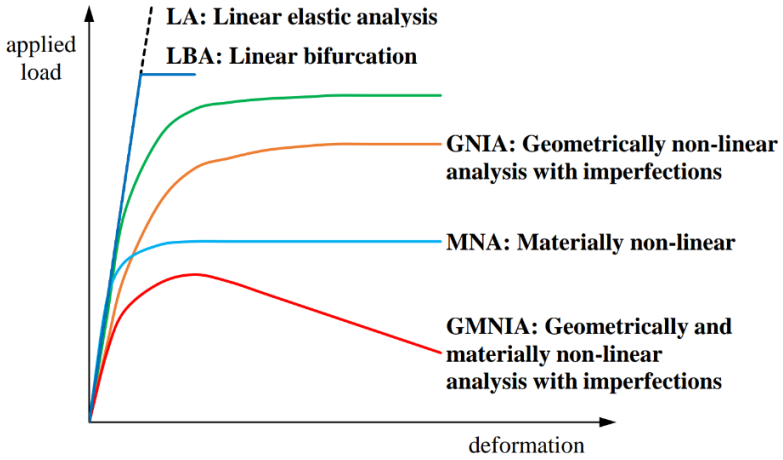

Figure 2.21: *Visualisation of load deformation curves with different non linear models by [Kuhlmann, 2022]*

2.5.2.2 Non linear proportional limits

To practice non linear modelling one approach is to use input parameters for specifying the breakpoints of the proportionality in the stress strain curves. This limits determines at what stresses or strains the material start to yield. Recommendations for these are given by [Kuhlmann, 2022]. $f_{1,c,0}$, compression parallel to the grain for tri-linear or multi linear stress- strain curves are given by equation 2.32

$$f_{1,c,0} = k_{lin,c,0} f_{2,c,0} \tag{2.32}$$

- $f_{2,c,0}$ is given as the compression strength parallel to the grain $f_{c,0,k}$
- $k_{lin,c,0}$ can be chosen as 0.75 for softwood and 0.65 beech LVL

For compression perpendicular to the grain the proportionality limit $f_{1,c,90}$ is given by equation 2.33

$$f_{1,c,90} = k_{lin,c,90} f_{2,c,90} \tag{2.33}$$

- $f_{2,c,90}$ is given as the compression strength parallel to the grain $f_{c,90,k}$
- $k_{lin,c,90}$ can be assumed as 0.75 for softwood.

[Kuhlmann, 2022] specifies that $f_{2,c,0}$ and $f_{2,c,90}$ should be modified with k_{mod} from EN-1995-1-1 in numerical simulations to consider the influence on moisture on the material behaviour.

2.5.2.3 Embedment stiffness and strength

Embedment is typically the only plastic behaviour of the wood in a timber joint. [Dorn and Bader, 2016] describes the embedement of fasteners in wood as an relationship how compressive forces from circular fasteners are moved to the wood when

the fasteners are loaded. [Xu et al., 2022] states that experiments are usually made to generate relationships and formulas for the embedment strength of timber, with full-hole or half-hole tests. The variation in these two methods relays on the test setup. In half-hole test, the dowel is loaded along its whole length with a movable loading apparatus. This prevents the dowel from bending which gives inaccurate deformation considering a whole connection's stiffness. In the other hand, the full-hole method allow bending of the dowel inside of timber, which for some applications could predict a more realistic embedment behaviour.

The article "*Embedment behaviour of fully threaded bolts in glued laminated timber*" reviews the results of full-hole and half-hole experiments for Glulam specimens of Pinus sylvestris wood. According to [Xu et al., 2022] the tests give rise to that the strength in a dowel-type connection depends on the wood species and density, the diameter and body threading of fastener and the loading angle. Although in case of threads on fasteners, most of the previous formulations don't take the fastener threading into account when calculating the embedment strength.

[Sandhaas et al., 2018] claims that out of 5 reviewed previous litterateurs, 3 of them have used the evaluation method according to EN 383:2007. This evaluation method calculates the embedment strength out of the load that causes a deformation of 5 mm accounting it as the ultimate load.

The embedment strength can be calculated with the relevant equations from Eurocode (EN 383:2007). for nails with diameter $\leq$ 8mm, and dowels according to equation 2.34 and 2.35 respectively to the loading-to-grain angle.

$$f_{h,0,mean} = 0.082 \cdot (1 - 0.01 \cdot d) \cdot \rho_m \tag{2.34}$$

$$f_{h,\alpha,mean} = \frac{f_{h,0,mean}}{k_{90} \cdot sin^2\alpha + cos^2\alpha} \tag{2.35}$$

for softwood $k_{90} = 1.35 + 0.015 \cdot d$
Where

- d - is the fastener diameter
- ρ_m - is the mean density of timber
- α - is the loading-to-grain angle

2.5.2.4 Embedment modulus for beam on elastic foundation modeling

The embedment modulus is described by [Reynolds et al., 2013] a stiffness parameter that describes the timber embedment stiffness in the area surrounding the fastener in a dowel-type connection. To estimate the embedment modulus in $[N/mm^3]$ for linar elastic behaviour, [Sandhaas et al., 2018] proposes that the mean embedment strength can be divided by a displacement of 1 mm according to equation 2.36.

$$m_{fh} = \frac{f_h}{1} \tag{2.36}$$

The foundation spring stiffness in [N/mm] are calculated with equation 2.37. This is the total spring stiffness along the embedment of the fastener. The stiffness should be divided into several springs that are spread out along the longitudinal direction of the fastener, depending on the distance between the springs. [Sandhaas et al., 2018] suggests that a proper discretization for the distance between each spring element should be as maximum as the fastener diameter.

$$K_d = m_{fh} \cdot d \cdot l \tag{2.37}$$

For a more sophisticated embedment modelling than assuming 1 mm displacement at embedment failure and linear stiffness, [Sandhaas et al., 2018] presents a nonlinear embedment model for circular fasteners. The nonlinear embedment modulus is then calculated according to equation 2.38

$$m_{fh}(u) = f_h \cdot (-ck \cdot (arctan(((u \cdot fk) + dk)^{ek} + ak) + bk)) \tag{2.38}$$

Where the embedment strength f_h can be calculated with Eurocode 5 equations and constants ak - fk:

$$ak = 1.33,\ bk = -1.57,\ ck = 1.79,\ dk = -1.65,\ ek = 4.0,\ fk = 2.8$$

Figure 2.22 shows the non linear model for embedement stiffness and strength as a function of displacement u based on $f_{h,0,m}$ for GL30c where the embedment strength as the black curve are the integral of the embedment modulus over the displacements.

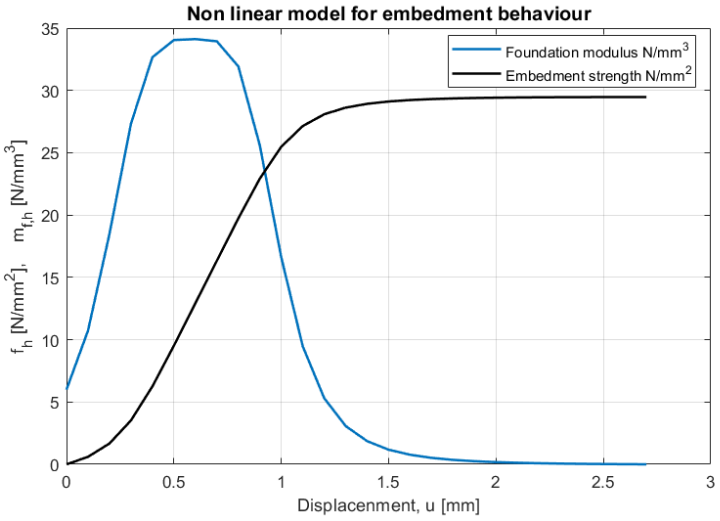

Figure 2.22: *Non linear model for embedment behaviour of circular fasteners. This figure is based on* $f_{h,0,m} = 29.6 N/mm^2$ *for Gl30c*

2.5.2.5 Plasticity model for modelling metal and fasteners

The basic principles for a stress strain curve of a ductile metal is explained by [Soutsos and Domone, 2010]. The linear elastic range is valid up to the yield stress,

then an abrupt decrease of stiffness is occurring and the metal can be assumed to have an almost perfect plastic behaviour. After yielding there is a region in the stress strain curve with almost constant stress and after this there will occur an increased strength which is called strain hardening or work hardening before fracture. Based on this, important parameters for metals besides the modulus of elasticity is the yield strength f_y and ultimate strength f_u as well as corresponding strain ϵ_y and ϵ_u. A typical stress strain curve for structural steel is shown to the left in figure 2.23 where $\epsilon_s h$ is strain when strain hardening starts.

In FEM software it is common to use models that approximates this stress strain relation. One basic model is to use bi-linear curve and isotropic strain hardening. A curve like this is visualized to the right in figure 2.23.

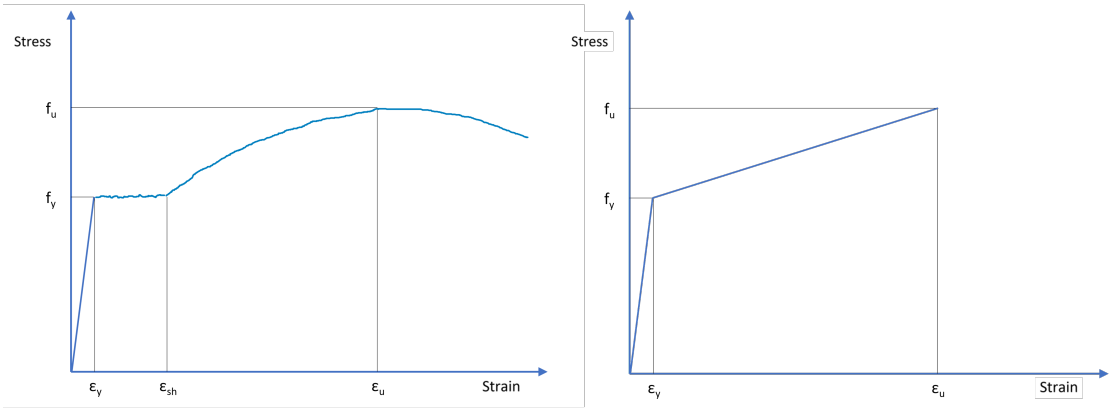

Figure 2.23: *To left, typical stress strain curve for ductile steel with structural engineering applications. To right, the implemented approximation in FEM*

2.5.2.6 Spring model for fasteners

[Sandhaas et al., 2018] presents different levels for modelling load-displacement for fasteners in wood as springs. Besides the full 3D element model with different solids for woods and fasteners with respective material model for plasticity and damage as well as contact models for interacting surfaces, simplified approaches for modelling fasteners as springs are explained.

Besides different approaches with solid finite elements, on method is to use a matrix of linear elastic shell elements which would approximate the deformations and stress states in the wood around the dowels. However stress distributions in the third dimension across the thickness of the members are not covered with this approach. If for instance two timber members are modeled with fasteners at their overlapping shear plane, springs are assigned at the shear planes and simulate deformations of the fastener and the relative deflections between the members which would occur in the local area around the fastener. [Sandhaas et al., 2018] specifies that the predetermined spring load -displacement curves should account for different properties for loading perpendicular and parallel to the grain. The coupling of the modelled fasteners to the wood matrix could include contact which allows separations on the

opposite side of where the fastener would be compressed to the wood. The interaction could also be created with a tie but this would result in tensions near the coupling which in reality would not be present and [Sandhaas et al., 2018] writes that the stresses obtained close to the fasteners then would become less accurate.

A further simplification is to use a rigid matrix around the spring elements as the fasteners in the connection. This would not give internal stresses in the members of the connection and neglect internal deformations in the wood. Distribution of forces on the fasteners could still be obtained, and [Sandhaas et al., 2018] explains that since deformations in the surrounding matrix are not taken to account, force distribution on fasteners would be less accurate for some load cases. The benefits with this approach are furthermore the reduced calculation effort for the software. [Sandhaas et al., 2018] also mentions the reduced effort required for creating the models as well as processing the results as advantages.

2.5.2.7 Frictional constants at contact surfaces

When modelling systems built up by several members as solids and surfaces in 3 dimensions, [Kuhlmann, 2022] writes that it may be important to consider the transfer of displacements and forces between the surfaces. Contact elements or interface elements can specify how the solids or surfaces interacts at their mutual boundary. According to [Kuhlmann, 2022] frictional constant can simulate how the interaction between solids plays and the frictional constants should have appropriate values between different materials based on test data or existing literature and standards.

[Basterrechea-Arévalo et al., 2021] compares the FE-analyses with real experiments on a moment transmitting beam-to-column timber connections. The modelling was implemented in Abaqus and the commandos surface-to-surface discretization and "hard contact" were used. The friction between two member elements (in this case column and beam) is expressed as normal forces applied to the tangent area between the two members. The friction pressure can be set to $0.1N/mm^2$ as in [Basterrechea-Arévalo et al., 2021]

In one more article about an FE-analysis *Modelling of steel-timber composite connections: Validation of finite element model and parametric study* [Hassanieh et al., 2017], the designer used surface-to-surface discretisation method and hard contact with the "Allow separation after contact" in Abaqus. However, they were more precised when formulating the friction between different materials accordingly to table 2.1

Table 2.1: Frictional constants

Materials	Frictional coefficient
steel to CLT	0.25
steel to LVL	0.3
steel to steel	0.4

2.5.2.8 Modeling verification

The relevant values or parameters that a finite element analysis gives are referred to as "System response quantity" and abbreviated to SRQ by [Kuhlmann, 2022]. The principle for verification of results could be to compare SRQ with analytical equations and check failure modes, for instance with available Eurocode 5 equations. [Kuhlmann, 2022] more specifically writes that the comparisons between results from numerical models should be made to benchmarks that have been established as reliable and accurate.

3
Methods

3.1 Case study

The reference building that is used to implement the analysis is an office building called Uppsala Lighthouse. The building is built by Castellum in Uppsala, Sweden and its inauguration is planned to be in 2025.

The 5-storey building is a timber column-beam structure with concrete floor slabs. Most of the structural glulam columns are designed continuous and stretches across all stories. Floor-carrying beams are hinged between the columns. At the short sides of the building there are cantilever beams furthest out towards the facade, and here the supporting timber columns are not continuous between the stories to allow the cantilever beams.

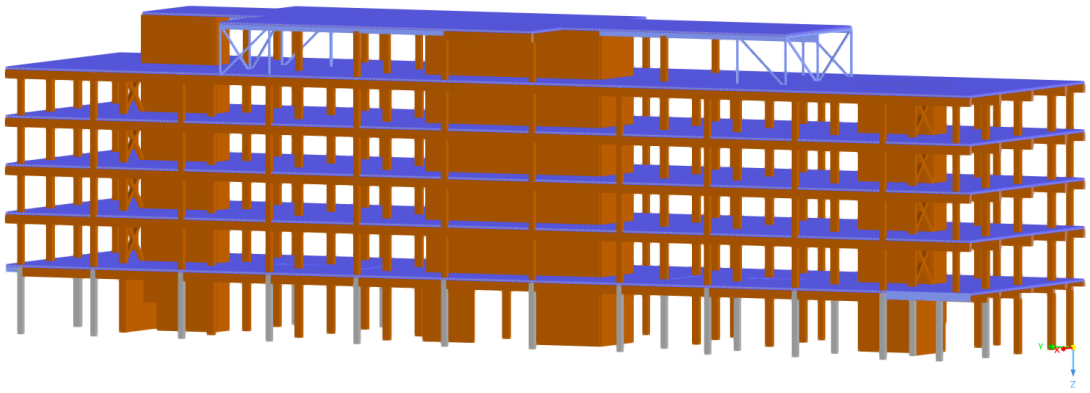

Figure 3.1: *The structural system of the reference building modelled in RFEM*

Some elements of the structural frame system are performed with steel beams, along the installation paths and as deep beams in some instances on the first floor level. Some timber columns are also replaced with reinforced concrete in the ground floor level, see figure 3.1. The building is stabilized against horizontal loads with inter alia CLT-stairwalls. The concrete floor slabs are hollow core one way slabs supported by rows of beams at every story. The load carrying direction of the slabs span in the direction that runs along the short side of the building.

To analyze the impact of the timber connections on the system level for the structural system, the mechanical behaviour of individual connections needs to be analysed and evaluated.
The connections in the structural system of the case study building that have been identified to have impact are the following:

- **Connections that support floor-carrying beams on the continuous columns:** The most duplicated type of connection of the building; due to that most of the columns are continuous and beams taking different forces are perpendicularly connected to them.

- **Connections between cantilever beams and columns:** This type of connection is similar to the previous one but instead, the force and moment bearing beam is a continuous beam laying on a column with a cantilever on one side.

- **Connections that support floor-carrying beams on CLT walls:** The connection between glulam beams and CLT-cores might become a critical one; where the two materials could behave differently and develop different movements.

- **Connections between bracing members, CLT walls and columns:** The connection between a beam or column to the inclined bracing trusses requires a rather different design the the other connectors. In addition to the special shape of connectors, bracing trusses are designed to stabilize the building and to withstand horizontal forces. Therefore the taken load combination is different to the previous perpendicular members.

The connection that have most instances in the structure and which stiffness are believed to play a large contribution to the global behaviour of the building are the connections between columns and floor carrying beams. The design of these connections are therefore the first priority in this project and will be the subject for a detailed evaluation.

The evaluation of the connections and its influence on the structural system are performed in 4 major steps accordingly:

- A preliminary load calculation is first made to adapt the basic load carrying demands in order to select an appropriate connection design.

- When suitable connection has been identified, its various components stiffness will be analyzed and calculated in the linear and non linear load deformation ranges.

- When the load deformation behaviour is obtained for individual fasteners that are present in the connection, models of the entire connections with its ma-

terial properties, and its geometries will be built and studied to generate the total load deformation behaviour.

- When stiffness parameters for rotational, and lateral deformations of the connections have been obtained and evaluated for different levels of loading, the rotational stiffness will be evaluated in simple frame models and for beams, as presented in figure 2.4. The whole structural system of the building are later modelled in 3 dimensions with the software, *RFEM* by *Dlubal*, to analyse the structural impacts and load redistributions resulting from the stiffness in the connections.

3.2 Preliminary design of connections

The preliminary design of the connections is done by calculating the design loads at the supports of different structural elements. For beams, the shear forces are calculated, axial loads for bracing trusses, and compression forces for columns at its bottom are calculated. Connections from manufactures are then selected based on these forces.

3.2.1 Assumptions

For hand calculations of design loads at joints in the case study building, no system effects was considered and the structural system was decoupled according to the following:

- Horizontal actions only load and act on the bracing system
- For columns, only vertical loads are considered
- Floor carrying beams are only loaded by vertical loads on the contributing area.
- Floor carrying beams between columns are assumed simply supported

For tall and slender buildings horizontal loads are inducing compression in columns as the structure works as a cantilever but this effect was here neglected.

3.2.2 Loads

The self weight except structural that was considered for floors walls and roofs are presented in table 3.1.

Table 3.1: *Self weight of non structural elements*

Floor structure	HDF slab	330	kg/m^2
	Screed+ coating	125	kg/m^2
	Installations	50	kg/m^2
	Ceiling	30	kg/m^2
Roof structure		70	kg/m^2
Exterior walls		50	kg/m^2

The characteristic imposed load for office buildings is set to $Q_k = 2.5kN/m^2$ according to EKS 12 [Boverket, 2022]. According to EN 1, the self-weight of movable partitions should be added to the imposed loads with the characteristic value of $Q_k = 0.5kN/m^2$

The building is located in Uppsala where The characteristic snow value is $s_k = 2kN/m^2$, and the reference wind speed reaches $v_b = 24m/s$, according to EKS 12 [Boverket, 2022]. The building is stabilized against wind loads by glulam trusses and three CLT-stairways. In figure 3.2, the blue and red elements are used to take the horizontal wind forces acting on the short and long side respectively. The magnitude of the horizontal load varies depending on the height and the exposed side. The calculation of the characteristic snow and wind load is shown in Appendix A.1 and A.2 respectively.

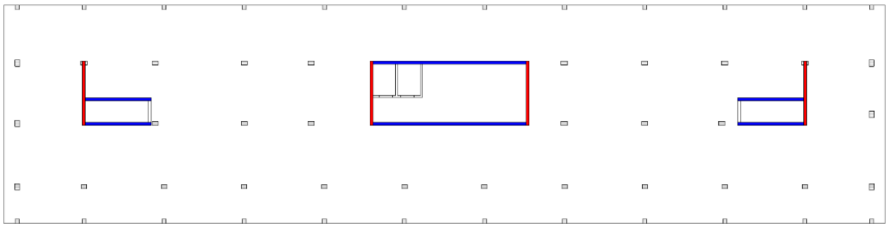

Figure 3.2: *The building's stabilizing elements against horizontal forces acting on the short side (in blue) and long side (in red) of the building*

3.2.3 Load combinations

The partial safety factors and combination coefficients for permanent and variable loads in ULS and SLS are determined according to Eurocode 1 as shown in table 3.2. Equation 3.1 present the principle how loads acting on structures are combined for ULS according to Eurocode 1.

$$\sum_{i\geq 1} \gamma_{g,i} \cdot G_{k,i}" + "\gamma_P \cdot P" + "\gamma_{Q,1} \cdot Q_{k,1}" + "\sum_{j>1} \gamma_{Q,j} \cdot \Psi_{0,j} \cdot Q_{k,j} \tag{3.1}$$

Equation 3.2 shows how loads are combined for characteristic combination in SLS according to Eurocode 1.

$$\sum_{i} G_{k,i} + Q_{k,1} + \sum_{j>1} \Psi_{0,j} \cdot Q_{k,j} \tag{3.2}$$

Equation shows how loads are combined for quasi-permanent combination in SLS according to Eurocode 1.

$$\sum_i G_{k,i} + \sum_{j \geq 1} \Psi_{2,i} \cdot Q_{k,j} \tag{3.3}$$

Table 3.2 shows the factors for load combinations and some of the relevant load combinations that are implemented in preliminary design and applied on the global FE-model of the reference building.

Table 3.2: Factors and load combinations that are used in hand calculations and simulations

Load case	Self weight $\gamma_{g,i}$	Imposed load $\Psi_{0,j} \cdot \gamma_{Q,1}$	Wind load $\Psi_{0,j} \cdot \gamma_{Q,1}$	Snow load $\Psi_{0,j} \cdot \gamma_{Q,1}$
ULS 1	1.35	1.5	$0.3 \cdot 1.5$	$0.7 \cdot 1.5$
ULS 2	1.35	$0.7 \cdot 1.5$	1.5	$0.7 \cdot 1.5$
ULS 3	1.35	$0.7 \cdot 1.5$	$0.3 \cdot 1.5$	1.5
ULS 4	1.35	1.5	0	0
Char. SLS 1	1.0	1.0	0.3	0.7
Char. SLS 2	1.0	0.7	1.0	0.7
Char. SLS 3	1.0	0.7	0.3	1.0
		$\Psi_{2,i}$	$\Psi_{2,i}$	$\Psi_{2,i}$
Quasi-perm. SLS	1.0	0.3	0	0.2

3.2.4 Results from hand calculations

The load combinations were implemented in order to calculate the support shear force of the most loaded timber beam, facade beam, cantilever beam and most loaded steel beam, see Appendix A.4. Table 3.3 displays the results of hand calculations from Appendix A.4.

Note that the actual length of the beams is smaller than the calculation inputs. In hand calculations, the beams' length is considered as a centre-to-centre distance, which corresponds the contributing floor span carried by the analysed beam, see figure 3.3 for clarification.

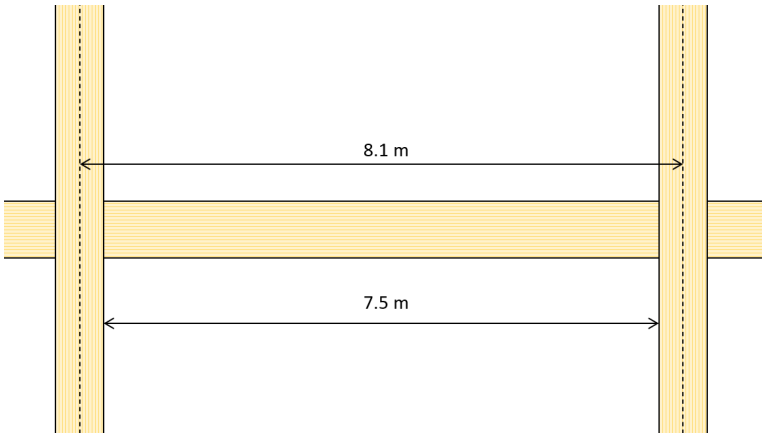

Figure 3.3: *Figure describing the beam length and the length of the contributing area used in hand calculations of design loads*

Table 3.3: Design shear force at end connections of floor carrying beams in the building. Calculated in Appendix A.4

Structural element	length	Shear force ULS	Shear force SLS	Quasi-permanent Shear force
Facade beam	8.1 m	159 kN	114 kN	89 kN
Beam with largest area	8,1 m	240 kN	171 kN	129 kN
Cantilever beam	7,95 m	241 kN	172 kN	129 kN
Max loaded steel beam	9 m	332 kN	236 kN	177 kN

3.2.5 Alumaxi connector and different fasteners

A connector that exist in the market, and that might fulfill the demands in the structural system of the case study builing is the *Alumaxi* connector manufactured by *Rothoblaas*. Its geometries, compatibale fasteners and some technical specifications are in this section presented. Figure 3.4 shows one specific varaint of the connector.

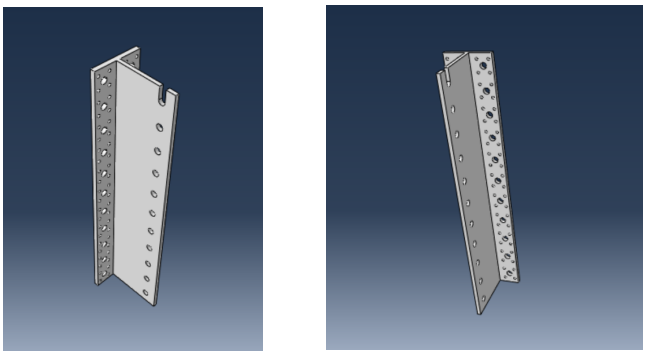

Figure 3.4: *Illustration of Alumaxi 704 STA connector*

It is manufactured of an Aluminium Alloy specified in table 3.20. Alumaxi is suitable for large scale glulam beams and can be used with cross sections up to 280x1200

mm. The connector geometries and the definitions of these are displayed in figure 3.5.

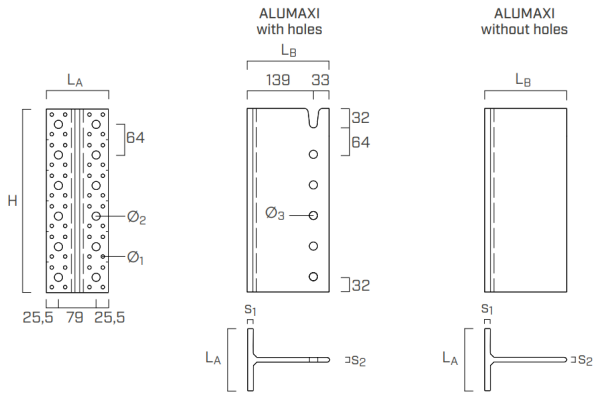

ALUMAXI			
flange thickness	s_1	[mm]	12
web thickness	s_2	[mm]	10
wing width	L_A	[mm]	130
web length	L_B	[mm]	172
small flange-holes	$Ø_1$	[mm]	7,5
large flange-holes	$Ø_2$	[mm]	17,0
web holes (dowels)	$Ø_3$	[mm]	17,0

Figure 3.5: *Definitions of geometries and dimension of the Alumaxi connector. Source: Rothoblaas*

The producer provides a multiple choice of fasteners to be combined with the Alumaxi connector. For The fasteners to be installed into the column, LBA anker nails and LBS screws are proposed. For the beam, STA and SBD dowels are suggested. Different configurations of the connector with STA dowel fasteners and SBD dowel fasteners are specified in table 3.4 and 3.8.

3.2.5.1 STA dowel

STA is a smooth dowel with 16 mm diameter to support timber beams. Table 3.4 reviews the possible lengths of STA with the used ones highlighted in yellow. Further material properties of STA dowels are displayed in table 3.5 and the shape of the dowel is shown in figure 3.6.

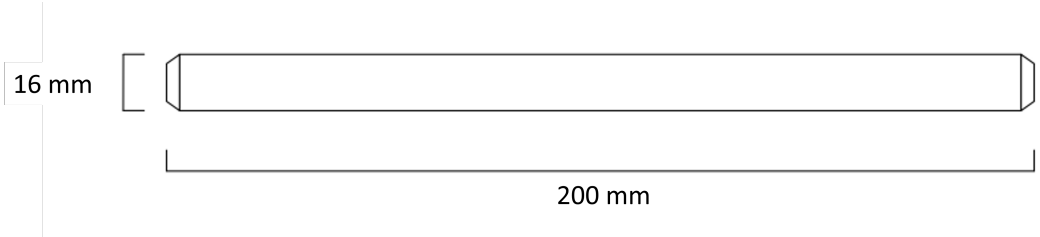

Figure 3.6: *Sketch of the STA dowel by Rothoblaas*

Table 3.4: *Technical data for Rothoblaas Alumaxi connection. Relevant connection configuration for beam end supports on columns marked in yellow. Source: Rothoblaas*

ALUMAXI with STA dowels

ALUMAXI	SECONDARY BEAM			MAIN BEAM			
				FASTENING THROUGH NAILS		FASTENING THROUGH SCREWS	
$H^{(1)}$	b_J	h_J	STA dowels Ø16[2]	LBA nails Ø6 x 80	$R_{v,k}$	LBS screws Ø7 x 80	$R_{v,k}$
[mm]	[mm]	[mm]	[pcs Ø x L]	[pcs]	[kN]	[pcs]	[kN]
384	160	432	6 - Ø16 x 160	48	122,8	48	130,3
448	160	496	7 - Ø16 x 160	56	152,0	56	152,0
512	160	560	8 - Ø16 x 160	64	173,8	64	173,8
576	160	624	9 - Ø16 x 160	72	195,5	72	195,5
640	200	688	10 - Ø16 x 200	80	246,0	80	246,0
704	200	752	11 - Ø16 x 200	88	270,6	88	270,6
768	200	816	12 - Ø16 x 200	96	295,2	96	295,2
832	200	880	13 - Ø16 x 200	104	319,8	104	319,8
896	200	944	14 - Ø16 x 200	112	344,4	112	344,4
960	200	1008	15 - Ø16 x 200	120	369,0	120	369,0

Table 3.5: *Input data STA dowels*

Diameter	Length	Material	Young's modulus	f_y	f_u	ϵ_u
16 mm	200 mm	S355	210 GPa	355 MPa	570 MPa	0.18

The studied beam has the dimensions 430x810 mm composed of two screw-glued 215x810 mm beams, and therefore two Alumaxi connectors placed next to each other are designed to carry the beam.
With 2 of these connectors at the ends of the beams, the capacity for the vertical support reaction at each end of the beams are presented in table 3.6.

With equation 3.4, $R_{v,D}$ for the connection in table 3.6 becomes:

$$R_{v,D} = \frac{R_{v,k} \cdot k_{mod}}{\gamma_m} \tag{3.4}$$

- $\gamma_m = 1.3$ for connections according to SS-EN 1995-1-1
- $k_{mod} = 0.8$ for glulam service class 1, medium load duration

Table 3.6: *Capacity of Alumaxi with STA dowels for vertical loading according to Rothoblaas*

ALUMAXI $H^{(1)}$	$R_{v,k}$	$R_{v,D}$	$2 \cdot R_{v,D}$
512 mm	173.8 kN	106.95 kN	213.9 kN
576 mm	195.5 kN	120.31 kN	240.6 kN
640 mm	246 kN	151.38 kN	302.8 kN
704 mm	270.6 kN	166.52 kN	333.0 kN

3.2.5.2 SBD dowels

SBD is another variation beside STA dowels which is recommended by Rothoblaas to be used in combination with the Alumaxi connector. For the studied beam width at this project, the dowel is chosen with the dimensions of 7,5x195 mm. Figure 3.25 shows the SBD dowel and the layout of SBD dowels at the web of Alumaxi 640 connector.

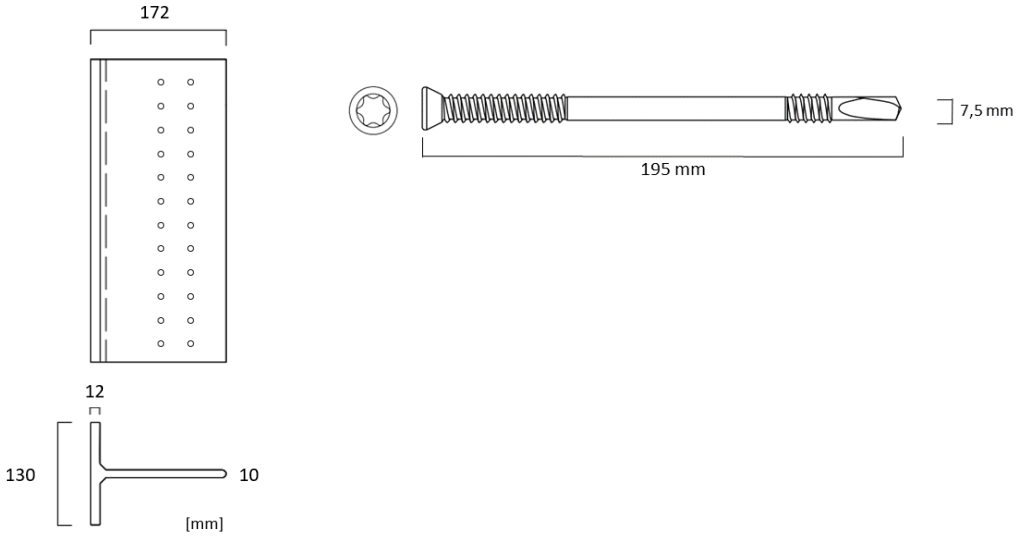

Figure 3.7: *Layout of SBD dowel (to the right), and layout of the web of Alumaxi with SBD dowels (to the left)*

The spacing between the dowels and distance between the dowel's centre and the beam's edges are designed according to Eurocode 5 (8.3.1.2 - Table 8.2). Table 3.7 shows the calculated minimum required distances according to EC5 and the actual spacing and distances used in this design.

Table 3.7: *The calculate minimum spacing and distances, also the design spacing and distances of SBD dowels, with the denotation according to figure 3.8*

Distance (see fig. 3.8)	Min. spacing acc. to EC5	Design distance
a_1	$38mm$	$40mm$
a_2	$23mm$	$50mm$
$a_{3,t}$	$80mm$	$80mm$
$a_{3,c}$	$40mm$	$3750mm$
$a_{4,t}$	$30mm$	$130mm$
$a_{4,c}$	$23mm$	$130mm$

The combination between the applied vertical load and bending moment on the beam results in variation of load-to-grain angles, see figure 3.8. The dowel displays different capacity related to the loading angle according to the producer Rothoblaas. In this project, the dowel is assumed to have capacity in two loading direction, parallel and perpendicular to grain. The actual resulting angle of the dowel is supposed to fall between these two values, see table 3.8. Further material properties of STA dowels are displayed in table 3.9

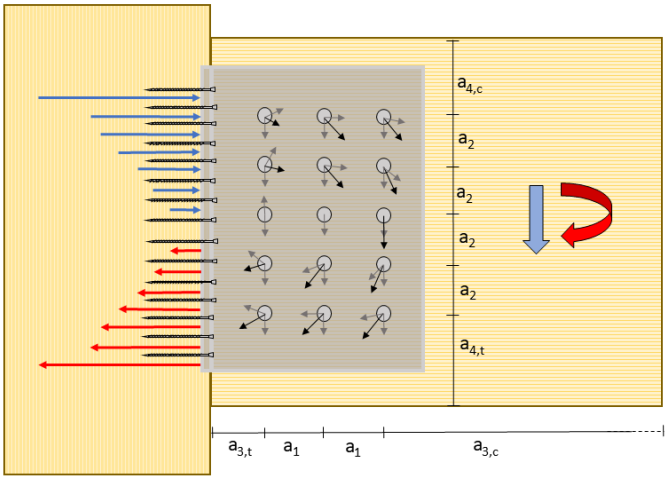

Figure 3.8: *An illustration of a column-beam timber joint, and the resulting load in the fasteners caused by loading the beam with a moment and a vertical load*

Table 3.8: *Technical data for SBD dowelsconnection. Relevant connection configuration for beam end supports on columns marked in yellow. Source: Rothoblaas*

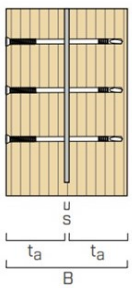

DOWEL HEAD INSERTION DEPTH 0 mm

FASTENING	SBD	[mm]	7,5x55	7,5x75	7,5x95	7,5x115	7,5x135	7,5x155	7,5x175	7,5x195	7,5x215	7,5x235
Beam width	B	[mm]	60	80	100	120	140	160	180	200	220	240
Head insertion depth	p	[mm]	0	0	0	0	0	0	0	0	0	0
Exterior wood	t_a	[mm]	27	37	47	57	67	77	87	97	107	117
$R_{v,k}$ [kN]	load-to-grain angle	0°	7,48	9,20	10,18	11,46	12,91	13,69	13,95	13,95	13,95	13,95
		30°	6,89	8,59	9,40	10,51	11,77	12,71	13,21	13,21	13,21	13,21
		45°	6,41	8,09	8,77	9,72	10,84	11,90	12,53	12,57	12,57	12,57
		60°	6,00	7,67	8,24	9,08	10,07	11,15	11,78	12,02	12,02	12,02
		90°	5,66	7,31	7,79	8,53	9,42	10,40	11,14	11,54	11,54	11,54

Table 3.9: *Input data SBD dowels, carbon steel for fasteners*

Diameter	Length	Material	Young's modulus	f_y	f_u	ϵ_u
7.5 mm	195 mm	Grade 8.8	210 GPa	640 MPa	800 MPa	0.2

3.3 FE-modelling of connections in Abaqus CAE

3.3.1 Beam on elastic foundation models

The 16x200 mm STA dowels was modeled as beam elements with circular cross section supported on springs with a 10 mm distance between every spring. Figure 3.9 shows the principles how the models were set up. For the STA dowels there is a 1 mm gap between the dowel and the hole in the slotted in aluminum plate and the beam elements representing the dowel was therefore allowed to rotate and move without interaction in this zone. Deformation in the contact zones between the slotted in aluminium plate and steel dowel was not considered. The load on the dowel from the aluminium plate was represented as two concentrated forces acting at the edge of the slotted in plate as visualized in figure 3.9. A 1 mm gap was assumed on both sides between the slotted in plate and where the dowel is embedded in the timber, i.e where the springs begin to act.

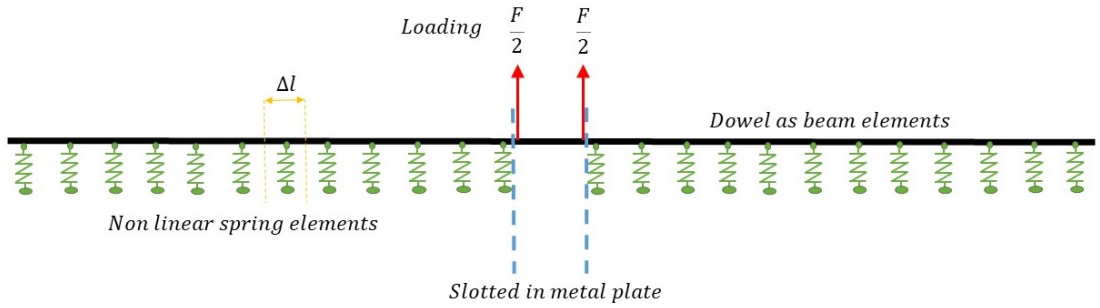

Figure 3.9: *Beam on foundation model implemented in Abaqus CAE*

First linear analysis were made with linear spring stiffness representing the behaviour of the timber. Elastic material model for the dowel with Young's modulus according to table 3.5 and poisons ratio 0.3. The spring stiffness was derived with equations 2.36 to 2.37. And the stiffness of every individual spring was assigned according to equation:

$$k_{spring} = \frac{f_h}{1mm} \cdot \phi \cdot \Delta l \tag{3.5}$$

Where f_h is the embedment strength, ϕ is the dowel diameter, and Δl is the distance

of where every spring acts as embedment, explained in figure 3.9.

The 7,5x195 mm SBD dowels are modelled with the same beam on elastic foundation methodology as for STA dowels, with input data according to table 3.9. As the diamter of SBD dowels is 7.5 mm and [Sandhaas et al., 2018] recommended the discretization for distance between springs to be equal or smaller then the diameter of the circular fastener, the maximum distances between springs in these analyses were reduced to 5 mm.

For the case when analysing SBD dowels with 6 shear planes, the loading with forces at the slotted in metal plate is replaced with displacements , see figure 3.10. This relies on that in case of 3 metal plates, the load is affecting the shear planes unequally, and fixed displacement at the walls of the plates could be a more accurate interpretation. When the loading was applied as displacements, the force acting on the system was obtained by taking the sum of reaction forces at the boundaries.

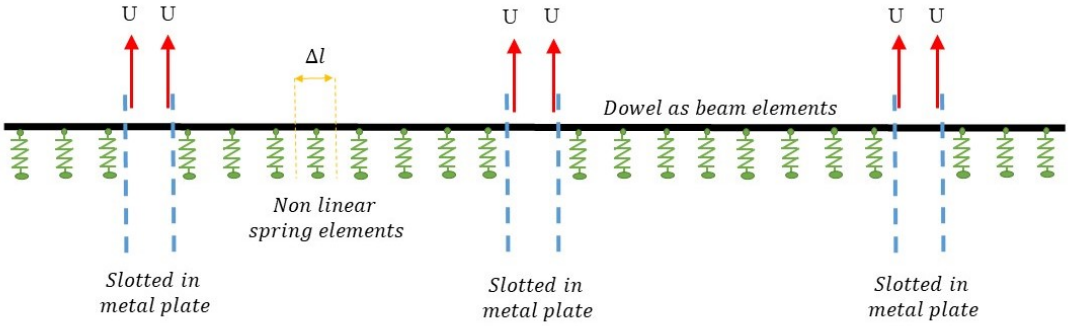

Figure 3.10: *Beam on foundation model of SBD dowel with 6 shear planes implemented in Abaqus CAE*

3.3.1.1 Non linear modelling with beam on elastic foundation

For more realistic results and load displacement relation of the the fasteners up to yielding and maximum loads, non linear analyses were made. These analyses were made by modifying the models mentioned in section 3.3.1 by implementing non linear springs, and activating plastic material model for the beam elements as the dowel. The plasticity model includes isotropic hardening according to section 2.5.2.5. The yield strength is set according to relevant material data with corresponding 0 plastic strain. The ultimate strength is also assigned with corresponding ultimate strain. These material properties were assigned according to tables 3.5 and 3.9. The non-linearity of springs are implemented as non linear connector elements in Abaqus, where the force in the connector element can be controlled by assigning what force should be given at specific displacements. In this way the non-linear embedment model presented in equation 2.38 and figure 2.22 was implemented. The force the connectors was assigned to give at different displacement was then based on this non linear development of the embedment strength for increasing displacement. Equation 3.6 states the development of spring stiffness in relation to

the non linear embedment modulus. Equation 3.7 define which force the springs were assigned with based on the displacement.

$$k_{spring}(u) = m_{fh}(u) \cdot \phi \cdot \Delta l \tag{3.6}$$

Where m_{fh} is the embedment modulus, ϕ is the dowel diameter, and Δl is the distance of where every spring acts as embedment.

$$F_{spring}(u) = \int k_{spring}(u)\, du \tag{3.7}$$

These non linear models are not able to simulate damage and the behaviour after failure for the applied material models. The simulations stops when the stress in the beam section has reached the assigned ultimate value presented in table 3.5 or 3.9. The non linear embedment model also assumes that the emnedment in timber is perfect plastic after the full embedment strength has been reached.

Figure 3.11 presents the values that were assigned for the non linear springs in Abaqus when modelling the embedment for the STA dowel based on mean embedment strength and action parallell to the grain direction. The left columns with header "*F or M*" is the force in [N] the springs are developing for the assigned degree of freedom in the model, and the right column with header "*U or UR*" is the displacements at the degree of freedom in [mm].

Outer springs Δl=9 mm

	F or M	U or UR
1	-4262	-50
2	-4262	-2
3	-4121	-1.2
4	-3908	-1
5	-3301	-0.8
6	-1371	-0.4
7	-901	-0.3
8	-507	-0.2
9	-241	-0.1
10	0	0
11	241	0.1
12	507	0.2
13	901	0.3
14	1371	0.4
15	3301	0.8
16	3908	1
17	4121	1.2
18	4262	2
19	4262	50

Mid springs Δl=10 mm

	F or M	U or UR
1	-4736	-50
2	-4736	-2
3	-4579	-1.2
4	-4343	-1
5	-3668	-0.8
6	-1523	-0.4
7	-1001	-0.3
8	-563	-0.2
9	-267	-0.1
10	0	0
11	267	0.1
12	563	0.2
13	1001	0.3
14	1523	0.4
15	3668	0.8
16	4343	1
17	4579	1.2
18	4736	2
19	4736	50

Inner springs Δl=5 mm

	F or M	U or UR
1	-2368	-50
2	-2368	-2
3	-2289	-1.2
4	-2171	-1
5	-1834	-0.8
6	-762	-0.4
7	-500	-0.3
8	-282	-0.2
9	-134	-0.1
10	0	0
11	134	0.1
12	282	0.2
13	500	0.3
14	762	0.4
15	1834	0.8
16	2171	1
17	2289	1.2
18	2368	2
19	2368	50

Figure 3.11: *Abaqus input data of non-linear springs for STA dowels based on mean embedment strength. Δl is length/spring for outer, mid and inner springs (closest to the plate), see figure 3.9*

The purpose with the non linear beam on foundation models are the following:

- Obtain load deformation relations for fasteners that can be used for analysing stiffness and ductility of different connections.
- Obtain more sophisticated load deformation relations than the analytical equations for k_{ser} and k_u from Eurocode 5 and SIA265.
- Identify failure modes and compare the stiffness and capacities with analytical equations to better understand the mechanical behaviour of fasteners loaded up to failure and also what stiffness values might be appropriate for analysing stiffness of different connections.

3.3.2 Stiffness and strength of fasteners based on beam on elastic foundation modelling

The results from beam on elastic foundation modelling that was done as the first step for analysing stiffness at beam to column connections are here presented, compared and discussed.

3.3.2.1 STA dowels with 2 shear planes, linear analysis

As a start, a linear analysis was created in order to test the beam on elastic foundation modelling method and as a reference for the non linear modelling. The results for stiffness k_{ser} from the linear model of the STA dowels are presented in table 3.10.

Table 3.10: *Stiffness from linear analysis of one dowel as beam elements on elastic springs in glulam material GL30c, without non linear material effects*

Embedment strength $[N/mm^2]$	Embedment modulus $[N/mm^3]$	$K_{ser,0}$ [kN/mm]	$K_{ser,90}$ [kN/mm]
$f_{h,0,m} = 29.6$	29.6	37	-
$f_{h,90,m} = 18.6$	18.6	-	26
$f_{h,0,k} = 26.9$	26.9	34	-
$f_{h,90,k} = 16.9$	16.9	-	24

3.3.2.2 STA dowels with 2 shear planes, nonlinear analysis

The load displacement curve from the non linear analyses of STA dowels are plotted in figure 3.12 with characteristic and mean strength for timber as well as parallel and perpendicular load to grain angle.

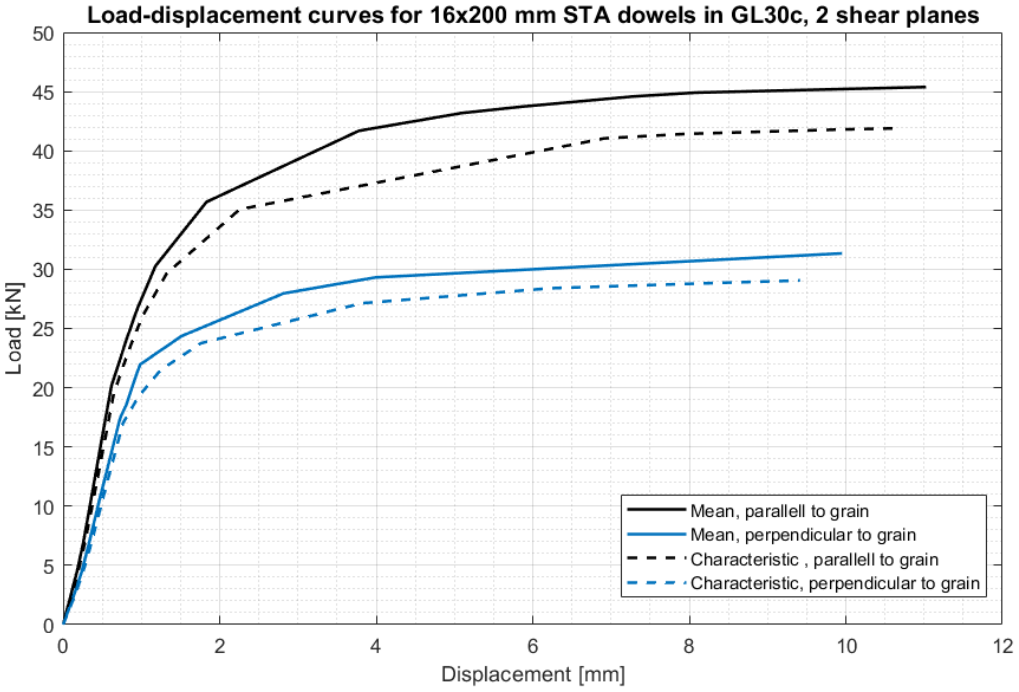

Figure 3.12: *Load displacement for the STA Alumaxi dowels, loaded parallell and perpendicular to the grain. Embedment model according to equation 2.38 with characteristic and mean embedment strengthts for GL30c*

The deformation shape which shows the failure mode of the STA dowel are plotted in figure 3.13. The legend displays the Von Mises stress in the beam elements as the dowel and the red regions are at yielding stress level.

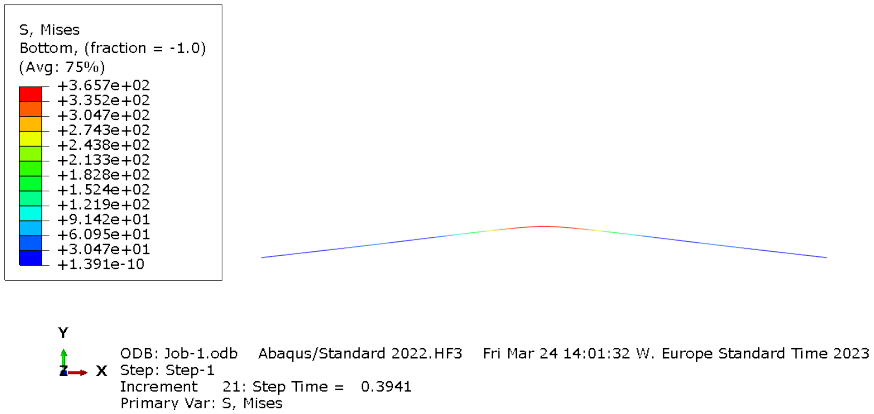

Figure 3.13: *The deformed shape of STA dowel with 2 shear planes, yielded parts displayed in red and deformation scale factor of 10*

As a step for verifying the results from the modelling, maximum loads for the dowels were calculated according to Eurocode 5. These calculations are presented in appendix A.5. The analytically calculated maximum loads are compared to maximum loads reached in the simulations as well as the load for which the connections starts to yield in the simulations.

Table 3.11: *Yield load and maximum load of the connection from non linear analysis of one STA dowel with 2 shear planes in glulam material GL30c, compared with analytical calculations from Eurocode 5 with Johansen equations*

	FEM	**FEM**	**Eurocode 5**
Embedment strength $[N/mm^2]$	Yield load [kN]	Maximum load [kN]	Calculated maximum load [kN]
$f_{h,0,m} = 29.6$	20.0	45.0	44.3
$f_{h,90,m} = 18.6$	17.0	30.0	30.5
$f_{h,0,k} = 26.9$	19.0	41.0	40.9
$f_{h,90,k} = 16.9$	16.5	29.0	28.3

The stiffness parameters k_{ser} and k_u are calculated with assumptions based on equation 2.14 and figure 2.18. k_{ser} is calculated between 10 and 40% of the maximum load, and k_u is calculated between 0 and 70% of the maximum load. Table 3.12 compares result for the stiffness parameters evaluated with beam on elastic foundation model for the STA Dowels with analytical equations according to Eurocode 5 and SIA265.

Table 3.12: *Stiffness from non linear analysis of one STA dowel as beam elements on elastic springs in glulam material GL30c, compared with analytical calculations*

Non linear analysis				
Embedment strength $[N/mm^2]$	$K_{ser,0}$ [kN/mm]	$K_{ser,90}$ [kN/mm]	$K_{u,0}$ [kN/mm]	$K_{u,90}$ [kN/mm]
$f_{h,0,m} = 29.6$	32.0	-	24.2	-
$f_{h,90,m} = 18.6$	-	25.1	-	22.9
$f_{h,0,k} = 26.9$	29.2	-	22.8	-
$f_{h,90,k} = 16.9$	-	22.0	-	18.5
Analytical values				
Eurocode 5	24.8	24.8	16.5	16.5
SIA265	26.4	13.2	17.6	8.8

3.3.2.3 SBD dowels with 2 shear planes

The load displacement curve from the non linear analyses of SBD dowels with 2 shear planes are plotted in figure 3.14, with characteristic and mean strength for timber as well as parallel and perpendicular load to grain angle..

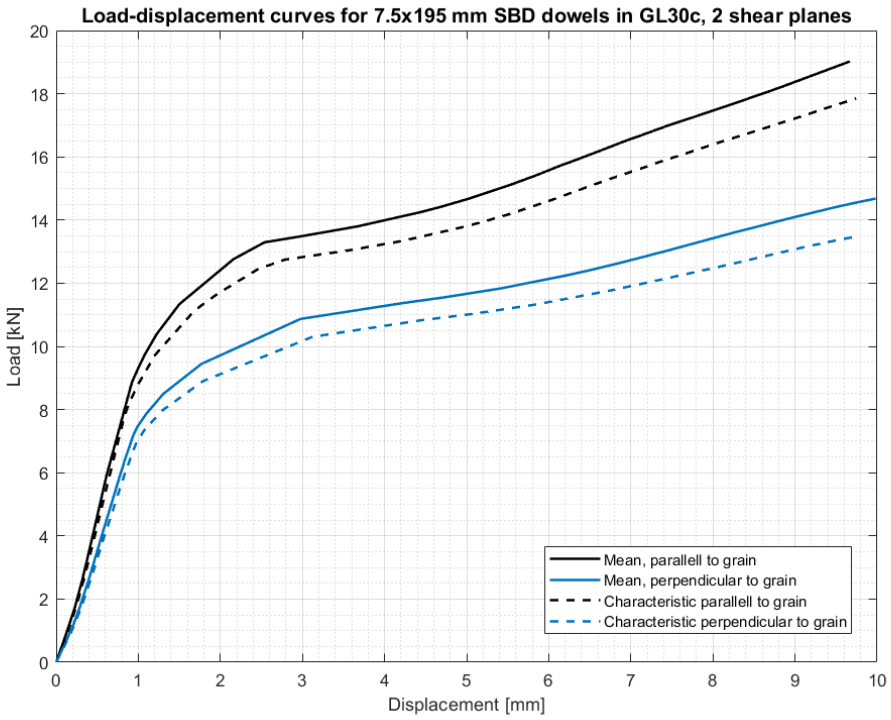

Figure 3.14: *Load displacement for the SBD dowel, loaded parallel and perpendicular to the grain. Embedment model according to equation 2.38 with mean material values for GL30c*

After the plateau reached after yielding in figure 3.14, a clear load increase is observed. This is due to the plasticity model in Abaqus which includes strain hardening and gives additional strength after yielding in the metal.

The deformation shape from the analysis and failure mode of the SBD dowel with 2 shear planes is plotted in figure 3.13. The legend displays the Von Mises stress in the beam elements as the dowel and the red regions are at yielding stress level.

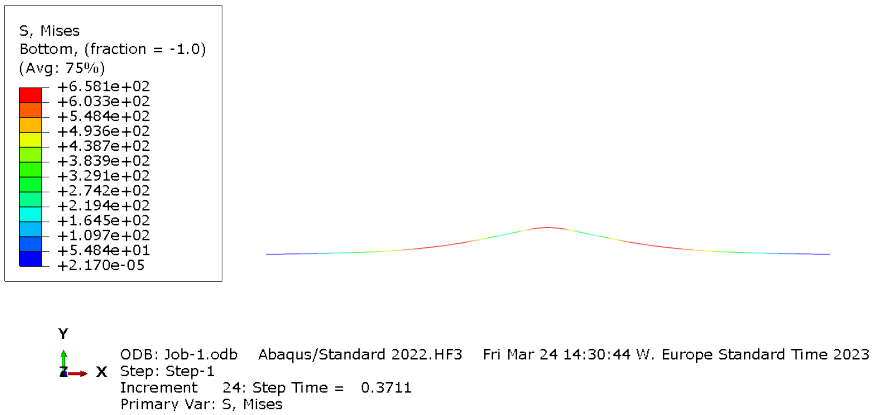

Figure 3.15: *The deformed shape of SBD dowel with 2 shear planes, yielded parts displayed in red and deformation scale factor of 5*

When comparing the failure mode of the STA dowel in figure 3.12 with the SBD dowel, it is observed that the more slender SBD dowel developes failure mode h in figure 2.13 with three plastic hinges and the STA dowel mode g with one plastic hinge. Another observable difference from the load displacement graphs in figures 3.12 and 3.14 is that the strain hardening does not appear as clear for the STA dowel as for the SBD dowel. This goes in hand with that more deformations might occur in the timber, rather in the metal fastener for the STA dowel.

The numerical yield and maximum loads at approximately 10 mm deformation, according to figure 3.14, are shown in table 3.13. The loads are to be compared with the calculated maximum load with *Johansen* equations according to Appendix A.5 for different embedment strengths.

Table 3.13: *Yield load and maximum load of the connection from non linear analysis of one SBD dowel with 2 shear planes in glulam material GL30c, compared with analytical calculations from Eurocode 5 with Johansen equations*

	FEM	**FEM**	**Eurocode 5**
Embedment strength $[N/mm^2]$	Yield load [kN]	Maximum load [kN]	Calculated maximum load [kN]
$f_{h,0,m} = 32.6$	6.5	18.8	14.7
$f_{h,90,m} = 22.3$	4.5	14.7	12.2
$f_{h,0,k} = 29.6$	6.2	17.8	14.0
$f_{h,90,k} = 20.2$	4.0	13.5	11.6

Table 3.14 compares results for the stiffness parameters evaluated by the beam on elastic foundation model for the SBD Dowels with one plate and/or two shear planes with the corresponding analytical values form Eurocode 5 and SIA265.

Table 3.14: *Stiffness from non linear analysis of one SBD dowel as beam elements on elastic springs in glulam material GL30c, compared with analytical calculations*

Non linear analysis				
Embedment strength $[N/mm^2]$	$K_{ser,0}$ [kN/mm]	$K_{ser,90}$ [kN/mm]	$K_{u,0}$ [kN/mm]	$K_{u,90}$ [kN/mm]
$f_{h,0,m} = 32.6$	9.0	-	4.9	
$f_{h,90,m} = 22.3$	-	7.1	-	4.0
$f_{h,0,k} = 29.6$	7.8	-	4.7	-
$f_{h,90,k} = 20.2$	-	6.2	-	3.4
Analytical values				
Eurocode 5	11.6	11.6	7.8	7.8
SIA265	7.3	3.6	4.9	2.4

3.3.2.4 SBD dowels with 4 shear planes

The dimensions of an SBD dowel in a connector with 4 shear planes are shown in figure 3.16. A paper by [Jockwer et al., 2021] presents recommendations for the side member thicknesses in relation to the inner timber member thickness for doweled slotted in plate connections. To obtain advantageous load distribution along the thickness, it is recommended that the side members have around 32-50% of the inner thickness. This recommendation was not exactly fulfilled for the case with 2 slotted in plates and 3 slotted in plates in section 3.3.2.5 since considerations to screw holes in the flange and other geometries also were needed. However further development should consider the recommendations better.

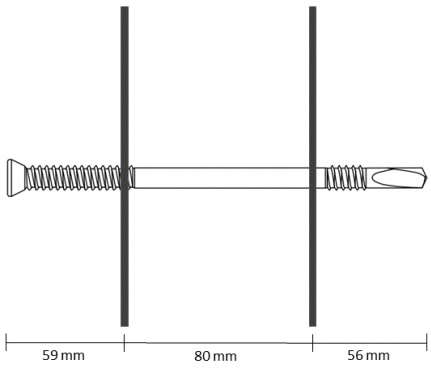

Figure 3.16: *An illustration of the dimensions of an SBD dowel placed in 2 slotted-in-steel plates with 5 mm thickness*

The deformed shape and failure mode from analysis of this configuration is displayed in figure 3.17.

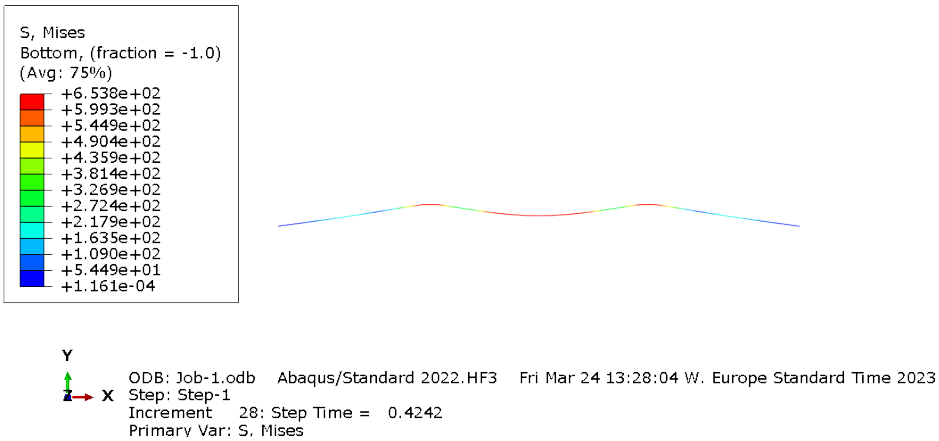

Figure 3.17: *The deformed shape of SBD dowel with 4 shear planes, yielded parts displayed in red and deformation scale factor of 5*

The load displacement curve from the non linear analyses of SBD dowel with 2 slotted in plates are plotted in figure 3.18 with characteristic and mean strength for

timber as well as parallel and perpendicular load to grain angle.

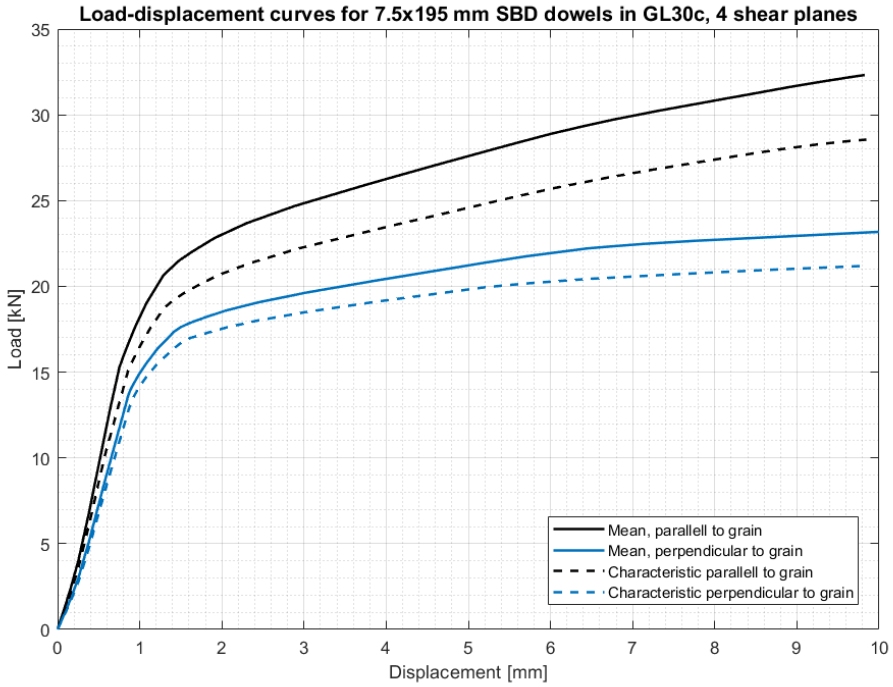

Figure 3.18: *Load displacement for the SBD dowels with two slotted in 5 mm plates, 4 shear planes, loaded parallel and perpendicular to the grain. Embedment model according to equation 2.38 with mean material values for GL30c*

The numerical yield and maximum loads at approximately 10 mm deformation, according to figure 3.18, are shown in table 3.15. The loads are to be compared with the calculated maximum load with *Johansen* equations according to Appendix A.5 for different embedment strengths.

Table 3.15: *Yield load and maximum load of the connection from non linear analysis of one SBD dowel with 4 shear planes in glulam material GL30c, compared with analytical calculations from Eurocode 5 with Johansen equations*

	FEM	**FEM**	**Eurocode 5**
Embedment strength $[N/mm^2]$	Yield load [kN]	Maximum load [kN]	Calculated maximum load [kN]
$f_{h,0,m} = 32.6$	15.0	32.0	29.5
$f_{h,90,m} = 22.3$	14.0	23.0	24.4
$f_{h,0,k} = 29.6$	14.5	26.5	28.1
$f_{h,90,k} = 20.2$	13.0	21.0	23.2

Table 3.16 compares results for the stiffness parameters evaluated by the beam on elastic foundation model for the SBD Dowels with two plates and/or 4 shear planes with the corresponding analytical values form Eurocode 5 and SIA265.

Table 3.16: *Stiffness from non linear analysis of one SBD dowel as beam elements on elastic springs with two 5mm slotted in steel plates and 4 shear planes. In glulam material GL30c, compared with analytical calculations*

Non linear analysis				
Embedment strength $[N/mm^2]$	$K_{ser,0}$ [kN/mm]	$K_{ser,90}$ [kN/mm]	$K_{u,0}$ [kN/mm]	$K_{u,90}$ [kN/mm]
$f_{h,0,m} = 32.6$	22.5	-	17.9	-
$f_{h,90,m} = 22.3$	-	20.1	-	13.4
$f_{h,0,k} = 29.6$	19.0	-	14.8	-
$f_{h,90,k} = 20.2$	-	17.5	-	12.2
Analytical values				
Eurocode 5	23.3	23.3	15.5	15.5
SIA265	14.6	7.3	9.7	4.9

3.3.2.5 SBD dowels with 6 shear planes

For the model of SBD dowels with 3 slotted-in-steel plates, the distances between the 5 mm thick plates along the 195 mm long dowel, is illustrated in figure 3.19.

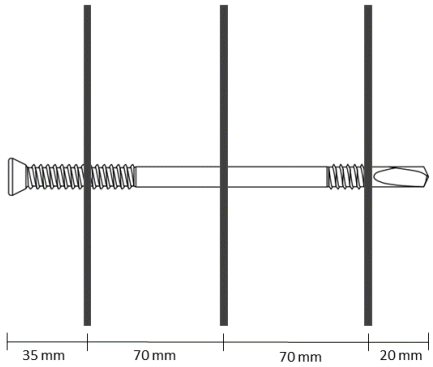

Figure 3.19: *An illustration of the dimensions of an SBD dowel placed in 3 slotted-in-steel plates*

The deformed shape and failure mode from analysis of the configuration of 3 plates is displayed in figure 3.20.

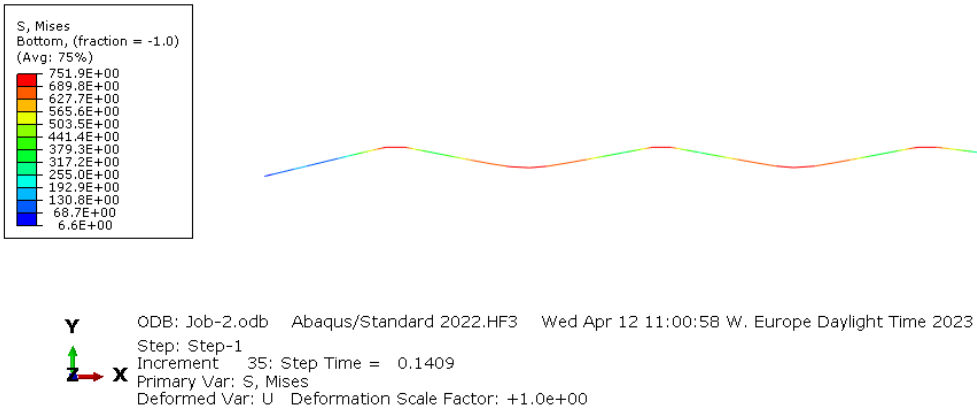

Figure 3.20: *The deformed shape of SBD dowel with 6 shear planes, yielded parts displayed in red and deformation scale factor of 5*

The load displacement curve from the non linear analyses of SBD dowel with 2 slotted in plates are plotted in figure 3.21 with characteristic and mean strength for timber as well as parallel and perpendicular load to grain angle.

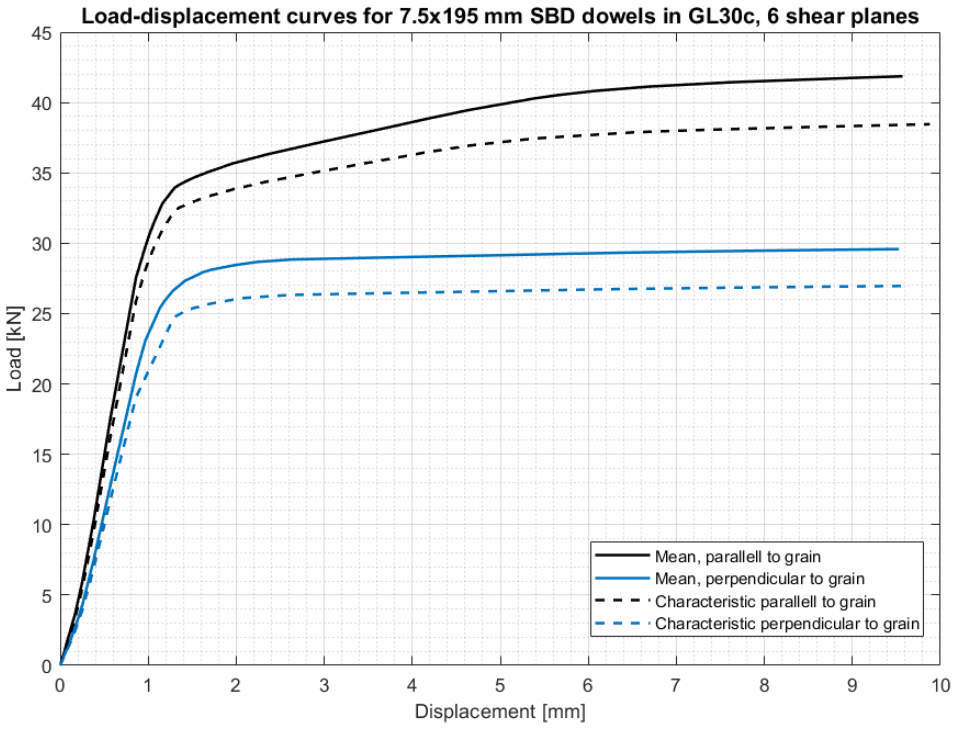

Figure 3.21: *Load displacement for the SBD dowels with three slotted in 5 mm plates, 6 shear planes, loaded parallell and perpendicular to the grain. Embedment model according to equation 2.38 with mean material values for GL30c*

The numerical yield and maximum loads at approximately 10 mm deformation, according to figure 3.21, are shown in table 3.17. The loads are to be compared

with the calculated maximum load with *Johansen* equations according to Appendix A.5 for different embedment strengths.

Table 3.17: *Yield load and maximum load of the connection from non linear analysis of one SBD dowel with 6 shear planes in glulam material GL30c, compared with analytical calculations from Eurocode 5 with Johansen equations*

	FEM	**FEM**	**Eurocode 5**
Embedment strength $[N/mm^2]$	Yield load [kN]	Maximum load [kN]	Calculated maximum load [kN]
$f_{h,0,m} = 32.6$	28.0	42.0	44.2
$f_{h,90,m} = 22.3$	22.0	29.0	36.5
$f_{h,0,k} = 29.6$	26.0	36.0	42.1
$f_{h,90,k} = 20.2$	19.0	27.0	34.8

Table 3.18 compares results for the stiffness parameters evaluated by the beam on elastic foundation model for the SBD Dowels with three plates and/or 6 shear planes with the corresponding analytical values form Eurocode 5 and SIA265.

Table 3.18: *Stiffness from non linear analysis of one SBD dowel as beam elements on elastic springs with three 5mm slotted in steel plates and 6 shear planes. In glulam material GL30c, compared with analytical calculations*

Non linear analysis				
Embedment strength $[N/mm^2]$	$K_{ser,0}$ [kN/mm]	$K_{ser,90}$ [kN/mm]	$K_{u,0}$ [kN/mm]	$K_{u,90}$ [kN/mm]
$f_{h,0,m} = 32.6$	34.2	-	30.3	-
$f_{h,90,m} = 22.3$	-	25.2	-	23.9
$f_{h,0,k} = 29.6$	31.7	-	29.1	-
$f_{h,90,k} = 20.2$	-	23.2	-	19.1
Analytical values				
Eurocode 5	34.9	34.9	23.3	23.3
SIA265	21.8	10.9	14.6	7.3

3.3.3 Component FE-models of beam to column connections

Component FE-models were developed to model the load deformation behaviour of different beam to column connectors. The purpose with the models was to simulate how different connectors behave mechanically and how the stiffness develops with increasing loading up to maximum load. The load deformation information that was of interest for the beam to column connections is the vertical displacement with increasing load from a beam, as well as the moment rotation relationship at the joint, when a beam connected to connector is subjected to an increasing moment.

Non linear FE-models with elastic - plastic non linear material models as well as non linear springs were developed in Abaqus CAE in 3 dimensions. The models are able

to simulate the planar behaviour of a beam and its connection at the end support. The models were built with the following components:

- Non linear spring elements representing individual fasteners and the deformation of fasteners in the timber.
- Shell elements representing metal plates of the connectors, with elastic-plastic material model and isotropic strain hardening according to section 2.5.2.5
- Solid elements to model the timber column where the metal connectors have contact to the column, orthotropic linear elastic material model.
- Beam elements to represent the loaded timber beam that the connector is supporting, with orthotropic linear-elastic material model.
- Rigid link between each spring element representing the dowels, and to which the loading from the beam is applied.

Figure 3.22 shows the various components of the model and its geometries.

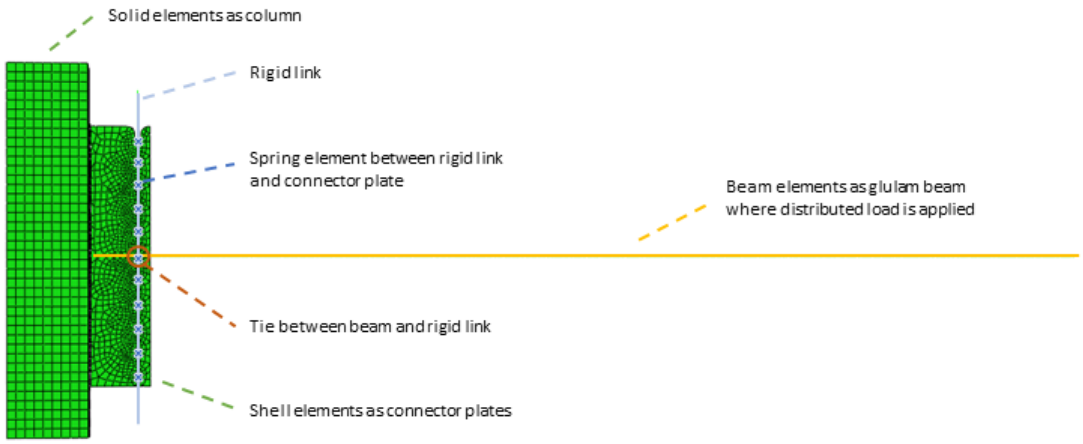

Figure 3.22: *Description of components of the FE-model of Alumaxi 704 STA connection, created in Abaqus*

The result for moment, rotation and displacement at the connection for all analyses are taken from the shear center for where the beam is supported on the connections, which in figure 3.22 is the point where the beam is tied to the rigid link.

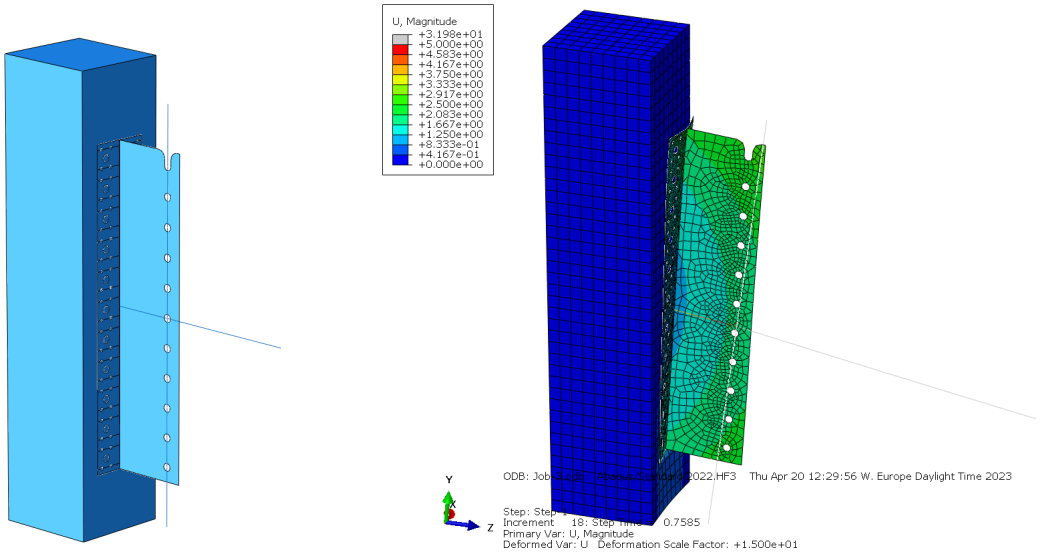

Figure 3.23: *To left: The assembly of the connection FE-model in 3D. To right: Deformed model with scale factor 15, load applied on the beam.*

3.3.3.1 Material properties

The FE-model of the timber connection includes the timber parts, the connector and the fasteners. Table 3.19 displays the timber's input data that is designed in GL30c. The material of the fasteners is presented respectively in table 3.5 and 3.9. The Alumaxi connector is usually manufactured with aluminium alloy and the material properties according to table 3.20. However, in this project, connectors is also studied with the material data of S235 shown in table 3.21.

Table 3.19: *Material properties' input data for the timber parts in glulam*

Glulam - GL30c		
Modulus of Elasticity	E_L	13000 MPa
	E_R	300 MPa
	E_T	300 MPa
Shear modulus	G_{LR}	650 MPa
	G_{LT}	650 MPa
	G_{RT}	65 MPa
Poisson ratio	v_{LR}	0.04
	v_{LT}	0.04
	v_{RT}	0.35

Table 3.20: *Material properties' input data for the Alumaxi connector in aluminium alloy*

Aluminium alloy - AW-6005A		
Elastic behaviour	Young's modulus	70 GPa
	Poisson's ratio	0.3
Plastic behaviour	Yield strength	250 MPa
	Ultimate strength	310 MPa
	Ultimate strain	0.1

Table 3.21: *Material properties' input data for the Alumaxi connector in steel*

Steel - S235		
Elastic behaviour	Young's modulus	210 GPa
	Poisson's ratio	0.3
Plastic behaviour	Yield strength	235 MPa
	Ultimate strength	360 MPa
	Ultimate strain	0.18

3.3.3.2 Fastening of the connector plate to the timber column

The support of the connector to the timber columns was modeled with non linear spring element of type "cartesian connector" in Abaqus. One spring element for each screw or nail was assigned and coupled to the holes in the shell elements representing the connector plate. These spring elements was not connecting the plate to the elements representing the column but instead connecting the plate with the assigned stiffness to the "ground" as referred in Abaqus. With other words, one end of the spring was asigned to have zero displacement and the other end was connected to the holes of the shell - metal plate.

The axial strength and stiffness of the springs representing the screws was assigned with analytical calculations according to Eurocode 5. The non linear behaviour is estimated with simplified bi-linear approach. The deformation was assumed to be 1 mm at withdrawal failure with the maximum load and the stiffness up to that load assumed linear elastic. After the maximum load, the withdrawal force was assigned to gradually decrease as the deformation decrease. The 1 mm displacement at whitdraval failure was based on the scales of the calculated axial stiffness in table 3.22. The force - displacement curve that was assigned to the non linear springs is plotted in figure 3.24.

Table 3.22 presents the withdrawal failure load and axial deformation for the fasteners that was implemented as spring elements in the component FE-models. Withdrawal loads are calculated according to Eurocode 5 and the calculations are reported in Appendix A.5.

Table 3.22: *Axial Strength and stiffness for different fasteners at the connection to the column*

	Anker nail (80 mm)	LBS screw (80mm)	LBS screw (100 mm)
Outer diameter	6 mm	7 mm	7 mm
Inner diameter	-	4.4 mm	4.4 mm
Penetration length	66 mm	68 mm	88 mm
$f_{ax,k}$ (Eurocode 5)	15.7 N/mm^2	15.2 N/mm^2	14.9 N/mm^2
$f_{ax,m}$ (Eurocode 5)	17.0 N/mm^2	16.5 N/mm^2	16.1 N/mm^2
$F_{ax,k}$ (Eurocode 5)	5.66 kN	6.35 kN	8.01 kN
$F_{ax,m}$ (Eurocode 5)	6.12 kN	6.86 kN	8.66 kN
$K_{ser,ax,90}$ (eq: 2.25)	-	22.1 kN/mm	26.4 kN/mm
$K_{ser,ax,90}$ (eq: 2.26)	-	14.3 kN/mm	18.5 kN/mm
$K_{ser,ax,90}$ (eq: 2.27)	-	10.1 kN/mm	11.2 kN/mm
$K_{ser,ax,90}$ (eq: 2.28)	-	6.59 kN/mm	9.49 kN/mm
$F_{ax,m} \div min(K_{ser,ax})$	-	1 mm	0.9 mm
Assumed deformation at withdrawal failure	1 mm	1 mm	1 mm

The lateral strength and stiffness of the screws was also assigned based on analytical equations and here only from Eurocode 5. The stiffness K_{ser} was assigned between 0 and 40 % of the ultimate load and K_u between 40 and 100 %. Table 3.23 shows these lateral strength and stiffness for the fasteners.

Table 3.23: *Latteral strength and stiffness for different fasteners at the connection to the column*

	Anker nail (80 mm)	LBS screw (80mm)	LBS screw (100 mm)
Outer diameter	6 mm	7 mm	7 mm
Inner diameter	-	4.4 mm	4.4 mm
Penetration length	66 mm	68 mm	88 mm
$f_{h,k}$ (Eurocode 5)	30.1 N/mm^2	19.9 N/mm^2	19.9 N/mm^2
$f_{h,m}$ (Eurocode 5)	33.1 N/mm^2	22.0 N/mm^2	22.0 N/mm^2
$F_{0,k}$ (Eurocode 5)	5.7 kN	4.3 kN	4.7 kN
$F_{0,m}$ (Eurocode 5)	6.0 kN	4.5 kN	5.0 kN
K_{ser} (Eurocode 5)	4.6 kN/mm	3.7 kN/mm	3.7 kN/mm
K_u (Eurocode 5)	3.1 kN/mm	2.5 kN/mm	2.5 kN/mm

Figure 3.24 shows the load deformation relation curves that was implemented for 80 mm LBS screws as non linear springs.

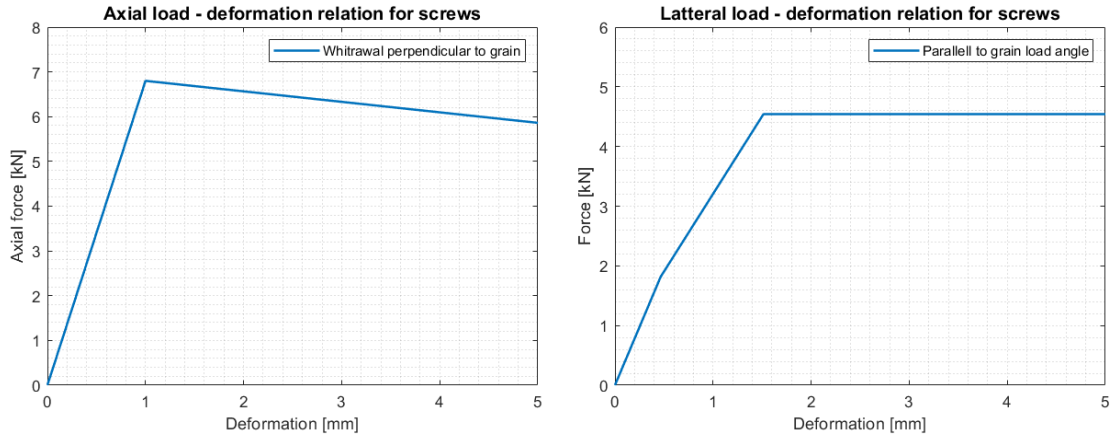

Figure 3.24: *Assumed load displacement curves for 80 mm LBS screws. To left: axial load deformation relation. To right: lateral load deformation relation.*

3.3.3.3 Timber column modeled as solid elements

The timber column was included in the model to simulate the interaction that occur at the contact zone between the connector and the column. As the moment in the connection increases, the rotation does so as well and there will become compression zone between the lower regions of the flange of the connector and the column. The column was assigned with solid 3D elements in Abaqus and material properties was set to orthotropic with enginnering constans as specified in table 3.19. The interaction between the column and the connector was assigned as hard contact with penelty in Abaqus, which means that a friction constant was defined to determine the tangential force in relation to the normal force. Assignment of friction coefficient is treated in section 2.1 and it was set to 0.25 in all simulations.

3.3.3.4 Dowels connecting the beam to the metal connector

The dowels were also represented with non linear springs implemented as cartesian connector elements in Abaqus. The load displacement relations obtained with the non linear beam on elastic foundation simulations were used as input data for the non linear springs to simulate the stiffness of each dowel. The springs were assigned to have different stiffness and strength in x and y direction to simulate the different behaviour in loading parallel and perpendicular to the grain direction. The x direction was used to represent the parallel grain direction and y the perpendicular. One end of the the cartesian connector elements, is tied to a reference point which in turn is connected to the holes for dowels in the web of the connector. The other end of the cartesian connector element is tied to a rigid link which joins all the the simulated dowels together.

The input data that was assigned to the cartesian connector elements are presented in figure 3.11, in which the load deformation relation for the STA dowels based on mean embedment strength are reported.

3.3.3.5 The glulam beam

Two-dimensional beam element was used for modeling the glulam beam, and was tied to the rigid link at the shear center of the dowel fastener group. The beam was modeled with half the length of the span, i.e. 7.5/2 with symmetry boundary conditions at the opposite end of the connection, which would be the center of the beam. As the spatial as well as rotation degrees of freedom of the beam was tied to the rigid link, moment in the beam can be transferred, and the stiffness of the connection can in this way effect the moment distribution in the beam. However This configuration spreads the loading from the timber beam more evenly on the dowels, and does not account for deformations within a beam, between the dowel fasteners which could result different load distribution on the dowels.

The beam was assumed to behave linear elastically and non linear material effects of the glulam beam was neglected. The material properties for the timber was assigned as orthotropic with engineering constants, as specified in table 3.19. A line load was assigned along the beam element as the distributed load that is increasing on the system with increments.

A different and more computational effort requiring approach for modelling the glulam beam was also tested in a sensitivity study. To identify how deformations in the timber between the dowels might influence the total stiffness of the connection, the rigid link was removed, and 2 dimensional beam elements as the glulam beam replaced with shell elements. These shell elements with a shell section thickness of 215 mm were then instead simulating the beam. With this configuation, the cartesian connector elements as the dowels instead were connected to nodes on the shell element beam.

3.3.4 Evaluation of stiffness and capacity of connections

To compare the performance of different connectors modeled accordingly with the principles described in section 3.3 , a reference context was implemented. A reference beam with material properties for GL30c is used. The context in which this beam is from the case study building, *Uppsala Lighthouse*. The span length of the beam is 7.5 m long and the beam is connected between columns as presented in figure 3.3. Table 3.24 presents data for the beam that was used in calculations, simulations and comparisons as well as shear force and moment capacity according to Eurocode 5.

Table 3.24: *The cross-section, material and capacity data of the studied beam from the case study building Uppsala Lighthouse*

Cross-section data	b	h	I	W
	215 mm	810 mm	$9.52 \cdot 10^{-3}$ m^4	$2.35 \cdot 10^{-2}$ m^3
Material data	$E_{0.05}$	$E_{0,m}$	$f_{m,k}$	$f_{v,k}$
	10.8 GPa	13 GPa	30 MPa	3.5 MPa
Capacity	$M_{y,k}$	$M_{y,D}$	$F_{v,k}$	$F_{v,D}$
	705 kNm	465 kNm	291 kN	186 kN

The results that are sought for from the analyses of different connectors are the following:

- Rotational stiffness of the connection
- Vertical stiffness of the connection
- Effect the connectors have on the moment distribution on the reference beam
- Yielding load and moment at the connection
- Maximum load and moment at the connection
- Ductility as ratio between maximum load and yield load

3.3.4.1 Verification

For comparisons of rotational stiffness from FE-models with analytical calculations, analytical stiffness values K_{ser} from Eurocode 5 and SIA265 was applied. By Using equation 2.16 the rotational stiffness could then be estimated. However this would only consider the contribution of all the laterally loaded dowels with polar moment of inertia in the connection. This method will not consider deformations occurring anywhere else in the connections, like in the connection to the column or deformations in the metal of the connector. Additional FE-simulations were therefor implemented to make the comparison more appropriate, by isolating the dowel group from the rest of the connections and only simulate the moment rotation relation for the dowel fastener group.

The simulations of load displacement relations for the connections were also made with two different ways of loading. One way of applying loads to the connections was to apply a pair of forces that only cause a moment at the connections. The other way was to connect the reference beam to the connections and then apply the loading to the system as a distributed load on the reference beam.

The results from analytical calculations compared with component FE-model is presented in table 4.4.

The interaction between the moment at the supports in the connections and in the mid span of the reference beam for different levels of loading was evaluated with the basis of Euler–Bernoulli beam theory. By studying Elementary case equations for linear elastic beams, the expression in 3.8 for the rotation θ at the supports could be written for beams loaded with equally distributed loads and where a moment is acting at the supports:

$$\theta = \frac{q \cdot L^3}{24 \cdot EI} - \frac{M_{s1} \cdot L}{3 \cdot EI} - \frac{M_{s2} \cdot L}{6 \cdot EI} \tag{3.8}$$

- q is the distributed load [N/m]
- M_{s1} and M_{s2} are the support moments [Nm]
- EI is the bending stiffness $[N \cdot m^2]$
- L is the beam span length [m]

As the beam beam is loaded with an equally distributed load and the connections at both ends of the beam are assumed to have the same stiffness, the support moments M_{s1} and M_{s2} will be equal. With the principles presented in section 2.2.1.1, the moment in the mid span of the beam can be calculated as follows:

$$M_b = M_{max} - M_s = \frac{q \cdot L^2}{8} - M_s \tag{3.9}$$

With the non linear simulation of the moment rotation with the component FE-models, data for the rotation in the joint together with corresponding moment in the mid span and at the support of the reference beam can be extracted. These extracted values from the modelling were then analytically checked against equation 3.8 and 3.9

3.4 Development and evaluation of alternative connection designs

The process for developing stiffer and possibly more efficient connections is here presented. Different variations of the connection design that are believed to give stiffer response will be evaluated. The following configurations of the beam to column connection will be treated:

- One slotted in metal plate with a larger flange that can host a circular pattern of STA dowels.
- Two slotted in steel plates with self drilling SBD dowels
- Three slotted in steel plates with self drilling SBD dowels

3.4.1 circular pattern with STA dowels

The first steps in an effort to achieve stiffer connection designs was to test some modifications on the Alumaxi 704 connector. In an preliminary attempt the web

and the pattern of holes for STA dowels was modified. A circular pattern with 12 STA Dowels with a radius of 230 mm was tested. The geometries of the modified connector are presented in figure 3.25 and the FEM model of this connection configuration is presented in figure 3.26. The material input data for the timber column and aluminium connector was the same as presented in tables 3.19 and 3.20 and the spring stiffness representing the screws to the column was the data for 80 mm LBS screws presented in table 3.22 and 3.23 for axial and lateral stiffness.

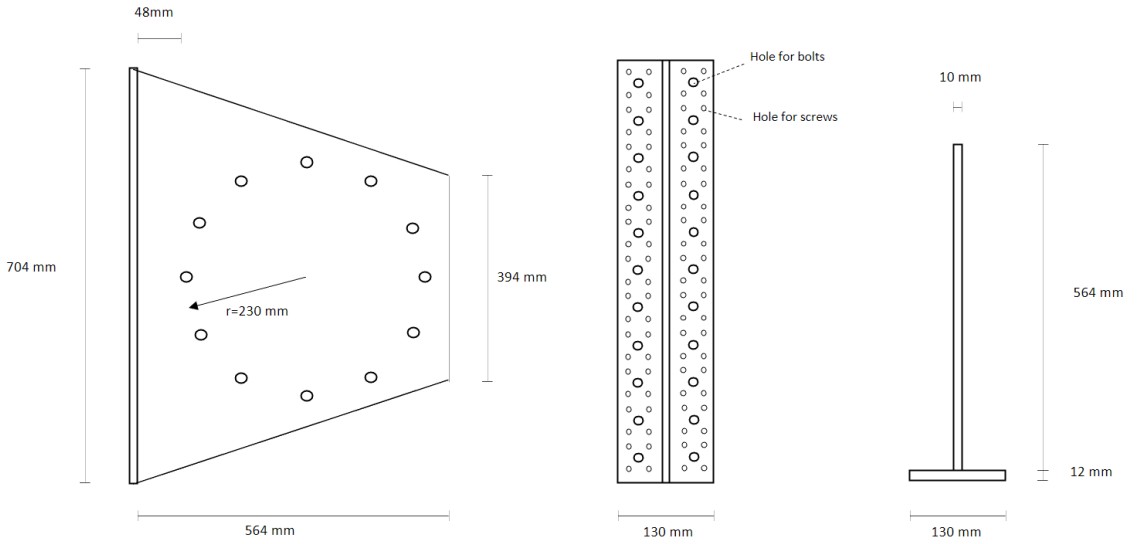

Figure 3.25: *The geometry and dimensions of the modified connector with circular pattern and STA dowels*

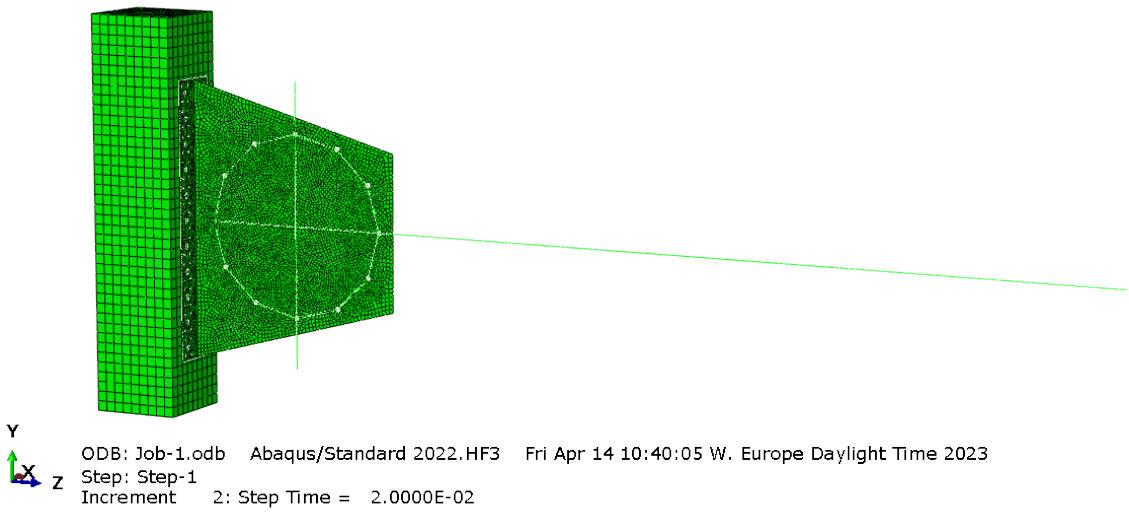

Figure 3.26: *The meshed FE-model of the modified connector with circular pattern and STA dowels*

The nonlinear springs that represent the mechanical behaviour of the STA dowels in the timber, were in this model assigned with the same method as the first model

described in section 3.3.1.

To improve the modified connection, further modifications where made and analysis where some parameters were changed to identify potential improvements for stiffer response. The chances and the results on the stiffness and moment at the support of the beam are presented in table 4.6 and the following modifications were analysed:

- Adding steel rods into the connection to the column. 16 screws were removed and 4x m16 or m24 steel rods of grade 8.8 were added. 2 at the bottom and 2 at the top of the connector plate. The material input data is presented in table 3.9. The rods were modeled as beam on elastic foundation.

- Changing material of the connector from aluminium to steel S235. The material input data is presented in table 3.21.

- Increasing the flange thickness, the plate that is connected with screws and bolts to the column. The initial flange thickness was 12 mm and it was increased to 20 mm.

Figure 3.27 shows a side view and sketch of the modified connectors with bolts through the column in between the beams. The connector is designed and modeled with two bolts/rods at the top, and two at the bottom.

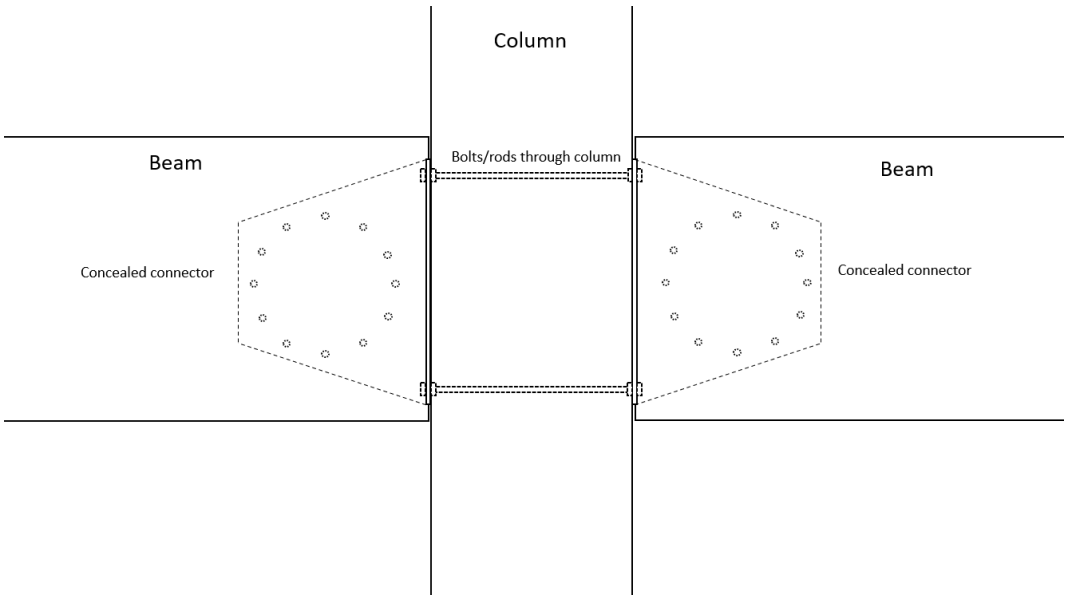

Figure 3.27: *A side view of the modified circular patterned connector with bolts connecting two beams and a column in between*

3.4.2 Two slotted in steel plates with self drilling SBD dowels

For a dowel-type connection, the number of shear planes influence its capacity significantly. A shear plane can be defined as the face of a connector's plate where shear stresses are produced in the dowel at its radial direction. The number of shear planes shapes the failure mode of the fastener according to figure 2.13. Increasing the number of shear planes increases the interfacing area between the plate and fastener which reduces the maximum stress in the dowel.

In order to investigate the impact of doubled number of shear planes, the Alumaxi connector with SBD dowels presented in section 3.2.5.2 was modified. The FE-model of this developed connector with 2 webs/4 shear planes is presented in figure 3.28, and figure 3.29 shows its geometry. In this configuration, the flange is broaden and number of screws into column is increased to 120 and the thickness of each web is decreased to 5 mm. The depth of the web is also increased in order to host several dowels in an row. Distances between the dowels are designed according to the minimum demands in EC5, see figure 3.29. Note that in this modification the flange and webs of connector are chosen to be in steel (S235), see table 3.21 for the material properties.

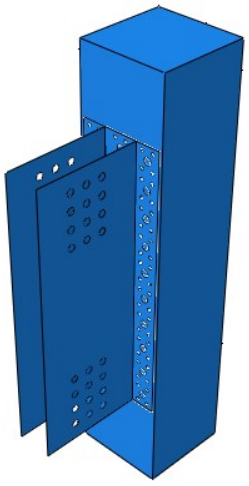

Figure 3.28: *The modified model of two slotted in steel plates with self drilling SBD dowels*

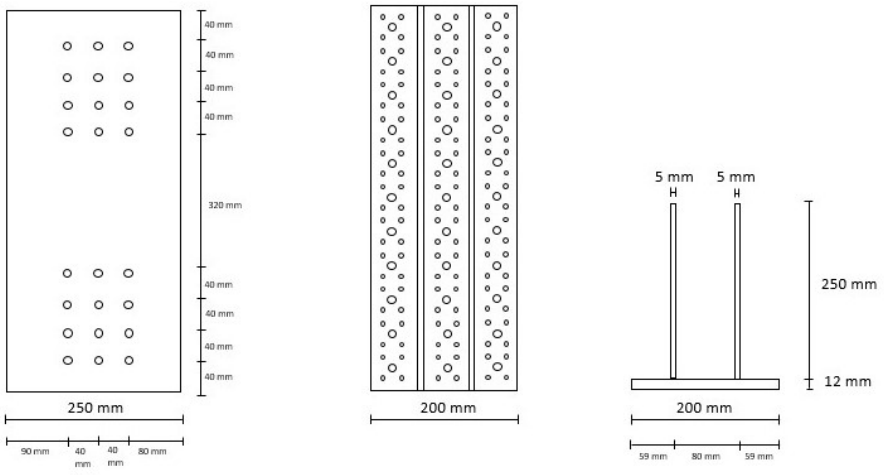

Figure 3.29: *The geometry and dimensions of the modified model of two slotted in steel plates with self drilling SBD dowels*

3.4.3 Three slotted in steel plates with self drilling SBD dowels

To investigate a stiffer model variation, an connector with three slotted in steel plates was also modelled, see figure 3.30. The flange is further widened, yet the number of screws if the same as the previous configuration, see figure 3.31. The dowel interspaces and web geometry are also the same as the 4-shear-plane model.

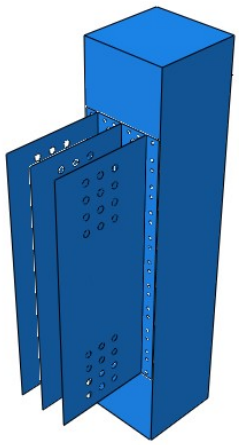

Figure 3.30: *The modified model of three slotted in steel plates with self drilling SBD dowels, 640 mm high*

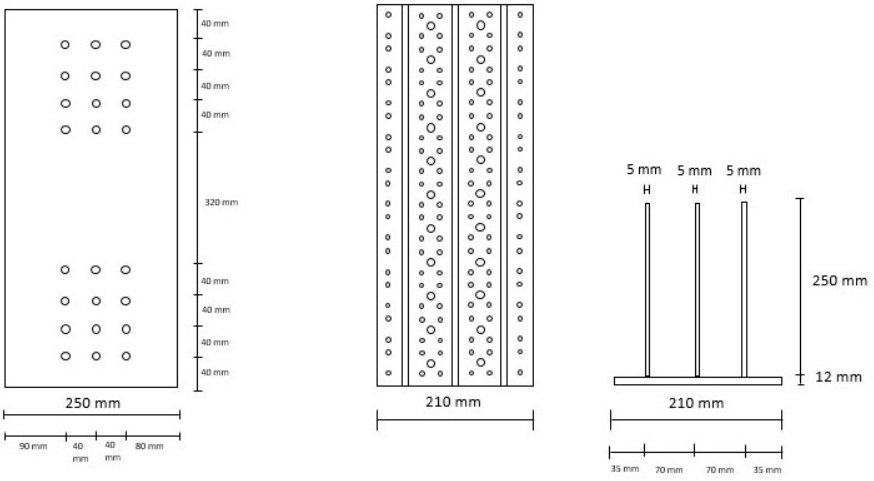

Figure 3.31: *The geometry and dimensions of the modified model of three slotted in steel plates with self drilling SBD dowels, 640 mm high*

The results of the simulations of the two Alumaxi versions are presented and discussed in the next chapter. The stiffness of the these exemplifications is to be compared with the pristine Alumaxi SBD connector.

3.5 Modelling of the structural system

The building is modelled in RFEM utilizing the same dimensions and material choice of different structural components as the original design. These dimensions are calculated by the structural engineers at a consultant company to withstand the relevant structural loads at the building.

The main frame work of the building is embodied of glulam columns and beams of different cross-sections. All glulam members in the model have the default material properties of GL30c and GL30h with isotropic linear elastic material model.

The shear walls are CLT-walls modelled as laminated surfaces with a thickness and stiffness built up by several 30 mm softwood laminates of timber grade C24. These layers are orientated perpendicular to each other's grain direction, see figure 3.32. With this input information of layers as the thickness of a surface, RFEM calculates an overall stiffness that is implemented for the surface in the model.

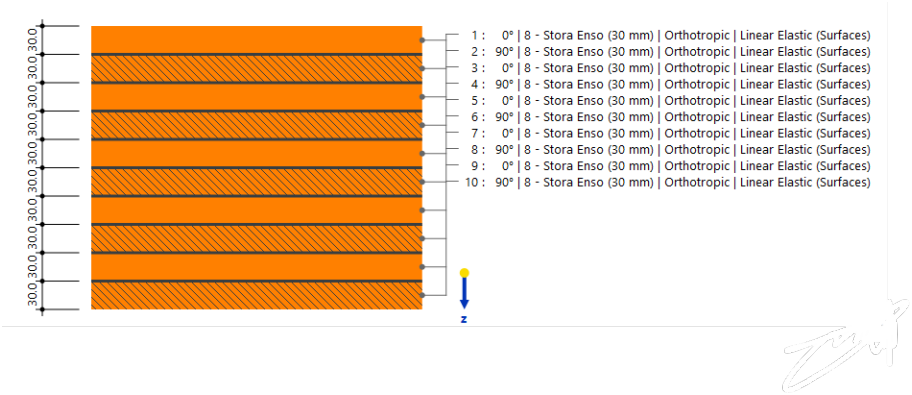

Figure 3.32: *Surface thickness composed of 10 layers CLT, used for modelling the 300 mm thick CLT walls in the building. Dimensions in mm*

The one way floor slabs are modelled as 250 mm thick surfaces with modified stiffness properties to simulate the one way action of the slabs. The stiffness in the load carrying direction was set to 33 GPa and the stiffness in the other direction was neglected. The shear modulus and density of the surface elements were set to the material properties of concrete class C30/37.

Some concrete columns are built in the first storey with concrete class C35/45, reinforcement class B500S. Lastly, steel beams with strength class S355 are designed to replace some glulam beams in the structural framework as shown in figure 3.1.

3.5.1 Assignment of stiffness at connections

The plates that model the stabilizing systems with CLT walls were assigned with "line hinges" in RFEM to represent joints between the CLT walls at each floor. The

plates were allowed to rotate freely at the boundary but the transnational degrees of freedom for shear was assigned with a stiffness that allows the plates to slide on the edges. The value of this stiffness is assigned in kN/m^2 which means kN/m of 1 meter support length. The stiffness values for the CLT supports were set to values recommended by Dlubal tutorials which was 7700 $[kN/m^2]$. This stiffness was not changed in simulations since the impact of the beam and column connections stiffness is the main subject to study in this case.

The rotational stiffness for supports of timber beams in the building were changed in simulations with different load cases to study the impact on global deformations and internal forces in some members. The magnitude of this rotational stiffness is based on the finite element analysis of connections according to section 3.3. As the beams in the reference building are carried out with double glulam beams with width of 215 mm and two connectors at each support, the calculated rotational stiffness for one connector is multiplied with 2 and assigned to the "member hinges" in RFEM. The different rotational stiffnesses that were simulated was 0, 11 MNm/rad and 22 MNm/rad. Simulations with infinite rotational stiffness was also tested to study how sensitive this structural system is to these parameters. The stiffness of supports of the glulam columns present in the building was never calculated but as there likely would be a significant stiffness at these supports, the same rotational stiffness as for the beams were assumed and assigned for the column supports.

The orthotropic plate that model the hollow core one way floor slabs are supported on the glulam beams and at these supports "line releases" are assigned in RFEM to decouple the rotation of the plate to the beams. This setting is assigned since it is more realistic that moments and rotations in the plate are not transferred to the beams as the plate should be simply supported.

4

Results

4.1 Alumaxi connector results

4.1.1 704 STA connector

Figure 4.1 shows the load displacement curves for Alumaxi 704 connector with STA dowels, from a simulation when the connector is supporting the reference beam as presented in section 3.2.5 and the beam is loaded with an increasing distributed load. The input data for this simulations was based on mean material values for glulam GL30c. The load for which yielding starts in the connection is marked yellow in the figure 4.1.

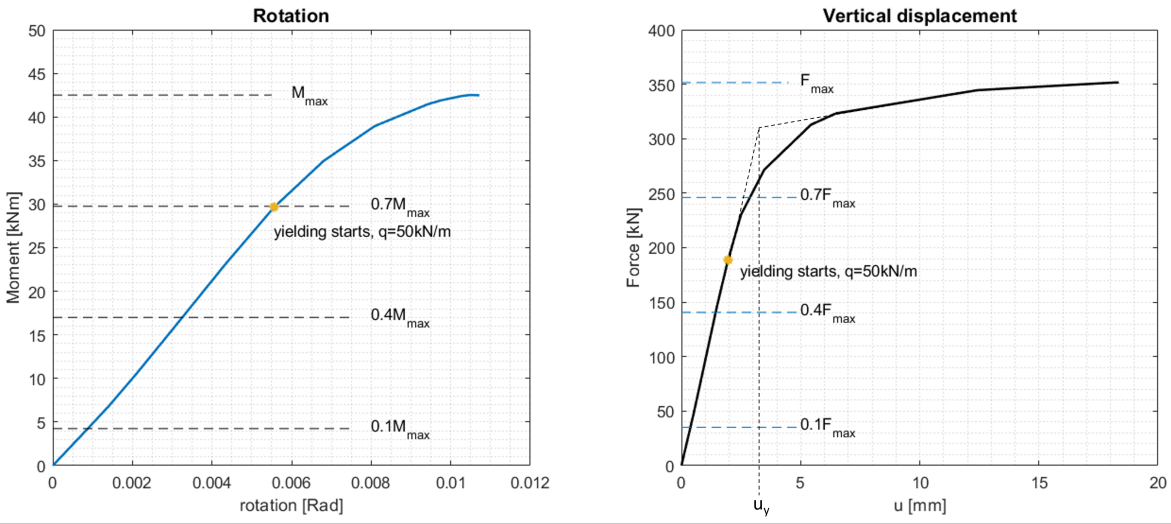

Figure 4.1: *Deformations at Alumaxi 704 STA connection when supporting a 7.5 m, 215x810 mm GL30c beam loaded with distributed load increasing up to 94 kN/m*

Table 4.1 shows stiffness parameters of the connection based on the simulation. k_{ser} is calculated between 10 and 40% of the maximum load, and k_u is calculated betwen 0 and 70% of the maximum load. These limits are marked in figure 4.1

Table 4.1: *The stiffness of Alumaxi 704 STA calculated out of moment-rotation and vertical force-displacement graph*

Alumaxi 704 STA	k_{ser}	k_u
Vertical action	99 kN/mm	83 kN/mm
Moment - rotation	5.5 MNm/rad	5.3 MNm/rad

The deformations of the model with applied distributed load on the reference beam are presented in figure 4.2 with scale factor 15 and [mm] in the legend.

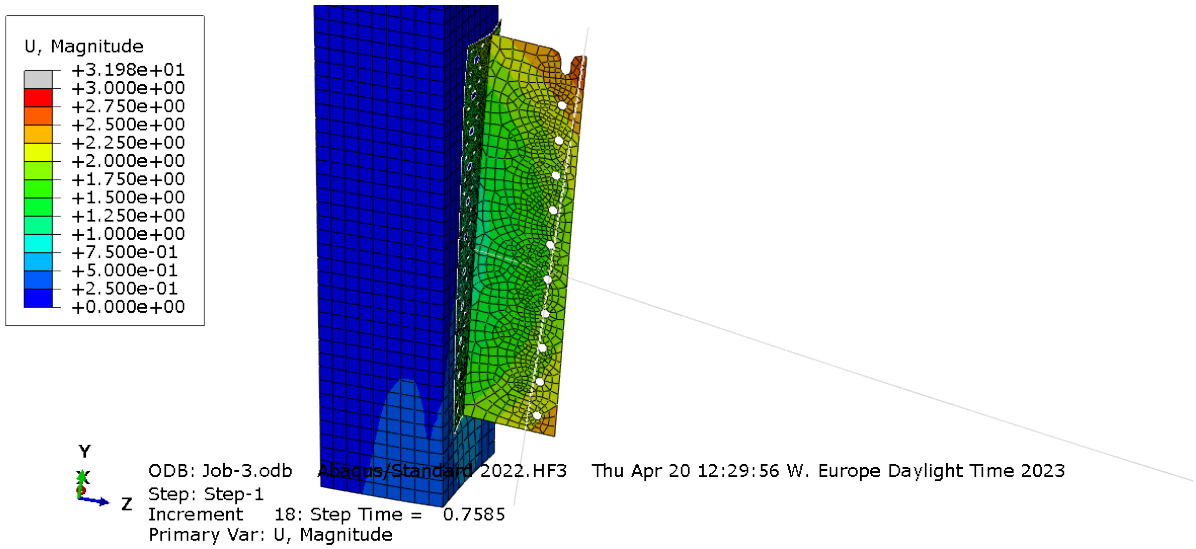

Figure 4.2: *Deformed model of the Alumaxi 704 STA connection, the reference beam is loaded with an distributed load. Deformation scale factor 15*

The deformations that cause the rotation at the connection in figure 4.2 are occurring at several locations. The springs that represent the stiffness of the dowels are deforming horizontally, which can be observed from the rigid link between the dowels and the beam. There are deformations at the flange of the connector, it bends in and out from the column. The flange is compressed in to the column at the lower regions and slightly withdrawn at the upper regions.

Figure 4.3 shows the moment distribution in the reference beam when supported by Alumaxi 704 STA and as the distributed load on the beam increases in the simulation. The moment at the connection, the moment in the mid span and the maximum moment which corresponds to the beam being simply supported without stiffness at the supports are plotted. The characteristic load and design load from the reference building is plotted as vertical dotted lines and the design moment capacity of the reference beam is plotted as a horizontal dotted line.

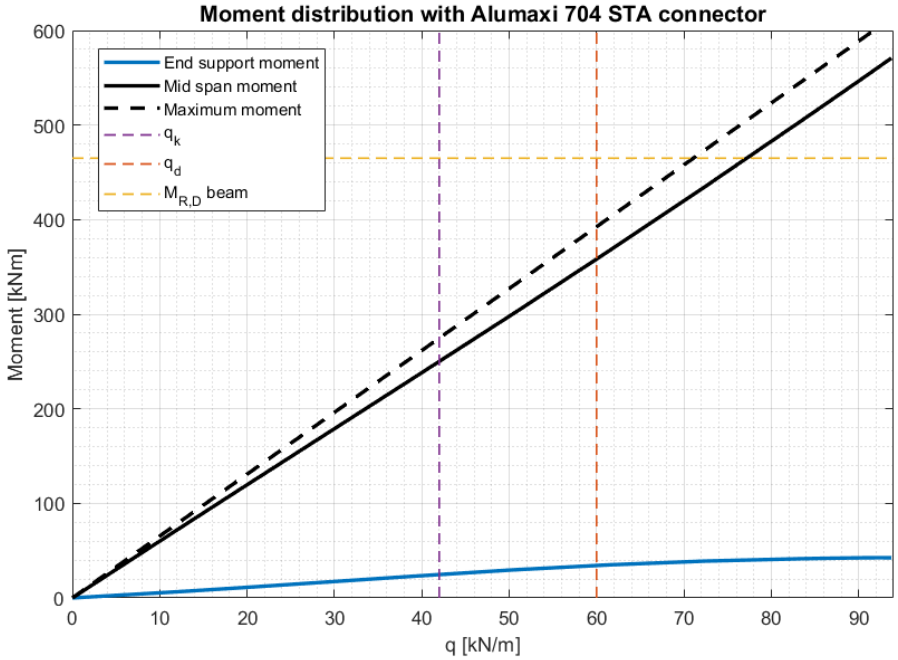

Figure 4.3: *The end support and mid span moment's distribution in relation to the increasing load in the reference beam, with Alumaxi 704 STA connector*

It can in figure 4.3 be observed that the moment in the beam is reduced from theoretical maximum span moment and that some moment is acting at the support. The moment in the support increases up to yielding and further on until the moment in the joint has reached its maximum level. After this, increasing loading on the beam only increases the moment in the span of the beam. This simulation of the connection result in that roughly 8-9% of the maximum moment is attracted to the support and the rest attracted to the span.

4.1.2 640 STA and SBD connector

The same analysis was made for different versions of the Alumaxi connector, one size smaller, i.e Alumaxi 640 with 10 STA dowels, and one version of Alumaxi 640 with 24 SBD dowels. These load deformation graphs from simulations are presented in figures 4.4 and 4.5 respectively.

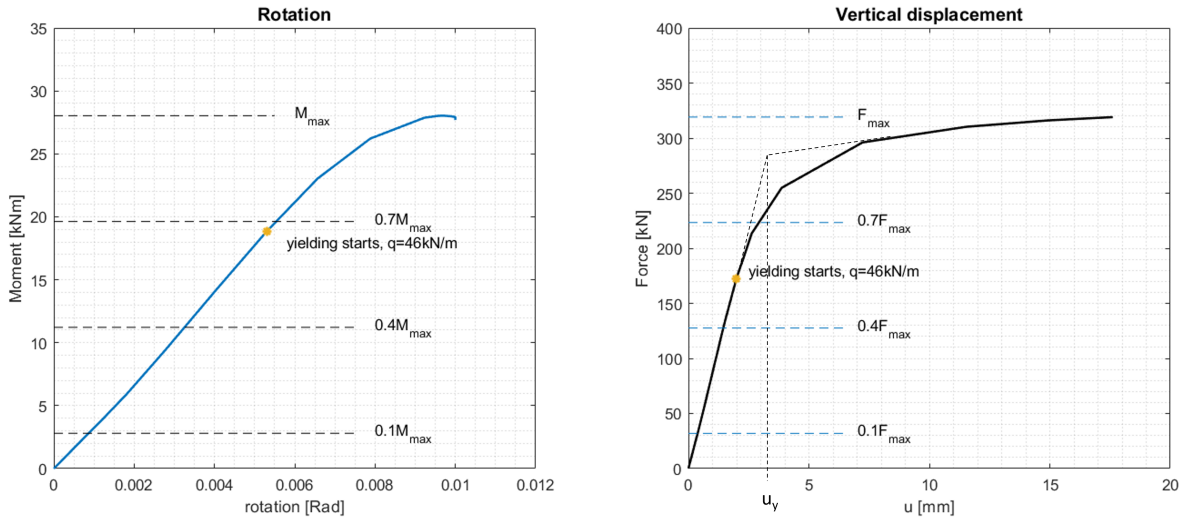

Figure 4.4: *Deformations at Alumaxi 640 STA connection when supporting a 7.5 m, 215x810 mm GL30c beam loaded with distributed load increasing up to 85 kN/m*

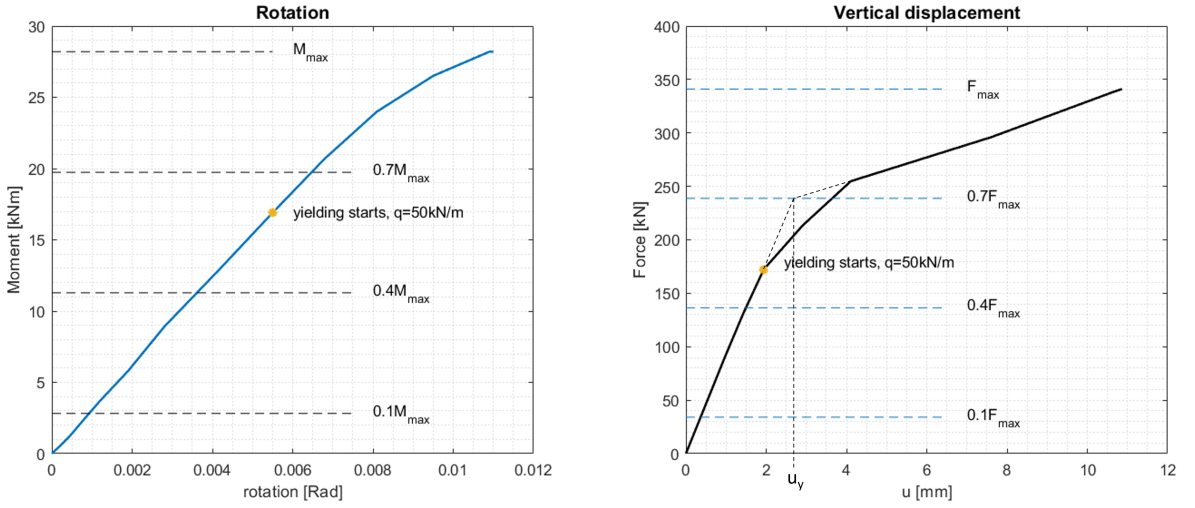

Figure 4.5: *Deformations at Alumaxi 640 SBD connection when supporting a 7.5 m, 215x810 mm GL30c beam loaded with distributed load increasing up to 94 kN/m*

Table 4.2 shows stiffness parameters of the connections based on the simulation. Where again k_{ser} is calculated between 10 and 40% of the maximum load, and k_u is calculated betwen 0 and 70% of the maximum load. These limits are marked in figures 4.4 and 4.5 for each case.

Table 4.2: *The stiffness of Alumaxi 640 with STA and SBD dowels, respectively calculated out of moment-rotation and vertical force-displacement graphs*

Alumaxi 640 STA	k_{ser}	k_u
Vertical action	89 kN/mm	82 kN/mm
Moment - rotation	3.7 MNm/rad	3.5 MNm/rad
Alumaxi 640 SBD	k_{ser}	k_u
Vertical action	88 kN/mm	62 kN/mm
Moment - rotation	3.1 MNm/rad	3.0 MNm/rad

4.1.3 Comparison of the connections

An approximate ductility factor can calculated for the vertical displacement as follows:

$$D \approx \frac{u_{max}}{u_y} \tag{4.1}$$

- u_{max} is the displacement when the maximum load is reached
- u_y is the displacement marked in the load-displacement graphs 4.1

The ductility of the previously presented versions of Alumaxi connections is approximated as in equation 4.1 and presented in table 4.3.

Table 4.3: *The ductility factor of Alumaxi connections calculated with u_{max} and u_y that are plotted from the load-displacement graph*

	u_y	u_{max}	ductility factor
Alumaxi 704 STA	3.2 mm	18.3 mm	5.7
Alumaxi 640 STA	3.2 mm	17.6 mm	5.5
Alumaxi 640 SBD	2.7 mm	10.3 mm	3.8

This principal of calculating the ductility factor agrees with the load-deformation graphs in figures 4.1, 4.4 and 4.5. The graphs show a milder slope of the force-displacement curve reaching out to failure beyond the yielding point in the stiffer connectors, which corresponds to ductile behaviour.

In table 4.4, the analytical stiffness according to Eurocode and SIA265 are compared with numerical results of the FE-model. As explained in section 2.4.6, the analytical stiffness calculation is load-independent. However, the numerical analysis in Abaqus shows dissimilarities in the obtained stiffness depending on the type of loading, such as the considered part of the model. In case of full model, the Alumaxi connector, the fasteners into the timber column, the timber beam and the dowels are contributing to the whole stiffness, unlike the case of only dowels loaded.

Table 4.4: *Moment stiffness of Alumaxi connector with different calculation approaches*

	Eurocode	SIA265	FE-model	FE-model	FE-model
load Version	only Dowels [MNm/rad]	only Dowels [MNm/rad]	only M only Dowels [MNm/rad]	only M full model [MNm/rad]	V and M full model [MNm/rad]
704 STA	11.2	11.9	13.0	7.0	5.5
640 STA	8.4	8.9	10.5	5.5	3.7
640 SBD	8.4	5.1	6.1	4.3	3.1

Comparing the numerical and analytical results of the case with only dowels, the Swiss standard SIA265 shows closer outcomes to the FE-model's outputs. The reason for this is that SIA265 takes into account the load-to-grain angle, which has a signification specially for tow rows of SBD dowels.

Setting the resulting moment of "full model" and "only dowels" analysis side by side, it can be observed that the pulled out nails and deformed metal plate of connectors gives lower stiffness.

4.2 Results for modified connectors

4.2.1 Connector with circular STA dowel pattern

Figure 4.6 shows the deformations with scale factor 10 and stresses in the connector when the beam is loaded with an distributed load that is increasing up to 110 kN/m.

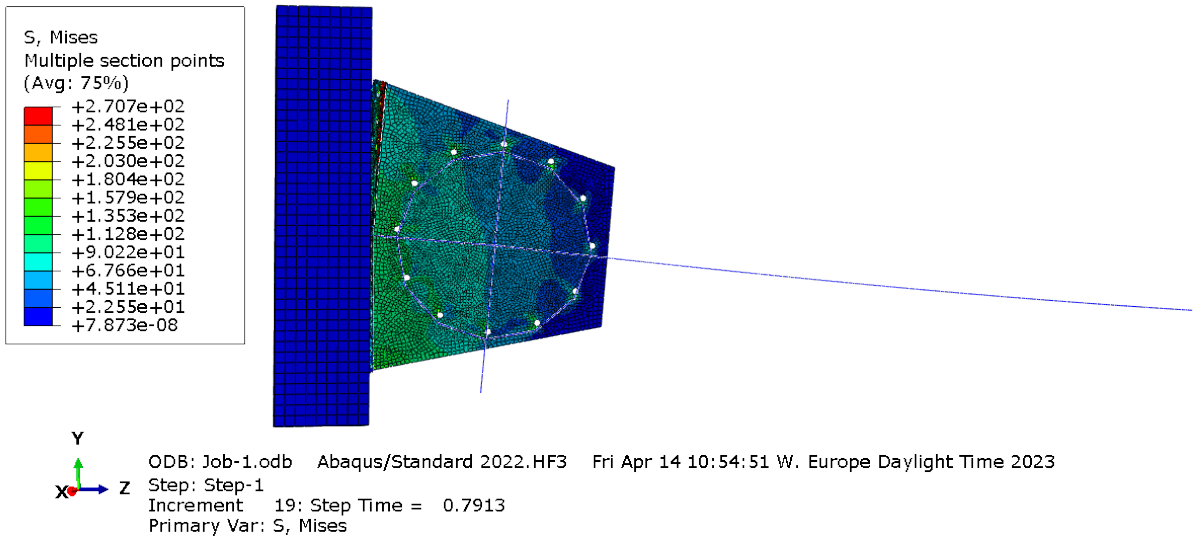

Figure 4.6:

It is in figure 4.6 observed that a lot of the deformation causing the rotation of the joint takes place in the metal at the column connection, but not as much deforma-

tion at the dowel fastener group of the web. It can be seen that yielding in the metal occurs in the top region where the flange and the web of the connector meet. This suggest that the connector is to week at the column for utilizing the stiffness of this circular pattern of dowels at the web.

To clarify this effect, the connection was disconnected from the beam in the model, and only a moment was applied at the connection. Table 4.5 shows results depending on how the loading were applied on the models of the Alumaxi 704 STA connection and the modified version of it.

Table 4.5: *Comparison of stiffness and maximum moment on the connection, with only moment applied on the models, and with loading a beam connected to the connector*

	k_{ser} joint [MNm/rad]	M_{yield} joint [kNm]	M_{max} joint [kNm]	θ_{max} joint [Rad]	M_{max} beam [kNm]
Alumaxi 704 STA					
only moment	6.7	-	86.2	0.100	-
Loaded beam	5.5	29.0	42.0	0.0107	570.8
Modified Alumaxi					
only moment	7.0	-	103.0	0.0716	-
Loaded beam	2.1	8.5	11.4	0.0115	616.5

The configuration with circular pattern for dowels shows less rotational stiffness compared to the orginial dowel configuration in Alumaxi 704. It is believed that this is due to that the shear center of the dowel fastener group is located further away from the flange, with the connection to the column. As referred from SIA265 in section 2.4.2, eccentricities in connections should be noticed when designing them. In this case an eccentricity might create an increased lever arm to the column that might cause larger deformation at the flange and the screws into the columns. Since the resultant of the loads on the beam act in the shear center, rotation of the connection might also be affected by this support reaction and not only the moment in the beam. As the load on the beam increase this effect also cause an increasing rotation at the joint.

The dowel group configuration is stiffer with this circular pattern, but the connection in total is less rotational stiff compared to the original Alumaxi 704 when the beam is loaded and both vertical force and moment act at the joint. Table 4.6 shows the impact of various design modification for the flange and fastening to the column of the connector with circular STA dowel pattern.

Table 4.6: *Comparison of stiffness and maximum moment on the connection, with different modifications of the connector, when supporting the glulam beam with increasing distributed load up to 110 kN/m*

	k_{ser} joint [MNm/rad]	M_{yield} joint [kNm]	M_{max} joint [kNm]	θ_{max} joint [Rad]	M_{max} beam [kNm]
Aluminium					
88 screws	2.1	8.5	11.4	0.0115	616.5
4x m16 rods, 72 screws	3.4	13.0	17.1	0.0113	607.5
Steel, 12 mm flange					
4x m16 rods, 72 screws	7.4	25.0	36.4	0.0105	578.1
Steel, 20 mm flange					
4x m16 rods, 72 screws	9.4	30.2	52.0	0.0100	559.2
4x m24 rods, 72 screws	10.9	33.9	55.1	0.0099	554.8

4.2.2 Connectors with multiple shear planes and SBD dowels

The results for load deformation at the joints from the simulations on the connectors with 2 and 3 slotted in steel plates i.e. 4 and 6 shear planes and with SBD dowels are presented in figures 4.7 and 4.8. These connectors show stiffer response and higher capacities than the previous results since the feature of multiple shear planes. Since the beam in the simulation is modeled as linear elastic without considering material failure, the simulations would continue beyond the loads at which the beam would fail. However the simulations show the structure behaves under loading through yielding and up to the maximum load.

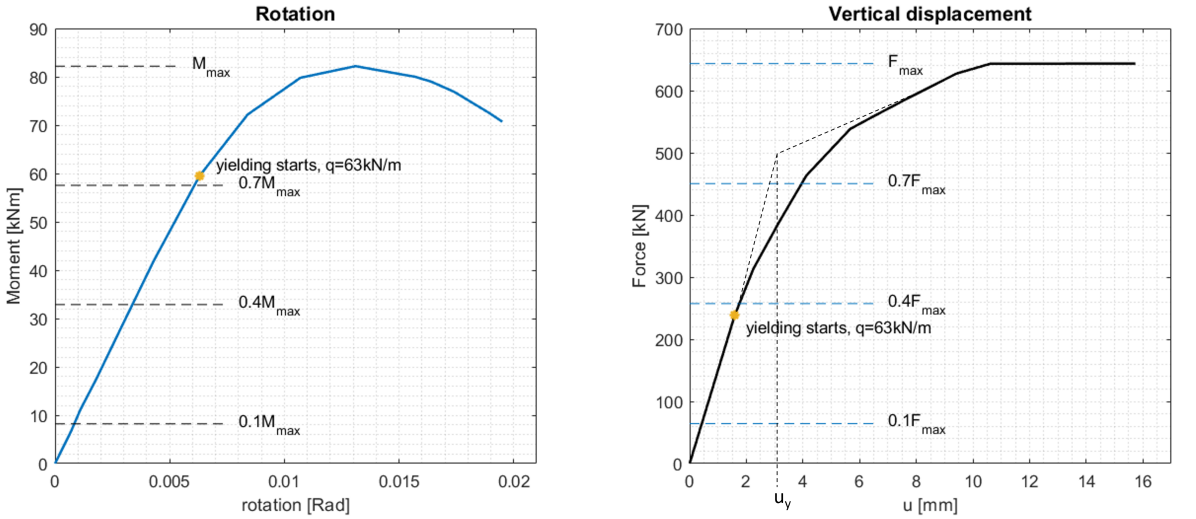

Figure 4.7: *Deformations at the connector with 4 shear planes and SBD dowels when supporting a 7.5 m, 215x810 mm GL30c beam loaded with distributed load increasing up to 170 kN/m*

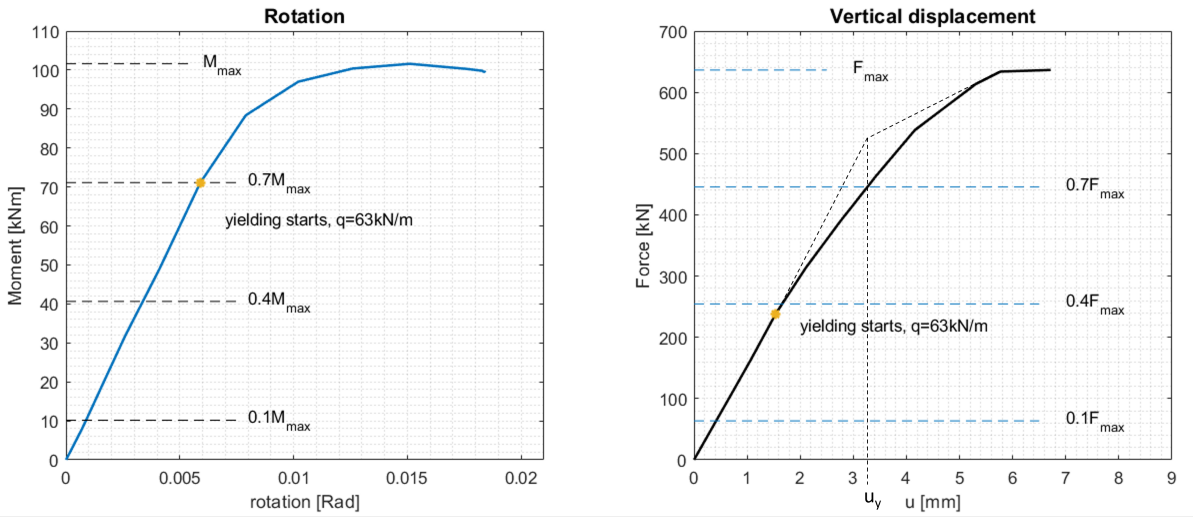

Figure 4.8: *Deformations at the connector with 6 shear planes and SBD dowels when supporting a 7.5 m, 215x810 mm GL30c beam loaded with distributed load increasing up to 170 kN/m*

As can be seen in figure 4.8, the analysis of SBD dowels in 3 slotted in steel plates/ 6 shear planes, shows that the load deformation curve shape of the single dowel connection follows the shape on the embedment modulus curve. This indicates that most of the deformation occurs in the wood for this configuration, and less yielding of the fastener.

As previously, k_{ser} is calculated between 10 and 40% of the maximum load, and k_u is calculated between 0 and 70% of the maximum load. The resulting stiffness parameters of the connection based on the simulation are presented in table 4.7. The displacement limits u_y and u_{max} are marked in figure 4.7 and 4.8 and are further used to determine the ductility factor of the connections as shown in table 4.8.

Table 4.7: *The stiffness of different modifications of SBD connector calculated based on moment-rotation and vertical force-displacement graphs*

SBD connector 640, 4 sh.p.	k_{ser}	k_u
Vertical action	150 kN/mm	112 kN/mm
Moment - rotation	9.8 MNm/rad	9.5 MNm/rad
SBD connector 640, 6 sh.p.	k_{ser}	k_u
Vertical action	148 kN/mm	135 kN/mm
Moment - rotation	12.1 MNm/rad	12.0 MNm/rad

The ductility factor in table 4.8 is calculated according to equation 4.1. Comparing these results with the one of 2 shear planes in table 4.3, it can be observed that with increasing number of shear planes, a significant reduction in ductility is obtained.

Table 4.8: *The ductility factor of Alumaxi SBD modified connections calculated with u_{max} and u_y that are plotted from the load-displacement graphs*

	u_y	u_{max}	Ductility factor
640, 4 sh.p.	3.1 mm	10.6 mm	3.4
640, 6 sh.p.	3.2 mm	5.6 mm	1.7

In table 4.9, the three versions of Alumaxi SBD are compared. It is noticed that beside the stiffness, a significant rise in yield and maximum moment at the joint by adding slotted in steel plates.

Table 4.9: *Comparison of stiffness, rotation and moments on the connection, with different modifications of the connector, when supporting the glulam beam with increasing distributed load*

	k_{ser} joint [MNm/rad]	M_{yield} joint [kNm]	M_{max} joint [kNm]	θ_{max} joint [Rad]	M_{max} beam [kNm]
One plate Aluminium, 80 screws	3.1	16.9	28.2	0.0110	574.3
Two plates Steel, 120 screws	9.8	59.5	82.2	0.0195	1041.0
Three plates Steel, 120 screws	12.1	71.1	101.6	0.0184	1001.3

Figure 4.9 is an example of the moment distribution of the reference beam with 4-shear plane SBD connector. The timber beam is assumed to have a linear elastic behaviour, therefore the span is increasing linearly with increased loading. Although, the end support moment increases up to 82,8 kNm before it start decreasing and failure in the joint takes place.

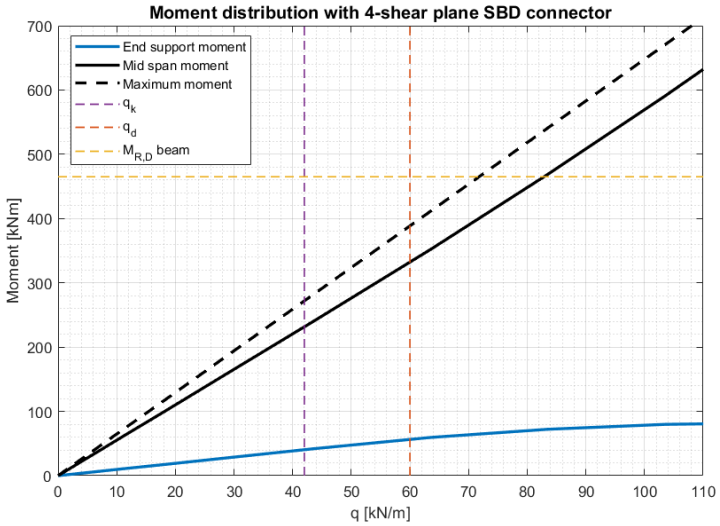

Figure 4.9: *The end support and mid span moment's distribution in relation to the increasing load in the reference beam, with SBD connector, 4-shear planes*

4.2.3 Connections in the moment distribution graph

Lastly, the graph of the moment distribution between span and end support moment that was presented in section 2.2.1.1, is here plotted with the connections' stiffness ratio as shown in figure 4.10.

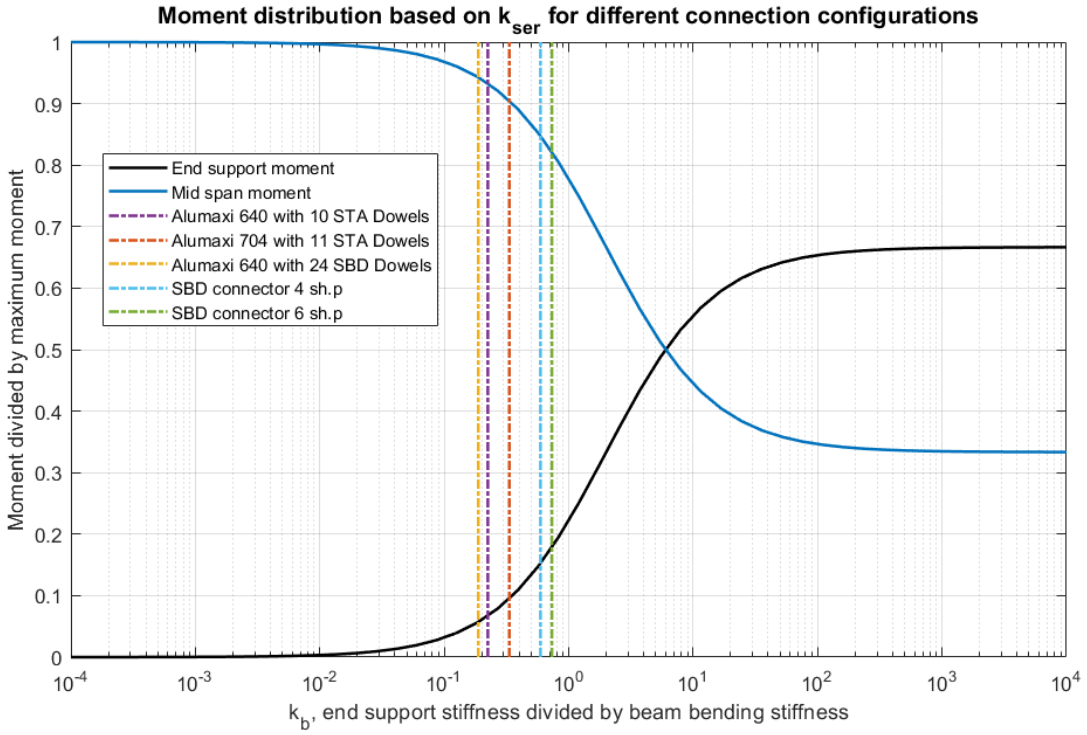

Figure 4.10: *Moment distribution for a 7.5 m GL30c beam with cross section 430x810 mm supported with 2 Alumaxi connections at each end*

As previously explained, the sought after connection is the one closest to the meeting point between end support and mid span moment curve. As can be seen in figure 4.10, Alumaxi SBD connector with 6 shear planes is the best alternative regarding the moment distribution between the beam and joints. However, many other aspects than stiffness and moment distribution that should be taken into account, make this connection undesirable to use. For instance, the low ductility ratio of this type of connections that might set additional demands to the structure. Nevertheless the economic aspect is out of importance, where Alumaxi SBD connector with 6 shear planes requires installing of 240 screws at each end of every beam, which considered time-consuming and economically inefficient.

4.3 Sensitivity study

4.3.1 Varying input parameters

A sensitivity study is implemented to investigate the potential impacts that different design choices, as well what varying material properties and assumptions in

the modelling method have on the resulting stiffness. The sensitivity study is done with comparison of Alumaxi connector (704 mm) with STA dowels and 80 mm LBS screws as a reference model.

First, the effect of material properties of timber is to be studied. The comparison is to see the output difference in case of using the value of $E_{0,05}$ instead of the mean elastic modulus $E_{0,mean}$ for GL30c, see figure 2.2. The glulam beam was assigned with characteristic material values and the stiffness for the non linear springs representing the dowels was changed to the characteristic load displacement curves as plotted in figure 3.12. Secondly, the effect of different fasteners into the column is to be studied. The fastener of the original analysis is LBD screw with the length if 80 mm. One analysis was generated with the same type of fastener but the length of 100 mm. Thereafter, the screws were replaced with anker nails LBA. Some relevant outputs from the sensitivity study are displayed in table 4.10 below.

Table 4.10: *The outcomes of the sensitivity study for Alumaxi 704 STA connector, with changing parameters of timber properties and type of fastener*

	k_{ser} joint [MNm/rad]	M_{yield} joint [kNm]	M_{max} joint [kNm]	θ_{max} joint [Rad]	M_{max} beam [kNm]
Timber properties					
$E_{0,mean}$ =13.0 GPa	5.5	29.6	42.5	0.0107	570.8
$E_{0,05}$ =10.8 GPa	5.8	28.3	47.7	0.0127	565.5
Type of fastener					
Screws (80 mm)	5.5	29.6	42.5	0.0107	570.8
Screws (100 mm)	6.0	31.9	46.9	0.0106	566.3
Anker nails (80 mm)	5.2	28.3	40.2	0.0108	573.2

In table 4.11, the percentage differences between the outcomes of the sensitivity study and the original analysis are calculated.

Table 4.11: *The percentage difference of the outcomes from sensitivity study compared to the original values*

	k_{ser} joint %	M_{yield} joint %	M_{max} joint %	θ_{max} joint %	M_{max} beam %
Timber properties					
$E_{0,05}$ =10.8 GPa	3.6	6.8	7.2	6.5	11.0
Type of fastener					
Screws (100 mm)	9.1	7.8	10.4	0.9	0.8
Anker nails (80 mm)	5.5	4.4	5.4	0.9	0.4

The greatest difference is of the maximum span moment influenced by the change of timber's Young's modulus. The end support stiffness and moments have the second

greatest outcome differences when changing the length of screw.

In any case, this sensitivity study might be useful for future projects to help with determining more accurate assumptions for the analysis.

4.3.2 Reference beam modeled as shell elements

As the simplification with the rigid link between the dowels and the reference beam neglect deformations occurring between dowels in the glulam beam, as mentioned in section 3.3.3.5, simulations were made to compare the effect of modelling the beam with shell elements. In this comparison, all parts of the connection except the dowels was removed and the non linear springs as the dowels were tied between the beam and the "ground" in Abaqus. The beam element beam with the rigid link between the dowels were also modeled without the other parts of the connection for this comparison. Figure 4.11 shows how the non linear springs were placed in the shell element beam as well as the mesh of the beam in this area. The loading was applied as shell edge load on top of the beam. Both versions of the beam were assigned with orthotropic linear elastic material model with engineering constants according to table 3.19.

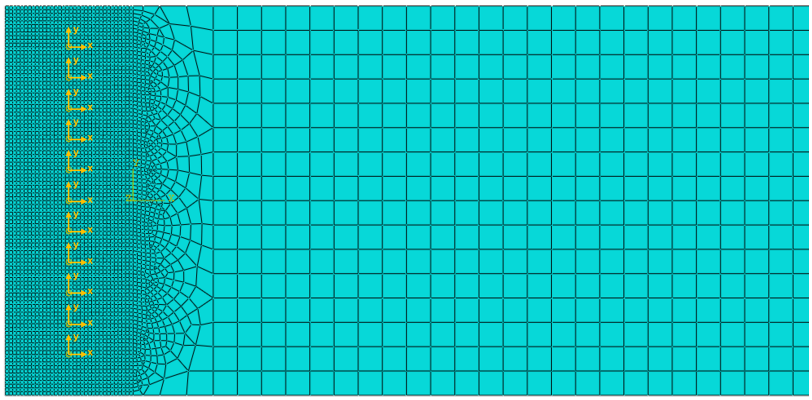

Figure 4.11: *The reference beam with mesh and connector elements marked in yellow, with their x and y direction for different stiffness parallel and perpendicular to the grain*

Figure 4.12 compares the deformations at the same load 61.4 kN/m for the shell element beam and beam element beam with the rigid link. A uniform deformation scale factor of 15 is assigned for both cases.

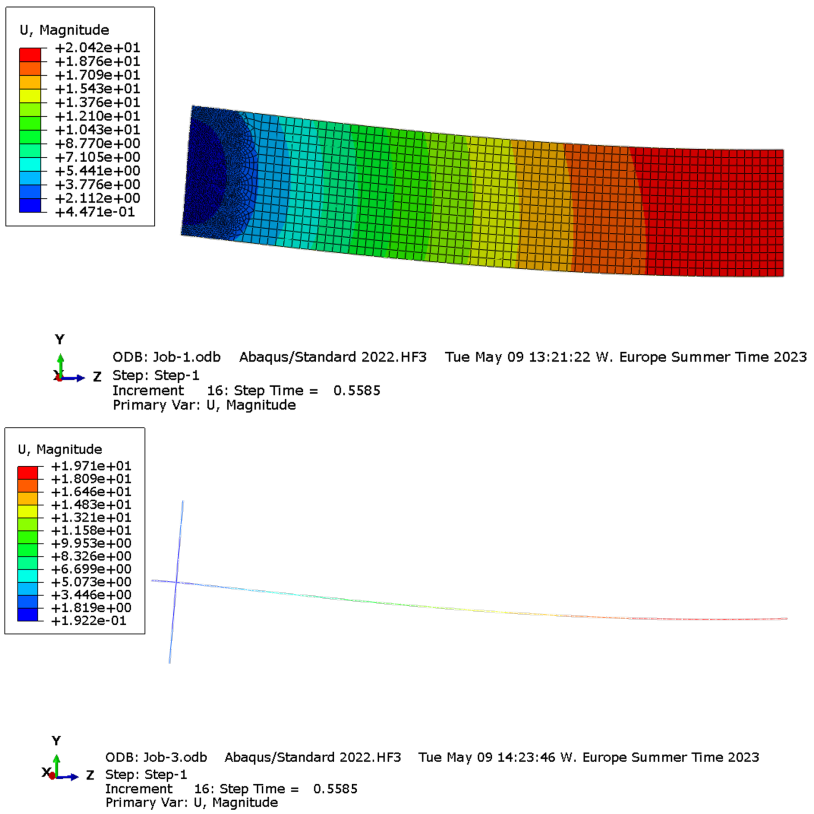

Figure 4.12: *The deformation (in mm) of the shell element beam (up) and the beam element beam (down) caused by the load of 61.4 kN/m*

Figure 4.13 shows the vertical displacement at the supports plotted with vertical force from both simulations.

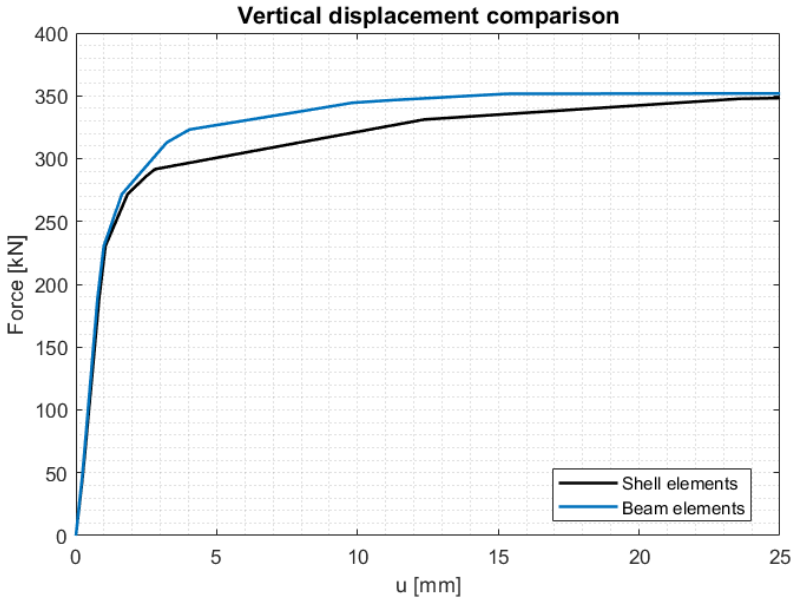

Figure 4.13: *The vertical displacement of the reference beam when modelling a shell element beam compared to a beam element beam*

As can be seen in figure 4.12 and 4.13, the maximum vertical displacement in mid of the span and at the joint are almost identical in case of modelling shell element beams or beam element beams.

Figure 4.14 shows the moment in mid span and at the end supports of the beams with increasing load.

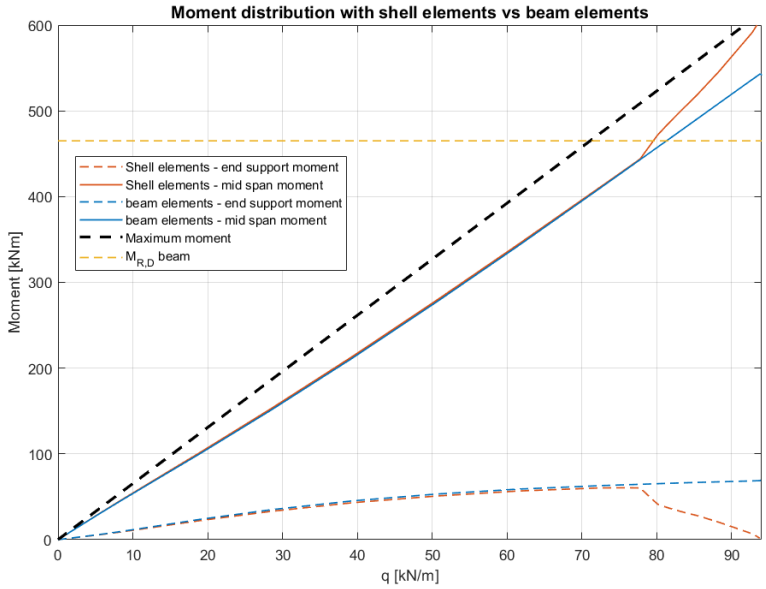

Figure 4.14: *The end support and mid span moment distribution in relation to the increasing load for both shell element beam and beam element beam model*

It is observed in figure 4.14 that there are deviations between the results from the simulations for higher loads when the dowels yield. The shell element beam has an sudden decrease in moment at the support and increase in mid span moment when the dowels fails. This occurs around a load level of 77 kN/m which corresponds to a vertical force in the connection of around 290 kN in figure 4.13.

4.4 Results from global FE-model of the reference building

Tables 4.12 to 4.15 show some extracted results from geometrical linear global analysis of the structural system with different rotational stiffness assigned between timber members in the model as presented in section 3.5.1. The tables include 4 different load cases in ULS that where applied on the model.
The internal forces presented in table 4.12 to 4.15 are extracted for the members highlighted yellow in figure 4.15. The mid span moments are extracted for the beams as well as the highest shear force at the supports of the two members. For the trusses the highest normal force is extracted.

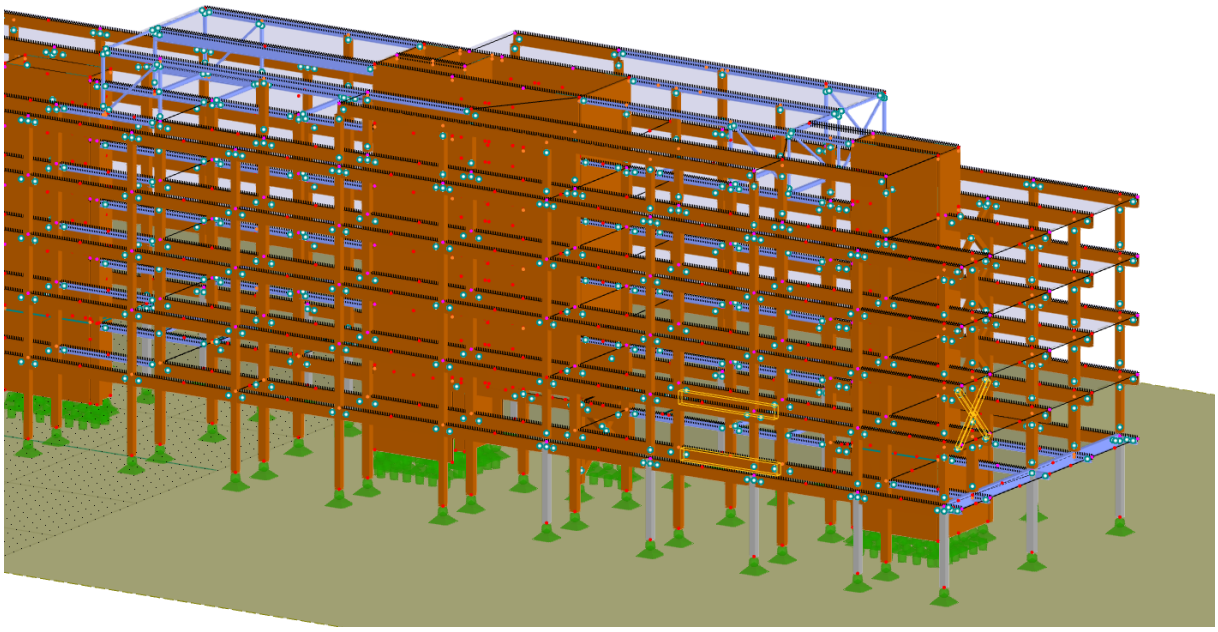

Figure 4.15: *The model of the building of the study case with the studied beams and truss marked in yellow*

Table 4.12: *The global elements and internal forces of the structural components. The load combination with wind load on the long side is the leading variable load*

Wind leading variable, long side ULS: $1.35 \cdot G_{k,i} + 0.7 \cdot 1.5 \cdot Q_{k,im} + 1.5 \cdot Q_{k.w} + 0.7 \cdot 1.5 \cdot Q_{k,s}$							
stiffness	Global deformations [mm]			Internal forces, beams and truss			
	$u_{x,max}$	$u_{y,max}$	$u_{z,max}$	$M_{max,1}$	$M_{max,2}$	V_{max}	N_{truss}
0 MNm/rad	55.6	10.0	68.3	676 kNm	529 kNm	157 kN	483 kN
11 MNm/rad	53.6	8.5	67.2	606 kNm	457 kNm	153 kN	462 kN
22 MNm/rad	52.6	8.0	66.7	558 kNm	414 kNm	150 kN	343 kN
∞ MNm/rad	49.8	7.6	64.0	284 kNm	195 kNm	107 kN	364 kN

Table 4.13: *The global elements and internal forces of the structural components. The load combination with wind load on the short side is the leading variable load*

Wind leading variable, short side ULS: $1.35 \cdot G_{k,i} + 0.7 \cdot 1.5 \cdot Q_{k,im} + 1.5 \cdot Q_{k,w} + 0.7 \cdot 1.5 \cdot Q_{k,s}$							
stiffness	Global deformations [mm]			Internal forces, beams and truss			
	$u_{x,max}$	$u_{y,max}$	$u_{z,max}$	$M_{max,1}$	$M_{max,2}$	V_{max}	N_{truss}
0 MNm/rad	12.7	12.0	68.9	677 kNm	528 kNm	165 kN	121 kN
11 MNm/rad	12.0	10.0	68.0	606 kNm	457 kNm	160 kN	105 kN
22 MNm/rad	11.6	9.2	67.5	559 kNm	414 kNm	155 kN	101 kN
∞ MNm/rad	12.5	8.7	64.7	282 kNm	194 kNm	114 kN	132 kN

Table 4.14: *The global elements and internal forces of the structural components. The load combination with imposed load is the leading variable load*

Imposed load leading variable ULS: $1.35 \cdot G_{k,i} + 1.5 \cdot Q_{k,im} + 0.3 \cdot 1.5 \cdot Q_{k,w} + 0.7 \cdot 1.5 \cdot Q_{k,s}$							
stiffness	Global deformations [mm]			Internal forces, beams and truss			
	$u_{x,max}$	$u_{y,max}$	$u_{z,max}$	$M_{max,1}$	$M_{max,2}$	V_{max}	N_{truss}
0 MNm/rad	26.0	13.0	69.9	749 kNm	584 kNm	176 kN	45 kN
11 MNm/rad	25.2	12.4	69.0	671 kNm	506 kNm	172 kN	42 kN
22 MNm/rad	24.9	11.9	68.5	618 kNm	458 kNm	166 kN	38 kN
∞ MNm/rad	26.0	10.8	65.5	314 kNm	215 kNm	122 kN	41 kN

Table 4.15: *The global elements and internal forces of the structural components. The load combination with snow load is the leading variable load*

Snow load leading variable ULS: $1.35 \cdot G_{k,i} + 0.7 \cdot 1.5 \cdot Q_{k,im} + 0.3 \cdot 1.5 \cdot Q_{k,w} + 1.5 \cdot Q_{k,s}$							
stiffness	Global deformations [mm]			Internal forces, beams and truss			
	$u_{x,max}$	$u_{y,max}$	$u_{z,max}$	$M_{max,1}$	$M_{max,2}$	V_{max}	N_{truss}
0 MNm/rad	26.6	13.0	72.4	677 kNm	528 kNm	159 kN	54 kN
11 MNm/rad	25.7	12.4	71.4	606 kNm	458 kNm	155 kN	51 kN
22 MNm/rad	25.4	11.9	70.9	559 kNm	414 kNm	150 kN	47 kN
∞ MNm/rad	25.5	10.8	67.9	284 kNm	194 kNm	110 kN	38 kN

The tables review the outcomes from the RFEM analyses where, firstly, the wind load is assumed to be leading variable load acting on the long side of the building (x-direction) and secondly, wind load acting on the short side of the building (y-direction). Thereafter, respectively the imposed and snow load are calculated to be the leading variable load assuming that the wind load is acting on the long side.

As it can be observed in tables 4.12 to 4.15, the global deformations and internal forces in beams and truss diminish with increasing stiffness of the joints. The span moments in two reference beams are changing due to the moment distribution occurring in the beam, but also, a reduction of the total moments loading the beams. This reduction explains the variation of the shear forces V_{max}, which originally are not influenced by the stiffness of the joint.

The reduction of the forces applied to the reference beams can be further explained by the force redistribution between the components of the structural system. Which can be noticed by the increment of internal forces in the truss and global deformation $u_{x,max}$ in some load cases for the infinite stiff connection. The condition is the same for some columns of the reference building.

It should also be mentioned that due to the lack of time and experience in using the software RFEM, it was late noticed that transnational degrees of freedom of the modelled concrete plates were not released from the nodes of the columns which

implies that the some portion of loads from the plates are directly carried by the columns and not all load by the beams. This proposition might have affected the outcomes of internal forces in the building. For more accurate results, the transnational degree of freedoms at concrete plates should have been released from the columns as the rotational degrees of freedom were released from the beams.
Figure 4.16 shows the deformation of the system wind is applied as the leading variable on the long side of the building.

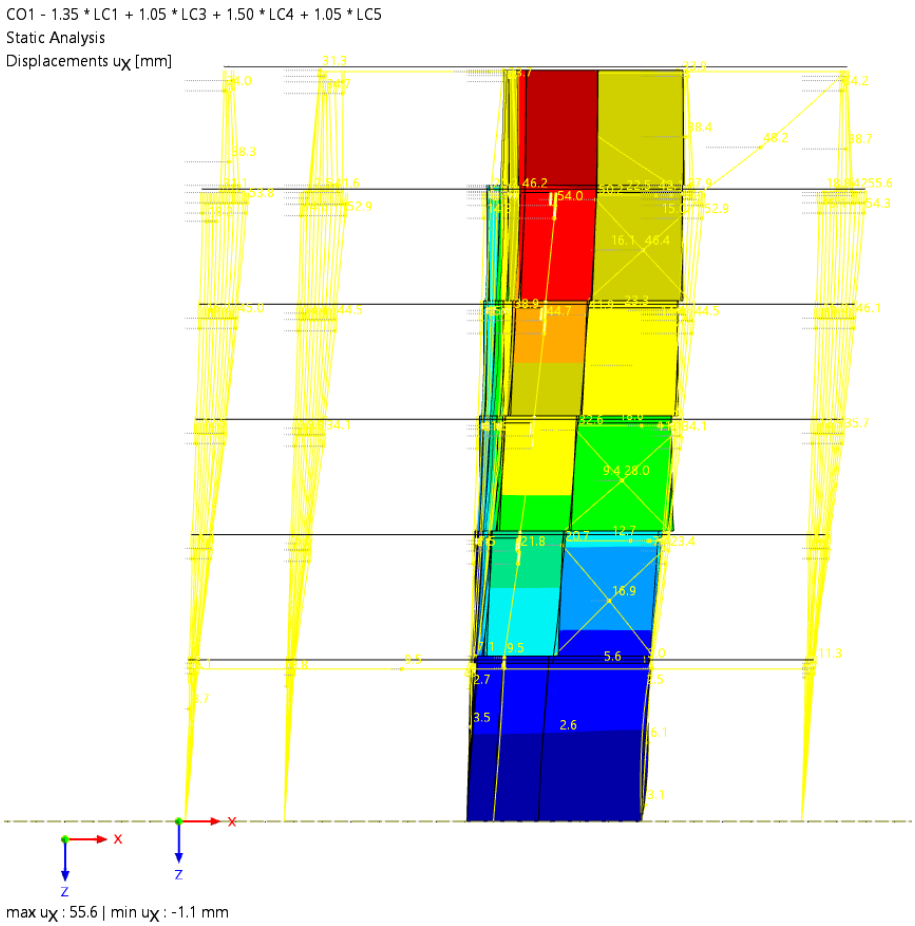

Figure 4.16: *The resulting global deformation of the reference building scaled up and caused by the wind load acting on the long side as the leading variable load*

5
Conclusion

The aim of this thesis was to study possible impacts from stiffness of timber connections which are suitable for large timber structures. This was done by first investigating proper ways to determine the stiffness of large dowel-type timber connections. As well as, to investigate how different design choices influence the stiffness of a connection and how this in turn affects the structural system behaviour.

Stiffness of connections

In a dowel-type timber connection, a lot of parameters are involved when calculating the stiffness. Material models for metal fasteners are reliable and provide accuracy for deformations and load capacity, while the varying properties of wood implies more uncertainties. Models can be established to deal with some complexities like orthotropy and non linearity and these models can be made more or less sophisticated. Consideration should be given to how necessary accurate results are in relative to the effort and time needed to develop the model and manage the results.

Linear analysis might overestimate the stiffness for connections, this was observed for 2D simulations with beam on elastic foundation. In these cases when linear material response was used, the stiffness was noticeably higher than the results obtained from non linear analysis with beam on elastic foundation. The non linear beam on elastic foundation modelling generated maximum loads on fasteners, that in general show good accordance with analytical equations in Eurocode 5 for the respective failure mode.

Eurocodes provide too simplified methods for calculating stiffnesses for more complex connections, specially when some fasteners are loaded axially. The Eurocode approaches are too general and cannot predict stiffness that depends on several parameters, which in this study have shown an impact, like load to grain angle, member thickness and deformation mode of the fastener.

The analyses that were studied in this project have indicated that the dimensions of both connector and fasteners, material choice of connector, fasteners and connected timber elements, all influence the stiffness of the connection. The fastening of the flange to the column for beam to column connectors show high impact on the rotational stiffness for the type of connectors that were studied. The parametric study with different fasteners, flange thickness and also rods indicate that the design of

these details should be done carefully to obtain stiff connection response.

Impact on structural system

With used input data and assumptions when modelling the structural system in RFEM, the impact of the connections' rotational stiffness on the analysis is comparatively low when the global deformations are accounted. However, the moment distribution and internal forces in members show a little bit higher dependency. It should be pointed out that the structural components of the studied building might be overdimensioned which could reduce the impact of the stiffness between the members. However depending on design choices for different structural systems, the stiffness at joints might have a more significant influence.

Moments in beams might be reduced depending on design choices doweled connections beam to column connections. Precise value of the moment and deflections decrease for single span beams for application in design is not investigated here. However, the outcomes indicate to a reduction around 5-15% could be realistic. This reduction is influenced by the properties of the beam and the design of the connection. Long term effects, which were neglected in this study, also need to be considered.

Overall summary

The methodology that was implemented to determine stiffness of a connection in this thesis might be time-consuming for engineers to learn and use as a new tool. Although when these methods have been tried, implementations can be considerably rapid. In particular, the development of similar models could help connection designers accounting for stiffness and simplify evaluation of variety of parameters that impact the performance of connections.

Lastly, a very important aspect that should be considered when designing stiff connections is ductility. As the results of this thesis indicate, relatively stiff connections are less ductile and might have a more brittle behaviour. It can be concluded that the most optimal connection is the one that achieves the balance between stiff and ductile with high capacity.

Further researches

Further researches can focus on how to increase the reliability and accuracy of the results from FE-modelling of timber connections. Development to the component FE-models could be made for possibly obtaining more accurate results since several simplifications were made in this project. For instance, by implementing more detailed and less simplified parameters for the fasteners into the column. In this study, assumptions were made for mechanical behaviour of screws, and nails and more detailed information of the load deformation for when these fasteners are both

laterally and the axially loaded would be useful. Also physical test on fasteners and entire connections to verify results and the modelling methods could be necessary.

It would also be useful to investigate if material damage and brittle failure mechanisms could be included in material models and component FE-models of connections. Another aspect is to include long term effects and enable the application of load redistribution due to connection stiffness to possibly reduce design forces.

The last suggestion is to further study the impact of some assumptions in the modelling. Some effects of using a rigid wood matrix around the spring elements were compared with using deformable shell elements. Future studies could investigate how much the internal forces around fasteners differ depending on these assumptions and if the overall stiffness and deformation are sensitive to them.

Bibliography

[Basterrechea-Arévalo et al., 2021] Basterrechea-Arévalo, M., Cabrero, J. M., Iraola, B., and Goñi, R. (2021). Modelling of moment transmitting beam-to-column timber connections accounting for frictional transmission. *Engineering Structures*, 247.

[Boverket, 2022] Boverket (2022). Boverkets föreskrifter om ändring i Boverkets föreskrifter och allmänna råd (2011:10) om tillämpning av europeiska konstruktionsstandarder (eurokoder), BFS 2022:4. Technical report.

[Burström, 2001] Burström, P. G. (2001). *Byggnadsmaterial: Tillverkning, egenskaper och användning*. Studentlitteratur AB.

[Caprio et al., 2022] Caprio, D., Jockwer, R., and Al-Emrani, M. (2022). Reliability of statically indeterminate timber structures: Modelling approaches and sensitivity study. In *Current Perspectives and New Directions in Mechanics, Modelling and Design of Structural Systems*.

[CEN, 2002] CEN (2002). EN 1990: 2002 - Basis of structural design.

[Dorn and Bader, 2016] Dorn, M. and Bader, T. K. (2016). Non-linear connection models in timber engineering. In *WCTE 2016 - World Conference on Timber Engineering*.

[Eurocode 5, 2004] Eurocode 5 (2004). EN 1995-1-1:2004. *Eurocode 5*, 1(2004).

[Gečys and Daniūnas, 2017] Gečys, T. and Daniūnas, A. (2017). Rotational stiffness determination of the semi-rigid timber-steel connection. *Journal of Civil Engineering and Management*, 23(8).

[Geiser et al., 2022] Geiser, M., Furrer, L., Kramer, L., Blumer, S., and Follesa, M. (2022). Investigations of connection detailing and steel properties for high ductility doweled timber connections. *Construction and Building Materials*, 324.

[Göts et al., 1989] Göts, K.-H., Hoor, D., Möhler, K., and Natterer, J. (1989). *Timber Design and Construction Sourcebook*. McGraw-Hill Publishing Company, Munich.

[Hanhijärvi and Kevarinmäki, 2008] Hanhijärvi, A. and Kevarinmäki, A. (2008). Timber failure mechanisms in high-capacity dowelled connections of timber to steel. Experimental results and design. Technical report.

[Harte, 2001] Harte, A. (2001). Introduction to timber as an engineering material. *ICE Manual of Construction Materials*.

[Hassanieh et al., 2017] Hassanieh, A., Valipour, H. R., Bradford, M. A., and Sandhaas, C. (2017). Modelling of steel-timber composite connections: Validation of finite element model and parametric study. *Engineering Structures*, 138.

[Jockwer et al., 2022] Jockwer, R., Caprio, D., and Jorissen, A. (2022). Evaluation of parameters influencing the load-deformation behaviour of connections with

laterally loaded dowel-type fasteners. *Wood Material Science and Engineering*, 17(1).

[Jockwer et al., 2021] Jockwer, R., Öberg, V., and Roberto, C. (2021). Några överväganden för effektiva och tillförlitiga träförband med inslitsade plåtar och dymlingar. *Tidningen Bygg och Teknik*.

[Johanides et al., 2021] Johanides, M., Kubíncová, L., Mikolášek, D., Lokaj, A., Sucharda, O., and Mynarčík, P. (2021). Analysis of rotational stiffness of the timber frame connection. *Sustainability (Switzerland)*, 13(1).

[Kaufmann et al., 2018] Kaufmann, H., Krötsch, S., and Winter, S. (2018). *Manual of Multi-Storey Timber Construction*. Detail Business Information GmbH, Munich, 2 edition.

[Kuhlmann, 2022] Kuhlmann, U. (2022). Guidelines for a Finite Element Based Design of Timber Structures. Technical report, Institute of structural design, Germany.

[Kuhlmann and Gauß, 2019] Kuhlmann, U. and Gauß, J. (2019). Component method in timber construction – Experimental and numerical research. *New Zealand timber design journal*, 28(3).

[Malo et al., 2016] Malo, K. A., Abrahamsen, R. B., and Bjertnæs, M. A. (2016). Some structural design issues of the 14-storey timber framed building "Treet" in Norway. *European Journal of Wood and Wood Products*, 74(3).

[Mirdad et al., 2022] Mirdad, M. A. H., Jucutan, A., Khan, R., Niederwestberg, J., and Chui, Y. H. (2022). Embedment and withdrawal stiffness predictions of self-tapping screws in timber. *Construction and Building Materials*, 345.

[Ottenhaus et al., 2021] Ottenhaus, L. M., Jockwer, R., van Drimmelen, D., and Crews, K. (2021). Designing timber connections for ductility – A review and discussion.

[Porteous and Kermani, 2013] Porteous, J. and Kermani, A. (2013). *Structural Timber Design to Eurocode 5*. Blackwell Publishing. Ltd, 2nd edition.

[Reynolds et al., 2013] Reynolds, T., Harris, R., and Chang, W. S. (2013). An analytical model for embedment stiffness of a dowel in timber under cyclic load. *European Journal of Wood and Wood Products*, 71(5):609–622.

[Rothoblaas, 2019] Rothoblaas (2019). Plates and connectors for timber. Buildings, structures and outdoor. Technical report.

[Sandhaas et al., 2018] Sandhaas, C., Munch-Andersen, J., and Dietsch, P. (2018). Design of Connections in Timber Structures. Technical report, A state-of-the-art report by COST Action FP1402 / WG3.

[Schweizer Norm, 2003] Schweizer Norm (2003). *SIA265*.

[Soutsos and Domone, 2010] Soutsos, M. and Domone, P. (2010). *Construction materials: Their nature and behaviour: Fourth edition*.

[Swedish Wood, 2016] Swedish Wood (2016). *Limträhandbok Del 1*. Swedish wood, Stockholm.

[Swedish Wood, 2022a] Swedish Wood (2022a). *Design of Timber Structures. Structural aspects of timber construction. Volume 1.*, volume 1. Swedish Forest Industries Federation, 3 edition.

[Swedish Wood, 2022b] Swedish Wood (2022b). Design of timber structures, Volume 2: Rules and formulas according to Eurocode 5. *Swedish Wood*, 3.

[Tomasi et al., 2010] Tomasi, R., Crosatti, A., and Piazza, M. (2010). Theoretical and experimental analysis of timber-to-timber joints connected with inclined screws. *Construction and Building Materials*, 24(9).

[Xu et al., 2012] Xu, B. H., Bouchaïr, A., and Racher, P. (2012). Analytical study and finite element modelling of timber connections with glued-in rods in bending. *Construction and Building Materials*, 34.

[Xu et al., 2022] Xu, B. H., Lin, J. B., Zhao, Y. H., and Bouchaïr, A. (2022). Embedment behaviour of fully threaded bolts in glued laminated timber. *European Journal of Wood and Wood Products*.

A

Appendix

A.1 Snow load

Snow load:

City: Uppsala

The characteristic snow load for Uppsala according to EN 1991-1-3:2003 (BFS 2008:19)

$s_k := 2 \ \frac{kN}{m^2}$

Snow load on the short side:

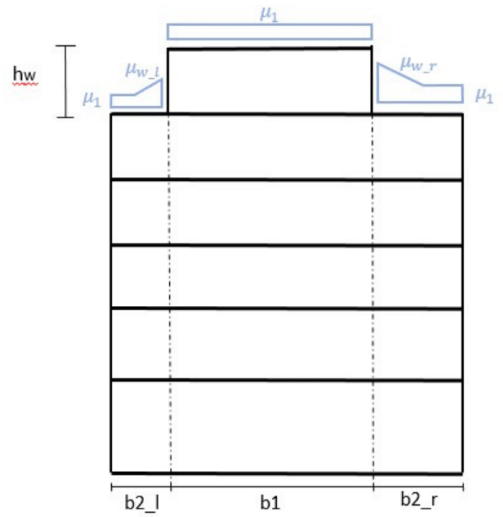

The hights of the floors:

$h_w := 4.250 \ m$

$h_{floor.3.4.5} := 4.025 \ m$

$h_{floor.2} := 4.375 \ m$

$h_{floor.1} := 5.775 \ m$

Total high of the building:

$h := h_{floor.1} + h_{floor.2} + 3 \cdot h_{floor.3.4.5} + h_w = 26.475 \ m$

Contributing widths of snow load, designation according the figure above:

$b_{2\_l} := 27.726 \ m$ $b_1 := 13.02 \ m$ $b_{2\_r} := 28.585 \ m$

Shape coefficients, designation according the figure above:

$\mu_1 := 0.8$ $\mu_{w\_r} := \frac{\langle b_1 + b_{2\_r} \rangle}{2 \cdot h_w} = 4.895$ $\mu_{w\_l} := \frac{\langle b_1 + b_{2\_l} \rangle}{2 \cdot h_w} = 4.794$

Snow load on the long side:

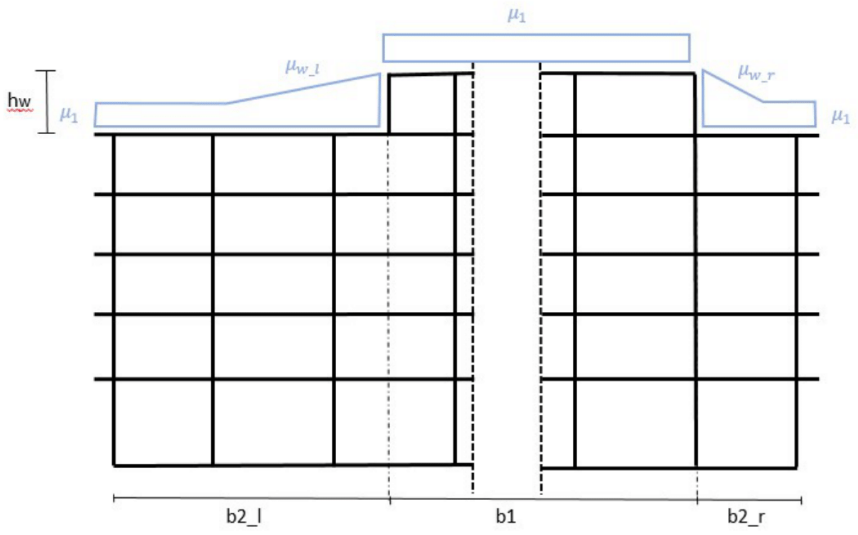

Contributing widths of snow load, designation according the figure above:

$b_{2\_l} := 40.468\ m$ $b_1 := 29.23\ m$ $b_{2\_r} := 19.92\ m$

Shape coefficients, designation according the figure above:

$\mu_1 := 0.8$ $\mu_{w\_r} := \frac{(b_1 + b_{2\_r})}{2 \cdot h_w} = 5.782$ $\mu_{w\_l} := \frac{(b_1 + b_{2\_l})}{2 \cdot h_w} = 8.2$

The snow load on the long side is decisive!

A restriction according to EN 1991-1-3:2003 (BFS 2008:19) is:

$0.8 \le \mu_w \le 4.0$ --> $\mu_w := 4$

$C_e := 1$ exposure coefficient

$C_t := 1$ thermal coefficient

The total decisive snow load:

$S := C_e \cdot C_t \cdot (\mu_1 + \mu_w) \cdot s_k = 9.6\ \frac{kN}{m^2}$

A.2 Wind load

Wind load:

Input data:

Geometrical input data of the building:

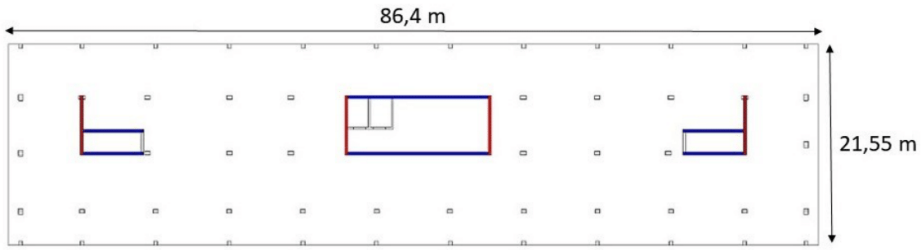

Hight: $h := 26.475\ m$
Length: $L := 86.4\ m$
Width: $W := 21.55\ m$

Terrain input data:

City: Uppsala
Reference wind speed: $v_b := 24\ \frac{m}{s}$

Terrain category: III
$z_0 := 0.3\ m$ $z_{min} := 5\ m$ $k_r := 0.22$

Wind peak velocity pressure:

$\rho := 1.25\ \frac{kg}{m^3}$ Air density

$q_b := \frac{v_b^2}{2} \cdot \rho = 0.36\ \frac{kN}{m^2}$ reference mean (basic) velocity pressure

$ce(z) := \left(k_r \cdot \ln\left(\frac{z}{z_0}\right)\right)^2 \cdot \left(1 + \frac{7}{\ln\left(\frac{z}{z_0}\right)}\right)$ exposure coefficient

peak velocity pressure:

$q_p(z) := ce(z) \cdot q_b$

Wind acting on the long side of the building:

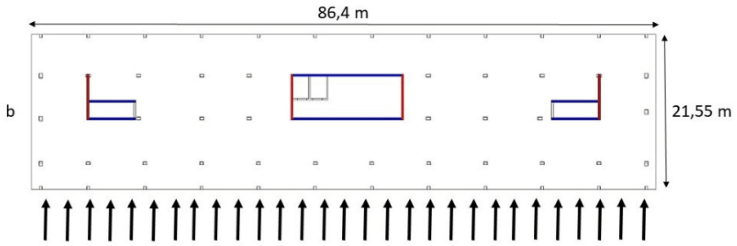

$q_{p1} := q_p(21.55\ m) = 839.671\ Pa$ At floors 1-5

$q_{p2} := q_p(26.475\ m) = 896.172\ Pa$ At floor 6 (top floor)

$b_{long} := W$ $d_{long} := b_{long}$ $\frac{h}{d_{long}} = 1.229$

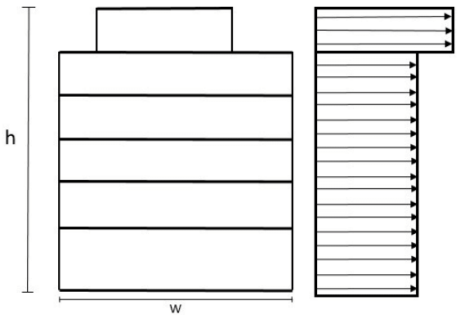

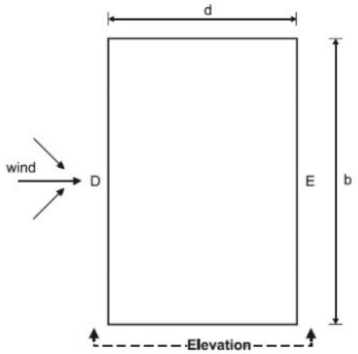

Pressure coefficient:

$c_{pe\_10D} := 0.8$ external

$c_{pe\_10E} := \frac{-0.7-(-0.5)}{5-1} \cdot 0.229 + (-0.5) = -0.511$ internal

Wind pressure on external surfaces:

$w_{eD1} := q_{p1} \cdot c_{pe\_10D} = 0.672\ \frac{kN}{m^2}$ Windward side wind load on floor 1-5

$w_{eD2} := q_{p2} \cdot c_{pe\_10D} = 0.717\ \frac{kN}{m^2}$ Windward side wind load on top floor level

Wind pressure on internal surfaces:

$w_{eE1} := q_{p1} \cdot c_{pe\_10E} = -0.429 \ \frac{kN}{m^2}$ Leeward side wind load on floor 1-5

$w_{eE2} := q_{p2} \cdot c_{pe\_10E} = -0.458 \ \frac{kN}{m^2}$ Leeward side wind load on top floor level

Wind acting on the short side:

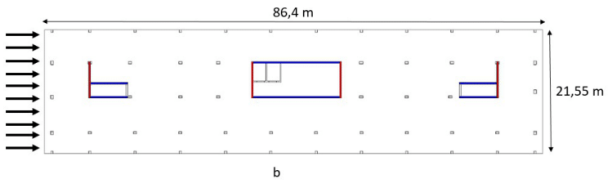

$q_{p\_s} := q_p(26.475 \ m) = 896.172 \ Pa$ At all floors (1-6)

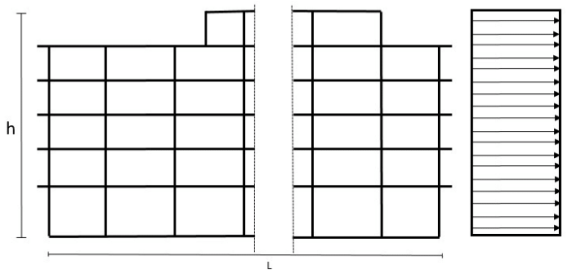

$b_{short} := L$ $d_{short} := b_{short}$ $\frac{h}{d_{short}} = 0.306$

Pressure coefficient:

$c_{pe\_10Ds} := \frac{0.8 - 0.7}{1 - 0.25} \cdot (0.306 - 0.25) + 0.7 = 0.707$ external

$c_{pe\_10Es} := \frac{-0.5 - (-0.3)}{1 - 0.25} \cdot (0.306 - 0.25) + (-0.3) = -0.315$ internal

Wind pressure on external surfaces:

$w_{eD} := q_{p\_s} \cdot c_{pe\_10Ds} = 0.634 \ \frac{kN}{m^2}$ Windload on windward side

Wind pressure on internal surfaces:

$w_{eE} := q_{p\_s} \cdot c_{pe\_10Es} = -0.282 \ \frac{kN}{m^2}$ Windload on leeward side

A.3 Self weights

Self-weights:

Self weight on the most loaded column:

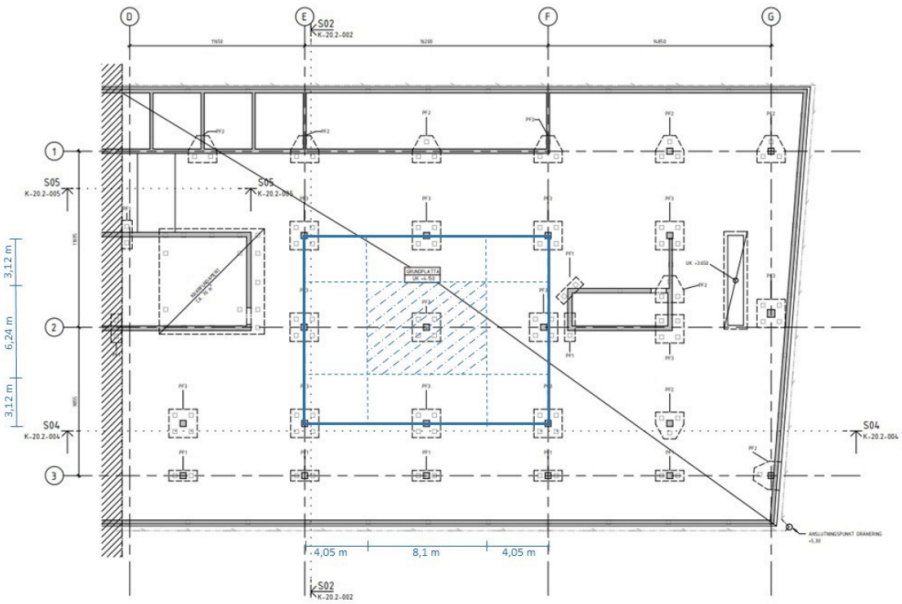

Density of the materials:

$\rho_{GL} := 430 \frac{kg}{m^3}$ Glulam, GL30h

$\rho_{HDF} := 330 \frac{kg}{m^2}$ Concrete slab HDF, thickness of 200 mm

$\rho_{screed} := 2500 \frac{kg}{m^3}$ Screed on concrete slab, thickness of 50 mm

$\rho_{steel} := 7850 \frac{kg}{m^3}$ Steel elements, beams and columns

Additional masses of the building according to Boverket:

$m_{vent} := 50 \frac{kg}{m^2}$ Weight of ventilation

$m_{undertak} := 30 \frac{kg}{m^2}$ Weight of suspended ceiling

$m_{roof} := 70 \ \frac{kg}{m^2}$ Weight of roof topping

Geometries of the contributing elements:

$L_{Cont.column.x} := 8.1 \ m$ $L_{Cont.column.y} := 6.24 \ m$ Length of contributin area

$A_{Cont.Column} := L_{Cont.column.x} \cdot L_{Cont.column.y} = 50.544 \ m^2$ Contributing area of floor/story

$A_{CS.Column} := 0.63 \ m \cdot 0.43 \ m = 0.271 \ m^2$ Cross section area glulam column

$L_{GL.Column} := 25.355 \ m$ Length of glulam column

$A_{CS.steel} := 0.014 \ m^2$ Cross section area of steel beams

$t_{screed} := 0.05 \ m$ Thickness of screed on top of the HDF floors

Total load on the bottom of the column:

$$m_{tot} := \left(\rho_{GL} \cdot A_{CS.Column} \cdot L_{GL.Column}\right) + \left(\rho_{HDF} \cdot A_{Cont.Column} \cdot 5\right) + \left(\rho_{steel} \cdot A_{CS.steel} \cdot L_{Cont.column.x} \cdot 6\right) + \left(\rho_{screed} \cdot A_{Cont.Column} \cdot t_{screed} \cdot 5\right) + \left(\left(m_{vent} + m_{undertak}\right)\right) \cdot A_{Cont.Column} \cdot 6 + m_{roof} \cdot A_{Cont.Column} = \left(1.511 \cdot 10^5\right) \ kg$$

$G_{Column} := m_{tot} \cdot 9.81 \ \frac{m}{s^2} = 1.482 \ MN$

Loads on beams:

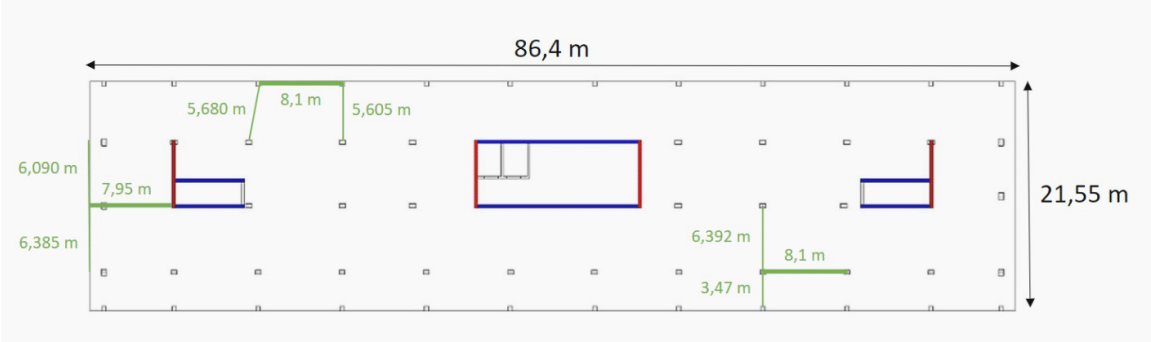

Longest/highest loaded beam:

Geometries of the beam:

$L_{beam} := 8.1\ m$ Length

$A_{CS.high} := 0.81\ m \cdot 0.43\ m = 0.348\ m^2$ Cross-sectional area

Contribution area:

$$A_{Cont.high} := \left(\frac{3.47}{2} + \frac{6.392}{2}\right) m \cdot L_{beam} = 39.941\ m^2$$

Total self-weight on the most loaded beam:

$$m_{high.beam} := A_{CS.high} \cdot \rho_{GL} \cdot L_{beam} + \left(\rho_{HDF} + \rho_{screed} \cdot t_{screed} + m_{vent} + m_{undertak}\right) \cdot A_{Cont.high} = \left(2.258 \cdot 10^4\right)\ kg$$

$$g_{k.high} := \frac{m_{high.beam}}{L_{beam}} \cdot 9.81\ \frac{m}{s^2} = 27.349\ \frac{kN}{m}$$

Cantilever:

Geometries of the beam:

$L_{c.a} := 1.2\ m \quad L_{c.b} := 6.75\ m$ Length

$A_{CS.cantilever} := 0.9\ m \cdot 0.43\ m = 0.387\ m^2$ Cross-sectional area

Contributing area:

$$A_{Cont.cantilever} := \left(\frac{6.090}{2} + \frac{6.385}{2}\right) m \cdot \left(L_{c.a} + L_{c.b}\right) = 49.588\ m^2$$

Total self-weight on the most loaded cantilever:

$$m_{cantilever.beam} := A_{CS.cantilever} \cdot \rho_{GL} \cdot \left(L_{c.a} + L_{c.b}\right) + \left(\rho_{HDF} + \rho_{screed} \cdot t_{screed} + m_{vent} + m_{undertak}\right) \cdot A_{Cont.cantilever} = \left(2.785 \cdot 10^4\right)\ kg$$

$$g_{k.cantilever} := \frac{m_{cantilever.beam}}{L_{c.a} + L_{c.b}} \cdot 9.81\ \frac{m}{s^2} = 34.369\ \frac{kN}{m}$$

Beam on facade:

Geometries of the beam:

$h_{floor} := 4.3\ m$ height of the contributing façade

$A_{CS.facade} := 0.72\ m \cdot 0.43\ m = 0.31\ m^2$ Cross-sectional area

Facade load:

$$m_{facade} := 50\ \frac{kg}{m^2} \cdot L_{beam} \cdot h_{floor} = \left(1.742 \cdot 10^3\right)\ kg$$

Contributing area:

$$x := \left(\frac{5.680^2}{5.605^2}\right)^{0.5} = 1.013$$

$$A_{Cont.facade} := \frac{\left(5.605\ m \cdot 8.1\ m + \left(5.605 \cdot \frac{x}{2}\right) m^2\right)}{2} = 24.12\ m^2$$

Total self-weight on the most loaded façade beam:

$$m_{facade.beam} := m_{facade} + A_{CS.facade} \cdot \rho_{GL} \cdot L_{beam} + \left(\rho_{HDF} + \rho_{screed} \cdot t_{screed} + m_{vent} + m_{undertak}\right) \cdot A_{Cont.facade} = \left(1.572 \cdot 10^4\right)\ kg$$

$$g_{k.facade} := \frac{m_{facade.beam}}{L_{beam}} \cdot 9.81\ \frac{m}{s^2} = 19.044\ \frac{kN}{m}$$

Additional loads:

Pointload at end of cantilever:

$$P_{g.facade} := \left(\frac{6.090}{2}\ m + \frac{6.385}{2}\ m\right) \cdot h_{floor} \cdot 50\ \frac{kg}{m^2} \cdot 9.81\ \frac{m}{s^2} = ?\ kN$$

Imposed loads for office buildings:

$$Q_{k\_im} := 0.5\ \frac{kN}{m^2} + 2.5\ \frac{kN}{m^2} = 3\ \frac{kN}{m^2}$$

A.4 Load combinations

Load combinations:

Facade beams:

SLS $g_{SLS.6.f} := 1.0 \cdot g_{k.facade} + 1.0 \cdot \frac{Q_{k\_im} \cdot A_{Cont.facade}}{L_{beam}} = 27.977 \ \frac{kN}{m}$

SLS quasi $g_{SLS.Q.f} := 1.0 \cdot g_{k.facade} + 0.3 \cdot \left(\frac{Q_{k\_im} \cdot A_{Cont.facade}}{L_{beam}} \right) = 21.724 \ \frac{kN}{m}$

ULS $g_{ULS.Q.f} := 1.35 \cdot g_{k.facade} + 1.5 \cdot \left(\frac{Q_{k\_im} \cdot A_{Cont.facade}}{L_{beam}} \right) = 39.109 \ \frac{kN}{m}$

Shear force at supports highest loaded facade beams

$F_{v.f.ULS} := g_{ULS.Q.f} \cdot L_{beam} \cdot \frac{1}{2} = 158.392 \ kN$

$F_{v.f.SLS} := g_{SLS.6.f} \cdot L_{beam} \cdot \frac{1}{2} = 113.307 \ kN$

Highest loaded glulam beams:

SLS $W_{SLS.6.h} := 1.0 \cdot g_{k.high} + 1.0 \cdot \frac{Q_{k\_im} \cdot A_{Cont.high}}{L_{beam}} = 42.142 \ \frac{kN}{m}$

SLS quasi $W_{SLS.Q.h} := 1.0 \cdot g_{k.high} + 0.3 \cdot \left(\frac{Q_{k\_im} \cdot A_{Cont.high}}{L_{beam}} \right) = 31.787 \ \frac{kN}{m}$

ULS $W_{ULS.6.h} := 1.35 \cdot g_{k.high} + 1.5 \cdot \left(\frac{Q_{k\_im} \cdot A_{Cont.high}}{L_{beam}} \right) = 59.11 \ \frac{kN}{m}$

Shear force at supports highest loaded timber beams

$F_{v.high.ULS} := W_{ULS.6.h} \cdot L_{beam} \cdot \frac{1}{2} = 239.397 \ kN$

$F_{v.high.SLS} := W_{SLS.6.h} \cdot L_{beam} \cdot \frac{1}{2} = 170.674 \ kN$

Cantilever beams:

SLS $W_{SLS.6.c} := 1.0 \cdot g_{k.cantilever} + 1.0 \cdot \frac{Q_{k\_im} \cdot A_{Cont.cantilever}}{L_{c.a} + L_{c.b}} = 53.082 \ \frac{kN}{m}$

SLS quasi $W_{SLS.Q.c} := 1.0 \cdot g_{k.cantilever} + 0.3 \cdot \left(\frac{Q_{k\_im} \cdot A_{Cont.cantilever}}{L_{c.a} + L_{c.b}} \right) = 39.983 \ \frac{kN}{m}$

ULS $W_{ULS.6.c} := 1.35 \cdot g_{k.cantilever} + 1.5 \cdot \left(\frac{Q_{k\_im} \cdot A_{Cont.cantilever}}{L_{c.a} + L_{c.b}} \right) = 74.467 \ \frac{kN}{m}$

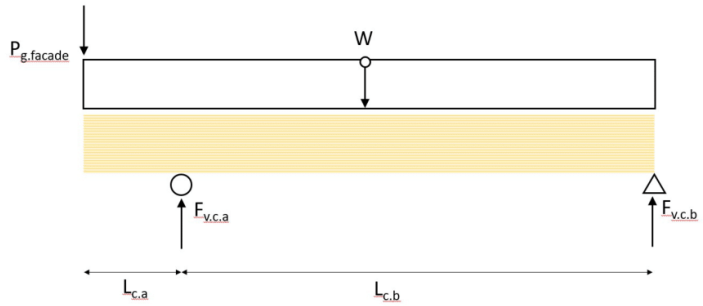

a)

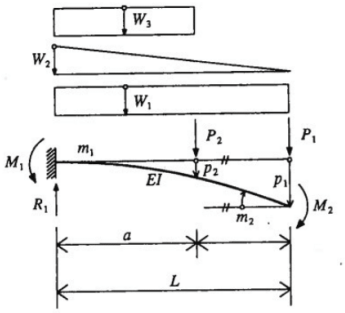

b)

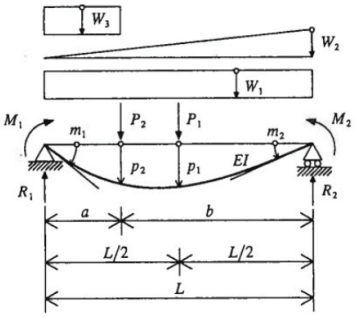

M1a=M1b

ULS

$$M_{1.a.ULS} := W_{ULS.6.c}\ \frac{{L_{c.a}}^2}{2} + L_{c.a} \cdot 1.35 \cdot P_{g.facade} = 74.929\ kN \cdot m$$

$$R_{1.a.ULS} := W_{ULS.6.c}\ L_{c.a} + 1.35\ P_{g.facade} = 107.121\ kN \qquad R_{1.b} := \frac{W_{ULS.6.c} \cdot L_{c.b}}{2} = 251.326\ kN$$

$$R_{1.ULS} := R_{1.a.ULS} + R_{1.b} = 358.447\ kN \qquad R_{2.ULS} := \frac{-M_{1.a.ULS}}{L_{c.b}} + \frac{W_{ULS.6.c} \cdot L_{c.b}}{2} = 240.226\ kN$$

$$F_{v.c.a.ULS} := R_{1.ULS} = 358.447\ kN \qquad F_{v.c.b.ULS} := R_{2.ULS} = 240.226\ kN$$

SLS

$$M_{1.a.SLS} := W_{SLS.6.c}\ \frac{{L_{c.a}}^2}{2} + L_{c.a} \cdot P_{g.facade} = 54.006\ kN \cdot m$$

$$R_{1.a.SLS} := W_{SLS.6.c}\ L_{c.a} + P_{g.facade} = 76.854\ kN \qquad R_{1.b.SLS} := \frac{W_{SLS.6.c} \cdot L_{c.b}}{2} = 179.15\ kN$$

$$R_{1.SLS} := R_{1.a.SLS} + R_{1.b.SLS} = 256.004\ kN \qquad R_{2.SLS} := \frac{-M_{1.a.SLS}}{L_{c.b}} + \frac{W_{SLS.6.c} \cdot L_{c.b}}{2} = 171.149\ kN$$

A.5 Fasteners' capacities

STA dowel

Units correction:

$f := 10^6 \cdot \frac{m^2}{s^2}$ $f_s := 10^6 \cdot mm^{0.3} \cdot \frac{m^2}{s^2}$ $my := mm^{0.4}$

Lateral capacity of one STA dowel:

$\rho := 390 \frac{kg}{m^3}$ the timber density
mean=430, characteristic= 390

$d_d := 16\ mm$ The dowel diameter

$t_d := 94\ mm$ the smaller of the thickness of the timber side member or the penetration depth

$f_{h\_0} := 0.082 \cdot \left(1 - 0.01 \cdot \frac{d_d}{1\ mm}\right) \cdot \rho \cdot f = 26.863 \frac{N}{mm^2}$ the embedment strength in the timber member, parallel to grain

From Structural Timber Design to Eurocode 5, Table 10.7 or EC5 8-32

$f_u := 630\ MPa$ the steel tensile strength (590 MPa for d=12mm)

$M_{y\_d} := 0.3 \cdot f_u \cdot d_d^{2.6} \cdot my = 255.372\ N \cdot m$ the yield moment (EC5 8-30)

For a steel plate of any thickness as the central member of a double shear connection. Failure modes f, g and h:

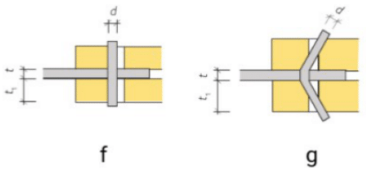

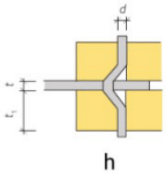

The lateral capacity of STA dowel loaded prallel to grain:

$$F_{v\_f} := f_{h\_0} \cdot t_d \cdot d_d = 40.402 \ kN$$

$$F_{v\_g} := f_{h\_0} \cdot t_d \cdot d_d \cdot \left(\sqrt{2 + \frac{4 \cdot M_{y\_d}}{f_{h\_0} \cdot d_d \cdot t_d^{\,2}}} - 1 \right) = 20.456 \ kN$$

$$F_{v\_h} := 2.3 \cdot \sqrt{M_{y\_d} \cdot f_{h\_0} \cdot d_d} = 24.096 \ kN$$

$$min\left(F_{v\_f}, F_{v\_g}, F_{v\_h}\right) = 20.456 \ kN$$ Failure mode g is decisive!

Lateral capacity of one dowel loaded perpendicular to grain:

$$\theta := 90 \cdot \frac{\pi}{180} = 1.571 \qquad k_{90} := 1.35 + 0.015 \cdot \frac{d_d}{1 \ mm} = 1.59$$

$$f_{h\_90} := \frac{f_{h\_0}}{k_{90} \cdot \sin(\theta)^2 + \cos(\theta)^2} = 16.895 \ MPa$$

$$F_{v\_f\_90} := f_{h\_90} \cdot t_d \cdot d_d = 25.41 \ kN$$

$$F_{v\_g\_90} := f_{h\_90} \cdot t_d \cdot d_d \cdot \left(\sqrt{2 + \frac{4 \cdot M_{y\_d}}{f_{h\_90} \cdot d_d \cdot t_d^{\,2}}} - 1 \right) = 14.181 \ kN$$

$$F_{v\_h\_90} := 2.3 \cdot \sqrt{M_{y\_d} \cdot f_{h\_90} \cdot d_d} = 19.11 \ kN$$

$$min\left(F_{v\_f\_90}, F_{v\_g\_90}, F_{v\_h\_90}\right) = 14.181 \ kN$$ Failure mode g is decisive!

SBD dowel

Lateral capacity of one SBD dowel:

Units correction:

$f := 10^6 \cdot \frac{m^2}{s^2}$ $f_s := 10^6 \cdot mm^{0.3} \cdot \frac{m^2}{s^2}$ $my := mm^{0.4}$

$\rho := 430 \frac{kg}{m^3}$ the timber density
mean=430, characteristic= 390

$d_{SBD} := 7.5\ mm$ The dowel diameter

$t_{SBD} := 97\ mm$ the smaller of the thickness of the timber side member or the penetration depth

$f_{h\_0\_SBD} := 0.082 \cdot \left(1 - 0.01 \cdot \frac{d_{SBD}}{1\ mm}\right) \cdot \rho \cdot f = 32.616 \frac{N}{mm^2}$ the embedment strength in the timber member

From Structural Timber Design to Eurocode 5, Table 10.7 or EC5 8-32

$M_{y\_SBD} := 42\ N \cdot m$ the yield moment (EC5 8-30)

For a steel plate of any thickness as the central member of a double shear connection. Failure modes f, g and h:

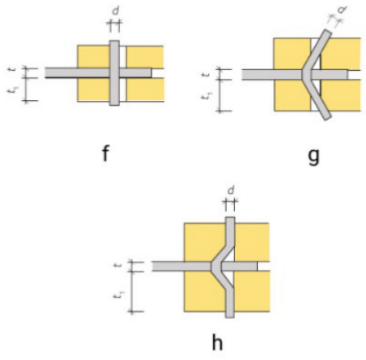

The lateral capacity of STA dowel loaded prallel to grain:

$$F_{v\_f\_SBD} := f_{h\_0\_SBD} \cdot t_{SBD} \cdot d_{SBD} = 23.728\ kN$$

$$F_{v\_g\_SBD} := f_{h\_0\_SBD} \cdot t_{SBD} \cdot d_{SBD} \cdot \left(\sqrt{2 + \frac{4 \cdot M_{y\_SBD}}{f_{h\_0\_SBD} \cdot d_{SBD} \cdot t_{SBD}^{\ 2}}} - 1 \right) = 10.435\ kN$$

$$F_{v\_h\_SBD} := 2.3 \cdot \sqrt{M_{y\_SBD} \cdot f_{h\_0\_SBD} \cdot d_{SBD}} = 7.372\ kN$$

$$min\left(F_{v\_f\_SBD}, F_{v\_g\_SBD}, F_{v\_h\_SBD}\right) = 7.372\ kN$$ Failure mode g is decisive!

Lateral capacity of one dowel (SBD) loaded perpendicular to grain:

$$\theta := 90 \cdot \frac{\pi}{180} = 1.571 \qquad k_{90} := 1.35 + 0.015 \cdot \frac{d_{SBD}}{1\ mm} = 1.463$$

$$f_{h\_90\_SBD} := \frac{f_{h\_0\_SBD}}{k_{90} \cdot \sin(\theta)^{2} + \cos(\theta)^{2}} = 22.301\ MPa$$

$$F_{v\_f\_90\_SBD} := f_{h\_90\_SBD} \cdot t_{SBD} \cdot d_{SBD} = 16.224\ kN$$

$$F_{v\_g\_90\_SBD} := f_{h\_90\_SBD} \cdot t_{SBD} \cdot d_{SBD} \cdot \left(\sqrt{2 + \frac{4 \cdot M_{y\_SBD}}{f_{h\_90\_SBD} \cdot d_{SBD} \cdot t_{SBD}^{\ 2}}} - 1 \right) = 7.325\ kN$$

$$F_{v\_h\_90\_SBD} := 2.3 \cdot \sqrt{M_{y\_SBD} \cdot f_{h\_90\_SBD} \cdot d_{SBD}} = 6.096\ kN$$

$$min\left(F_{v\_f\_90\_SBD}, F_{v\_g\_90\_SBD}, F_{v\_h\_90\_SBD}\right) = 6.096\ kN$$ Failure mode g is decisive!

LBS screw

$\rho := 390 \frac{kg}{m^3}$

Axial capacity of one LBS screw (80 mm):

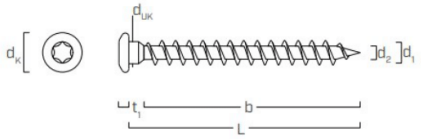

Nominal diameter	d_1	[mm]	5	7
Head diameter	d_K	[mm]	7,80	11,00
Tip diameter	d_2	[mm]	3,00	4,40
Underhead diameter	d_{UK}	[mm]	4,90	7,00
Head thickness	t_1	[mm]	2,40	3,50
Pre-drilling hole diameter(1)	d_V	[mm]	3,0	4,0
Characteristic yield moment	$M_{y,k}$	[Nm]	5,4	14,2
Characteristic withdrawal-resistance parameter(2)	$f_{ax,k}$	[N/mm²]	11,7	11,7
Associated density	ρ_a	[kg/m³]	350	350
Characteristic head-pull-through parameter(2)	$f_{head,k}$	[N/mm²]	10,5	10,5
Associated density	ρ_a	[kg/m³]	350	350
Characteristic tensile strength	$f_{tens,k}$	[kN]	7,9	15,4

(1) Pre-drilling valid for softwood.
(2) Valid for softwood - maximum density 440 kg/m³.
For applications with different materials or with high density please see ETA-11/0030.

$d_{scr} := 7\ mm$ the outer thread diameter

$$k_{d\_scr} := min\left(\frac{d_{scr}}{8\ mm}, 1\right) = 0.875$$

$l_{ef\_scr} := 68\ mm$ the penetration length of the threaded part

$$f_{ax} := 0.52 \cdot \left(\frac{d_{scr}}{1\ mm}\right)^{-0.5} \cdot \left(\frac{l_{ef\_scr}}{1\ mm}\right)^{-0.1} \cdot \left(\frac{\rho}{1\ \frac{kg}{m^3}}\right)^{0.8} = 15.242$$

$$f_{ax\_scr} := f_{ax} \cdot 1\ \frac{N}{mm^2} = 15.242\ \frac{N}{mm^2}$$

$n_{\_scr} := 1$ $\quad n_{ef} := n_{\_scr}^{0.9} = 1$ the effective number of screws

$\alpha := 90 \cdot \frac{\pi}{180}$ the angle between the screw axis and the grain direction, with $\alpha \geq 30\ °$

The withdrawal capacity (8-38):

$$F_{ax\_scr} := \frac{n_{ef} \cdot f_{ax\_scr} \cdot d_{scr} \cdot l_{ef\_scr} \cdot k_{d\_scr}}{1.2 \cdot \cos(\alpha)^2 + \sin(\alpha)^2} = 6.348\ kN$$

The pull-through resistance of connections with axially loaded screws should be taken as:

$\rho_a := 350\ \frac{kg}{m^3}$ the associated density

$f_{head\_scr} := 10.5\ \frac{N}{mm^2}$ the pull-through parameter of the screw

$d_h := 11\ mm$ the diameter of the screw head

$$F_{ax\_a\_scr} := n_{ef} \cdot f_{head\_scr} \cdot d_h^2 \cdot \left(\frac{\rho}{\rho_a}\right) = 1.416\ kN \qquad \text{(8-40b)}$$

The tensile resistance of the connection (head tear-off or tensile capacity of shank), should be taken as:

$f_{tens\_scr} := 15.4\ kN$ the tensile capacity of the screw

$F_{tens\_scr} := n_{ef} \cdot f_{tens\_scr} = 15.4\ kN$ (8-40c)

$$min\left(F_{ax\_scr}, F_{ax\_a\_scr}, F_{tens\_scr}\right) = 1.416\ kN$$

Lateral capacity of one LBS screw (80 mm):

Full shank screw

$d_{scr\_root} := 4.4\ mm$

$d_{scr\_ef} := 1.1 \cdot d_{scr\_root} = 4.84\ mm$ The diameter of the screw (8.7.1(3))

$t_{scr} := 68\ mm$ The penetration depth of the screw (smaller than timber thickness)

$f_{h\_scr} := 0.082 \cdot \rho \cdot {d_{scr\_ef}}^{-0.3} \cdot f_s = 19.926\ \frac{N}{mm^2}$ embedment strength, without predrilled holes (8-15)

$M_{y\_scr} := 14.2\ N \cdot m$

For a thick steel plate in single shear. Failure modes c, d and e:

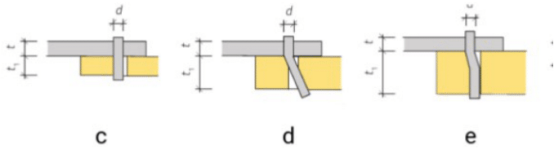

$F_{v\_c} := f_{h\_scr} \cdot t_{scr} \cdot d_{scr\_ef} = 6.558\ kN$

$F_{v\_d} := f_{h\_scr} \cdot t_{scr} \cdot d_{scr\_ef} \cdot \left(\sqrt{2 + \frac{4 \cdot M_{y\_scr}}{f_{h\_scr} \cdot d_{scr\_ef} \cdot {t_{scr}}^2}} - 1 \right) + \frac{F_{ax\_scr}}{4} = 4.594\ kN$

$F_{v\_e} := 2.3 \cdot \sqrt{M_{y\_scr} \cdot f_{h\_scr} \cdot d_{scr\_ef}} + \frac{F_{ax\_scr}}{4} = 4.279\ kN$

$min\left(F_{v\_c}, F_{v\_d}, F_{v\_e}\right) = 4.279\ kN$

Failure mode e is decisive for one screw!
Failure mode c is decisive for 3 or more screws!

LBA nails

Axial capacity of one LBA nail:

GEOMETRY AND MECHANICAL CHARACTERISTICS | LBA

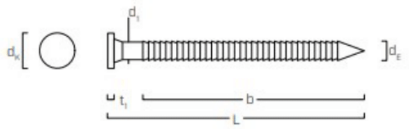

Nominal diameter	d_1	[mm]	4	6
Head diameter	d_K	[mm]	8,00	12,00
External diameter	d_E	[mm]	4,40	6,65
Head thickness	t_1	[mm]	1,40	2,00
Pre-drilling hole diameter	d_V	[mm]	3,0	4,5
Characteristic yield moment	$M_{y,k}$	[Nm]	6,5	19,0
Characteristic withdrawal-resistance parameter	$f_{ax,k}$	[N/mm²]	7,5	7,5
Characteristic tensile strength	$f_{tens,k}$	[kN]	6,9	11,4

$d_{n\_nom} := 6\ mm$ the inner thread diameter

$d_{n\_head} := 12\ mm$

$d_{n\_ef} := 1.1 \cdot d_{n\_nom} = 6.6\ mm$ the outer/eff. thread diameter

$t_{n\_head} := 2\ mm$

$t_{n\_pen} := 80\ mm - 12\ mm - t_{n\_head} = 66\ mm$ the penetration length of the threaded part

$$k_{n\_d} := min\left(\frac{d_{n\_ef}}{8\ mm}, 1\right) = 0.825$$

$$f_{ax} := 0.52 \cdot \left(\frac{d_{n\_ef}}{1\ mm}\right)^{-0.5} \cdot \left(\frac{t_{n\_pen}}{1\ mm}\right)^{-0.1} \cdot \left(\frac{\rho}{1\ \frac{kg}{m^3}}\right)^{0.8} = 15.744$$

$$f_{ax\_n} := f_{ax} \cdot 1\ \frac{N}{mm^2} = 15.744\ \frac{N}{mm^2}$$

$n_{\_n} := 1$ $\quad n_{ef\_n} := n_{\_n}^{0.9} = 1$ the effective number of screws

$\alpha := 90 \cdot \frac{\pi}{180}$ the angle between the screw axis and the grain direction, with $\alpha \geq 30\ °$

the withdrawal capacity (8-38):

$$F_{ax\_n} := \frac{n_{ef\_n} \cdot f_{ax\_n} \cdot d_{n\_ef} \cdot t_{n\_pen} \cdot k_{n\_d}}{1.2 \cdot \cos(\alpha)^2 + \sin(\alpha)^2} = 5.658\ kN$$

Lateral capacity of one LBA nail:

EN 5 8.3.1.1 (2) Timber should be pre-drilled when the diameter d of the nail exceeds 6 mm:

The embedment strength in timber with pridrelled holes:

$$f_{n\_h\_k} := 0.082 \cdot \left(1 - 0.01 \cdot \frac{d_{n\_nom}}{1\ mm}\right) \cdot \rho \cdot f = 30.061\ \frac{N}{mm^2}$$

$M_{n\_y} := 19\ N \cdot m$ yield moment

$$F_{n\_v\_c} := f_{n\_h\_k} \cdot t_{n\_pen} \cdot d_{n\_nom} = 11.904\ kN$$

$$F_{n\_v\_d} := f_{n\_h\_k} \cdot t_{n\_pen} \cdot d_{n\_nom} \cdot \left(\sqrt{2 + \frac{4 \cdot M_{n\_y}}{f_{n\_h\_k} \cdot d_{n\_nom} \cdot t_{n\_pen}^2}} - 1\right) + \frac{F_{ax\_n}}{4} = 6.748\ kN$$

$$F_{n\_v\_e} := 2.3 \cdot \sqrt{M_{n\_y} \cdot f_{n\_h\_k} \cdot d_{n\_nom}} + \frac{F_{ax\_n}}{4} = 5.672\ kN$$

$min\left(F_{n\_v\_c}, F_{n\_v\_d}, F_{n\_v\_e}\right) = 5.672\ kN$ Failure mode e is decisive for one nail!